Chapter 20

The Boundary Element Method for Structural Problems

Chapter details

Chapter DOI:

https://doi.org/10.4322/978-65-86503-83-8.c20

Chapter suggested citation / reference style:

Albuquerque, Éder L., et al. (2022). “The Boundary Element Method for Structural Problems”. *In* Jorge, Ariosto B., et al. (Eds.) *Fundamental Concepts and Models for the Direct Problem*, Vol. II, UnB, Brasilia, DF, Brazil, pp. 733–808. Book series in Discrete Models, Inverse Methods, & Uncertainty Modeling in Structural Integrity.

P.S.: DOI may be included at the end of citation, for completeness.

Book details

Book: Fundamental Concepts and Models for the Direct Problem

Edited by: Jorge, Ariosto B., Anflor, Carla T. M., Gomes, Guilherme F., & Carneiro, Sergio H. S.

Volume II of Book Series in:

Discrete Models, Inverse Methods, & Uncertainty Modeling in Structural Integrity

Published by: UnB City: Brasilia, DF, Brazil Year: 2022

DOI: https://doi.org/10.4322/978-65-86503-83-8

The Boundary Element Method for Structural Problems

E. L. Albuquerque[1*], P. Sollero[2], M. H. Aliabadi[3]

[1*]Department of Mechanical Engineering, University of Brasilia, Brazil. E-mail: eder@unb.br
[2]Faculty of Mechanical Engineering, University of Campinas, Brazil. E-mail: sollero@fem.unicamp.br
[3]Department of Aeronautics, Imperial College London, London, UK. E-mail: m.h.aliabadi@imperial.ac.uk

*Corresponding author

Abstract

In this chapter, some boundary element formulations applied to anisotropic materials are reviewed. Firstly, the plane elasticity is presented, with special attention to dynamic problems. Then, the thin plate formulation is shown, with application to transient dynamic problems, modal analysis, and buckling. Finally, thin shallow shell formulation is presented. Body forces are treated by the dual reciprocity boundary element method or by the radial integration method. Some numerical examples are presented in order to access the accuracy of the formulations.

1 Introduction

The extensive use of composite material structures in engineering design has demanded reliable and accurate numerical procedures for the treatment of anisotropic material structural problems. As anisotropy increases the number of material elastic constants, difficulties in the modelling arise in the analysis of laminate composite structures. Particularly, in boundary element formulation, larger number of variables means far more difficulties in deriving fundamental solutions. This aspect is evident in literature. It can be noted that the number of references in which boundary element method is applied for anisotropic structures is significantly smaller than those treating isotropic ones. However, in the last ten years, important advances on boundary element techniques applied to anisotropic materials were published in the literature. For example, plane elasticity problems were analysed by Sollero and Aliabadi [1993, 1995], Deb [1996], and Albuquerque et al. [2002, 2003a,b, 2004], out of plane elasticity problems by Zhang [2000], tri-dimensional problems by Kogl and Gaul [2000a,b, 2003], Kirchhoff plates by Shi and Bezine [1988], Rajamohan and Raamachandran [1999], Albuquerque et al. [2006], and shear deformable plates by Wang and Schweizerhof [1995, 1996, 1997].

Many alternative procedures have been presented to treat domain integrals in the BEM as shown in books like Nowak Nowak and Neves [1994] and Partridge *et al.* Partridge et al. [1992]. Among them, the most established is the dual reciprocity boundary element method (DRM), proposed by Nardini and Brebbia Nardini and Brebbia [1982] for the analysis of dynamic problems in plane elasticity and extended by many other authors for different applications (see the book of Partridge *et al.* Partridge et al. [1992]).

Boundary element formulations have been applied to plate bending anisotropic problems considering Kirchhoff as well as shear deformable plate theories. Shi and Bezine [1988] presented a boundary element analysis of plate bending problems using fundamental solutions proposed by Wu and Altiero [1981] based on Kirchhoff plate bending assumptions. Rajamohan and Raamachandran [1999] proposed a formulation that the singularities were avoided by placing source points outside the domain. Paiva et al. [2003] presented an analytical treatment for singular and hypersingular integrals of the formulation proposed by Shi and Bezine [1988]. Shear deformable plates have been analysed using boundary element method by Wang and Schweizerhof [1996, 1997] with the fundamental solution proposed by Wang and Schweizerhof [1995].

In general plate bending boundary element method, domain integrals arise in the formulation due to the distributed load in the domain. In order to evaluate these integrals, cell integration scheme can give accurate results, as carried out by Shi and Bezine [1988] for anisotropic plate bending problems. However, the discretization of the domain into cells reduces one of the main advantages of boundary element method that is the boundary only discretization. An alternative for this procedure was presented by Rajamohan and Raamachandran [1999] which proposes the use of particular solutions to avoid domain discretization. Nevertheless, the use of particular solutions demands to find a suitable function which satisfy the governing equation. Depending on how complicated the governing equation is, this function is quite difficult to be found.

Although the large majority of papers about the numerical analysis of composite shells are related to the finite element method, there are few works in literature that present boundary element formulations applied to orthotropic or even anisotropic shells Wang [1992], Lu and Mahrenholtz [1994], Wang and Schweizerhof [1995]. However, all these works involve complicated fundamental solutions that need to be computed numerically. An alternative approach to the these previous formulations is the coupling of plate bending and plane elasticity formulations, as proposed by Zhang and Atluri Zhang and Atluri [1986] who derived a formulation for static and dynamic analysis of isotropic classical shallow shells. Domain integrals were computed by the domain discretization into cells. Dirgantara and Aliabadi Dirgantara and Aliabadi [1999] extended this approach to the analysis of shear deformable isotropic shallow shells. Later, Wen, Aliabadi, and Young Wen et al. [2000] used the formulation proposed by Dirgantara and Aliabadi Dirgantara and Aliabadi [1999] and transformed the domain integrals into boundary integrals using the dual reciprocity method (DRM). Baiz and Aliabadi Baiz and Aliabadi [2006] presented a boundary element formulation for the analysis of linear buckling of shear deformable shallow shells.

In this report, boundary element formulations are presented for anisotropic problems. In all problems, the static fundamental solution is used and domain integrals which come from domain distributed loads are transformed into boundary integrals by exact transformation using the radial integration method or by the dual reciprocity boundary element method. The radial integration method was initially presented by Venturini [1988] in 1988 for isotropic plate bending problems. Recently, Gao [2002] extended it for three dimensional isotropic elastic problems. Two cases of loading are considered: uniformly distributed and linearly distributed loads. As stated by Gao [2002], this method can be applied to transform any of domain integral to the boundary. The most attractive feature of the method is its simplicity since only the radial variable is integrated. For domain integrals which include unknown variables, the proposed procedure can be performed using radial basis function as in the dual reciprocity method as suggested by Gao [2002]. The formulations are presented for plane elasticity, plate bending, and shallow shell problems.

2 Boundary element method applied to the dynamic analysis of anisotropic plane elasticity

2.1 Introduction

Nowadays, the structural dynamic analysis of anistropic plates by the boundary element method (BEM) has been treated by two different approaches. In the first, the fundamental solution is obtained considering all terms of the equation of motion. As a consequence, this approach has no domain integrals but uses complicated fundamental solutions (Wang and Schweizerhof Wang and Schweizerhof [1997]). In the second, the static fundamental solution is used and the inertia term of the equation of motion is considered as a body force. This body force generates domain integrals that can be computed by the discretization of the domain into cells. However, this procedure eliminates, to a certain extent, one of the most interesting advantage of the BEM that is the absence of domain discretization. The DRM has been successfully used in the dynamic analysis of anisotropic structures as presented by Albuquerque *et al.* Albuquerque et al. [2002, 2003a,b, 2004] for bidimensional problems, and by Kögl and Gaul Kogl and Gaul [2000a,b, 2003] for three-dimensional problems. Due to the complexity of governing equations of anisotropic materials, the analytical computation of particular solutions used in the DRM is restricted to some approximation functions, all of them are functions of material properties.

In this chapter, a boundary element formulation applied to transient dynamic anisotropic problems is presented. The fundamental solutions for elastostatics presented by Cruse and Swedlow Cruse and Swedlow [1971] are used and the inertia terms are treated as body forces. The dual reciprocity boundary element is used to transform the domain integral into a boundary integral. The particular solutions and the approximation function used here are both simple. The results are stable and strongly dependent on the material anisotropy. When they are compared with results obtained by other formulations, there is a good agreement in all the cases.

2.2 Anisotropic Elasticity

The equilibrium and compatibility equation are independent of the type material. However, the stress-strain relationship depends on the specific type of material behaviour. The constitutive equations for linear elastic anisotropic materials, leading to the governing differential equations of the stress function, will be reviewed in this section.

2.3 Constitutive equations

A linear relationship between stress and strain is assured only when the strain energy W is a quadratic function of strain. If W is the quadratic function

$$W = \frac{1}{2} C_{ijkl} \epsilon_{ij} \epsilon_{kl} \tag{1}$$

the equation (1) yields the generalized Hooke's law, or constitutive equation for fully anisotropic three-dimensional body, given by

$$\sigma_{ij} = C_{ijkl} \epsilon_{kl} \ . \tag{2}$$

The components of the fourth-order tensor C_{ijkl} are known as elastic constants of the material. Symmetry of the stress and strain tensors requires the $C_{ijkl} = C_{jikl}$ and $C_{ijkl} = C_{ijlk}$, respectively. The condition for the existence of a strain energy function also requires that $C_{ijkl} = C_{klij}$. These latter conditions reduce the number of elastic constants from 81 to 21.

For two-dimensional elasticity a fully anisotropic material can be described using only six independent elastic constants, rewriting equation (2) as

$$\epsilon_i = \sum_j a_{ij} \sigma_j \qquad\qquad i, j = 1, 2, 6 \tag{3}$$

where a_{ij} are compliance coefficients with $a_{ij} = a_{ji}$. The simplified notation for the strains in equation (3) is defined as

$$\epsilon_i = \left\{ \begin{array}{c} \epsilon_1 \\ \epsilon_2 \\ \epsilon_6 \end{array} \right\} = \left\{ \begin{array}{c} \epsilon_{11} \\ \epsilon_{22} \\ \epsilon_{12} \end{array} \right\} \ , \tag{4}$$

and for stresses

$$\sigma_j = \left\{ \begin{array}{c} \sigma_1 \\ \sigma_2 \\ \sigma_6 \end{array} \right\} = \left\{ \begin{array}{c} \sigma_{11} \\ \sigma_{22} \\ \sigma_{12} \end{array} \right\} \ . \tag{5}$$

The compliance coefficients can be expressed in terms of engineering constants as:

$$\begin{array}{ll} a_{11} = 1/E_1 & a_{12} = -\nu_{12}/E_1 = -\nu_{21}/E_2 \\ a_{16} = \eta_{12,1}/E_1 = \eta_{1,12}/G_{12} & a_{22} = 1/E_2 \\ a_{26} = \eta_{12,2}/E_2 = \eta_{2,12}/G_{12} & a_{66} = 1/G_{12} \end{array} \tag{6}$$

where E_k are the Young's moduli referring to the axes x_k , G_{12} is the shear modulus for the plane, ν_{ij} are the Poisson's ratios and $\eta_{jk,l}$ and $\eta_{l,jk}$ are the mutual coefficients of first and second kind respectively. For orthotropic materials $a_{16} = a_{26} = 0$.

2.3.1 Governing Differential Equation

The Airy stress function can be used to compute the stresses and displacements in a loaded anisotropic body by the method described in References Lekhnitskii [1968].

$$a_{11} \frac{\partial^4 F}{\partial x_2^4} - 2a_{16} \frac{\partial^4 F}{\partial x_1 \partial x_2^3} + (2a_{12} + a_{66}) \frac{\partial^4 F}{\partial x_1^2 \partial x_2^2} - 2a_{26} \frac{\partial^4 F}{\partial x_1^3 \partial x_2} + a_{22} \frac{\partial^4 F}{\partial x_1^4} = 0 \tag{7}$$

Equation (7) can be integrated in the characteristic complex planes

$$z = x_1 + \mu x_2 \ , \qquad \mu = r + is \ , \tag{8}$$

where r and s are the real and imaginary parts of μ, respectively.

Using equation (8), equation (7) can be rewritten as

$$\frac{d^4F}{dz^4}\left[a_{11}\mu^4 - 2a_{16}\mu^3 + (2a_{12} + a_{66})\,\mu^2 - 2a_{26}\mu + a_{22}\right] = 0 \ . \tag{9}$$

The existence of non trivial solutions of equation (9) requires the fulfillment of its characteristic equation

$$a_{11}\mu^4 - 2a_{16}\mu^3 + (2a_{12} + a_{66})\,\mu^2 - 2a_{26}\mu + a_{22} = 0 \ . \tag{10}$$

The roots of equation (10) are always complex or pure imaginary, occur in conjugate pairs (μ_k and $\overline{\mu}_k$) and s is always positive, as shown by Lekhnitskii Lekhnitskii [1968]. Thus, the characteristic directions become

$$z_k = x_1 + \mu_k x_2 \ , \qquad k = 1, 2 \tag{11}$$

and their conjugates.

The general form of the stress function is then given by

$$F(x_1, x_2) = 2Re[F_1(z_1) + F_2(z_2)] \ . \tag{12}$$

Introducing the notation

$$\frac{\mathrm{d}F_k(z_k)}{\mathrm{d}z_k} = \Phi_k(z_k) \ , \tag{13}$$

where no summation is implied on k. From equation (12), we obtain the stress components

$$\begin{aligned}
\sigma_{11} &= 2\mathrm{Re}[\mu_1^2\Phi_1^{(1)}(z_1) + \mu_2^2\Phi_2^{(1)}(z_2)] \ ,\\
\sigma_{22} &= 2\mathrm{Re}[\Phi_1^{(1)}(z_1) + \Phi_2^{(1)}(z_2)] \ ,\\
\sigma_{12} &= -2\mathrm{Re}[\mu_1\Phi_1^{(1)}(z_1) + \mu_2\Phi_2^{(1)}(z_2)] \ ,
\end{aligned} \tag{14}$$

where $\Phi_k^{(1)}$ denotes the first derivative of Φ_k.

Substituting equation (14) into equation (3), neglecting rigid body motion and integrating, we obtain the displacements

$$\begin{aligned}
u_1 &= 2\mathrm{Re}[p_{11}\Phi_1(z_1) + p_{12}\Phi_2(z_2)] \ ,\\
u_2 &= 2\mathrm{Re}[p_{21}\Phi_1(z_1) + p_{22}\Phi_2(z_2)] \ ,
\end{aligned} \tag{15}$$

where

$$[p_{ik}] = \begin{bmatrix} a_{11}\mu_k^2 + a_{12} - a_{16}\mu_k \\ a_{12}\mu_k + a_{22}/\mu_k - a_{26} \end{bmatrix} \tag{16}$$

is a matrix of complex parameters.

Equations (14) and (15) together with traction boundary conditions

$$t_j = \sigma_{ij}n_i = g_j \tag{17}$$

or displacements boundary conditions

$$u_j = h_j \tag{18}$$

constitute the mathematical problem to be solved.

2.4 Anisotropic Elastostatics Fundamental Solutions

The solution of a point force in the infinite anisotropic plane is called fundamental solution and is the basic relation for the development of integral equations for the solution of the anisotropic elasticity problem. The fundamental solutions U_{ij} and T_{ij} are the displacements and tractions in the j-direction at $\mathbf{z}$ due to a unit point force acting in the i-direction at $\mathbf{z}^{'}$. The points $\mathbf{z}$ and $\mathbf{z}^{'}$ are the source (or load) and field points and are defined by

$$\mathbf{z}^{'} = \left\{ \begin{array}{c} z_1^{'} \\ z_2^{'} \end{array} \right\} = \left\{ \begin{array}{c} x_1^{'} + \mu_1 x_2^{'} \\ x_1^{'} + \mu_2 x_2^{'} \end{array} \right\} \tag{19}$$

and

$$\mathbf{z} = \left\{ \begin{array}{c} z_1 \\ z_2 \end{array} \right\} = \left\{ \begin{array}{c} x_1 + \mu_1 x_2 \\ x_1 + \mu_2 x_2 \end{array} \right\} \tag{20}$$

where μ_k are the complex roots of equation (10).

If we consider a closed contour Γ surrounding the source point and use the tractions computed by equation (17) and the stresses defined by equation (14), it can be shown that

$$\int_\Gamma t_1 \mathrm{d}\Gamma = 2\mathrm{Re}\, [\![\mu_1 \Phi_1 + \mu_2 \Phi_2]\!] \quad ,$$

$$\int_\Gamma t_2 \mathrm{d}\Gamma = 2\mathrm{Re}\, [\![\Phi_1 + \Phi_2]\!] \quad , \tag{21}$$

where the double brackets denote the jump in the function for a closed contour surrounding the source point. If the contour Γ encloses $\mathbf{z}^{'}$, the point of load application, then the results of equations (21) will be non-zero.

The fundamental solutions in an infinite anisotropic plane can be obtained by finding the Airy stress function resulting from the fundamental tractions. The Airy stress function for a point load in the x_i direction can be represented by Φ_{ik}. As the contour integrals of equation (21) are of opposite signs to the applied loads it can be expressed for the point load solution as

$$\begin{aligned} 2\mathrm{Re}\, [\![\mu_1 \Phi_{i1} + \mu_2 \Phi_{i2}]\!] &= -\delta_{i1} \quad , \\ 2\mathrm{Re}\, [\![\Phi_{i1} + \Phi_{i2}]\!] &= \delta_{i2} \quad . \end{aligned} \tag{22}$$

Equation (22) may be satisfied for any closed contour enclosing $\mathbf{z}^{'}$ by taking

$$\Phi_{ik} = A_{ik} \ln \left(\mathbf{z} - \mathbf{z}^{'}\right) \tag{23}$$

where A_{ik} are complex constants. It can be shown that for any contour enclosing the point $\mathbf{z}^{'}$

$$\ln \left(\mathbf{z} - \mathbf{z}^{'}\right) = 2\pi i \quad . \tag{24}$$

Using equations (22), (23), and (24) it can be obtained two equations for the unknown constants A_{ik}, or

$$\begin{aligned} A_{i1} - \overline{A}_{i1} + A_{i2} - \overline{A}_{i2} &= \delta_{i2}/(2\pi i) \\ \mu_1 A_{i1} - \overline{\mu_1}\overline{A}_{i1} + \mu_2 A_{i2} - \overline{\mu_2}\overline{A}_{i2} &= -\delta_{i1}/(2\pi i) \quad . \end{aligned} \tag{25}$$

The remaining two equations result from the requirement that the displacements be single valued, or

$$[\![u_i]\!] = 0 \ . \tag{26}$$

Using the displacements equation (15) and equation (23) and (24), equation (26) can be rewritten as

$$\begin{aligned} p_{11}A_{i1} - \overline{p_{11}}\overline{A_{i1}} + p_{12}A_{i2} - \overline{p_{12}}\overline{A_{i2}} &= 0 \ , \\ p_{21}A_{i1} - \overline{p_{21}}\overline{A_{i1}} + p_{22}A_{i2} - \overline{p_{22}}\overline{A_{i2}} &= 0 \ , \end{aligned} \tag{27}$$

where p_{ik} is given by equation (16) and the overbar denotes the conjugate of the complex constant. Equations (25) and (27) can be rearranged in the usual matricial form as

$$\begin{bmatrix} 1 & -1 & 1 & -1 \\ \mu_1 & -\overline{\mu}_1 & \mu_2 & -\overline{\mu}_2 \\ p_{11} & -\overline{p}_{11} & p_{12} & -\overline{p}_{12} \\ p_{21} & -\overline{p}_{21} & p_{22} & -\overline{p}_{22} \end{bmatrix} \begin{Bmatrix} A_{i1} \\ \overline{A}_{i1} \\ A_{i2} \\ \overline{A}_{i2} \end{Bmatrix} = \begin{Bmatrix} \delta_{i2}/(2\pi i) \\ -\delta_{i1}/(2\pi i) \\ 0 \\ 0 \end{Bmatrix} , \tag{28}$$

which is sufficient to find the complex constants A_{ik}.

The fundamental solution for displacements can be obtained by inserting the stress function given by equation (23) into the displacements equation (15) to give

$$U_{ij}(\mathbf{z}', \mathbf{z}) = 2\mathrm{Re}\left[p_{j1}A_{i1}\ln(z_1 - z_1') + p_{j2}A_{i2}\ln(z_2 - z_2')\right] \ . \tag{29}$$

Similarly, the fundamental solution for tractions is obtained by substituting equation (23) into the stress equations (14) and using equation (17) to give

$$T_{ij}(\mathbf{z}', \mathbf{z}) = 2\mathrm{Re}\left[\frac{1}{(z_1 - z_1')}\, q_{j1}(\mu_1 n_1 - n_2)A_{i1} + \frac{1}{(z_2 - z_2')}\, q_{j2}(\mu_2 n_1 - n_2)A_{i2}\right] \ . \tag{30}$$

where

$$[q_{jk}] \ = \ \begin{bmatrix} \mu_1 & \mu_2 \\ -1 & -1 \end{bmatrix} \tag{31}$$

and n_k are the components of the normal outward vector.

2.5 Boundary Integral Equation

Since the governing partial differential equation (7) of the anisotropic elasticity problem admits no real characteristic surface, the problem is elliptic and the continuity of the stresses and displacement fields is assured. Consequently, it can be verified that Betti's reciprocal work theorem for two self-equilibrated states $(\mathbf{u}, \mathbf{t}, \mathbf{b})$ and $(\mathbf{u}^*, \mathbf{t}^*, \mathbf{b}^*)$ must be valid and expressed as

$$\int_\Omega b_i^* u_i \mathrm{d}\Omega + \int_\Gamma t_i^* u_i \mathrm{d}\Gamma = \int_\Omega b_i u_i^* \mathrm{d}\Omega + \int_\Gamma t_i u_i^* \mathrm{d}\Gamma \ . \tag{32}$$

The self-equilibrated states are described by the displacements $\mathbf{u}$ and $\mathbf{u}^*$, the tractions $\mathbf{t}$ and $\mathbf{t}^*$ and the body forces $\mathbf{b}$ and $\mathbf{b}^*$. It is assumed that the domain Ω with boundary

Γ and the domain Ω^* with boundary Γ^* encompass the states $(\mathbf{u}, \mathbf{t}, \mathbf{b})$ and $(\mathbf{u}^*, \mathbf{t}^*, \mathbf{b}^*)$, respectively. The problem under consideration in domain Ω is contained within a general region Ω^*, having the same anisotropic properties.

For the present purposes it is convenient to let the state $(\mathbf{u}, \mathbf{t}, \mathbf{b})$ be the required solution, and the state $(\mathbf{u}^*, \mathbf{t}^*, \mathbf{b}^*)$ be the fundamental solution. The displacement and traction field corresponding to the solution of the governing equation can be written as

$$
\begin{aligned}
u_i^* &= u_j^* \delta_{ij} = U_{ij}(\mathbf{z}', \mathbf{z}) \delta_{ij} e_i \ , \\
t_i^* &= t_j^* \delta_{ij} = T_{ij}(\mathbf{z}', \mathbf{z}) \delta_{ij} e_i \ ,
\end{aligned} \tag{33}
$$

where δ_{ij} is the Kronecker's delta, U_{ij} and T_{ij} are the anisotropic fundamental solution for elastostatics given by equations (29) and (30), respectively, and e_i are the components of the unit vector corresponding to a unit force in the i direction applied at $\mathbf{z}'$. The body force component b_i^* corresponds to a point force and is given by

$$
b_i^* = \delta(\mathbf{z} - \mathbf{z}') e_i \ , \tag{34}
$$

where $\delta(\mathbf{z} - \mathbf{z}')$ is the Dirac delta function, that has the property

$$
\int_\Omega g(x) \delta(\mathbf{z} - \mathbf{z}') \mathrm{d}\Omega(\mathbf{z}) = g(\mathbf{z}') \ . \tag{35}
$$

From this property of the Dirac delta function, the first integral in equation (32) can be written as

$$
\int_\Omega b_i^* u_i \mathrm{d}\Omega = u_i(\mathbf{z}') e_i \ . \tag{36}
$$

Using equations (33) and (36), equation (32) can be rewritten as

$$
u_i(\mathbf{z}') + \int_\Gamma T_{ij}(\mathbf{z}', \mathbf{z}) u_j(\mathbf{z}) \mathrm{d}\Gamma(\mathbf{z}) = \int_\Gamma U_{ij}(\mathbf{z}', \mathbf{z}) t_j(\mathbf{z}) \mathrm{d}\Gamma(\mathbf{z}) + \int_\Omega U_{ij}(\mathbf{z}', \mathbf{z}) b_j(\mathbf{z}) \mathrm{d}\Omega(\mathbf{z}) \tag{37}
$$

which is known as Somigliana's identity that in absence of body forces is expressed as

$$
u_i(\mathbf{z}') + \int_\Gamma T_{ij}(\mathbf{z}', \mathbf{z}) \ u_j(\mathbf{z}) \ \mathrm{d}\Gamma(\mathbf{z}) = \int_\Gamma U_{ij}(\mathbf{z}', \mathbf{z}) \ t_j(\mathbf{z}) \ \mathrm{d}\Gamma(\mathbf{z}) \ . \tag{38}
$$

Equation (38) does not constitute a solution to a well-posed boundary value problem because the boundary tractions and boundary displacements are not simultaneously known for all boundary points. A relation between boundary tractions and displacements is obtained when the source point is taken to the boundary, which represents the solution for the elastic problem.

When there is body forces in the formulation, the integral equation is given by:

$$
c_{ij}(\mathbf{z}') u_j(\mathbf{z}') + \int\!\!\!\!\!\!- _\Gamma T_{ij}(\mathbf{z}', \mathbf{z}) \ u_j(\mathbf{z}) \ d\Gamma(\mathbf{z}) = \int_\Gamma U_{ij}(\mathbf{z}', \mathbf{z}) \ t_j(\mathbf{z}) \ d\Gamma(\mathbf{z}) + \int_\Omega U_{ij}(\mathbf{z}', \mathbf{z}) \ b_j(\mathbf{z}) \ d\Gamma(\mathbf{z}). \tag{39}
$$

where $b_j(\mathbf{z})$ is a load distributed along the domain Ω.

2.6 The dual reciprocity boundary element method for dynamic problems

The reciprocal relation between the fundamental solution and another elastostatic state defined over a domain Ω is given by the following integral equation

$$c_{ik}u_i + \int_\Gamma T_{ik}u_i d\Gamma = \int_\Gamma U_{ik}t_i d\Gamma - \int_\Omega U_{ik}\rho\ddot{u}_i d\Omega \tag{40}$$

where c_{ik} is equal to $\delta_{ik}/2$ to smooth boundary.

In order to transform the domain integral of equation (40) into a boundary one, the dual reciprocity boundary element method will be used. In this method, the acceleration is approximated as a sum of M function $f^m(x)$ multiplied by unknown time dependent coefficients $\ddot{\alpha}_k(\tau)$

$$\ddot{u}_i(x,\tau) = \sum_{m=1}^{M} \ddot{\alpha}_k(\tau) f^m(x) \tag{41}$$

The domain integral in equation (40) can be written as

$$\int_\Omega U_{li}\rho\ddot{u}_i = \rho \sum_{m=1}^{M} \ddot{\alpha}_i^m \int_\Omega U_{li} f^m d\Omega \tag{42}$$

The solutions of the equilibrium equation

$$C_{mnrs}\hat{u}^j_{rk,ns} = f^j_{mk} \tag{43}$$

are required in order to transform the domain integral into an equivalent boundary integral. The solutions $\hat{u}_{rk}$ are known as particular solutions.

The reciprocal relation between the fundamental solution and the particular solution is given by

$$c_{li}\hat{u}^m_{in} + \int_\Gamma T_{li}\hat{u}^m_{in} d\Gamma = -\int_\Omega f^m U_{ln} d\Omega + \int_\Gamma U_{li}\hat{t}^m_{in} d\Gamma \tag{44}$$

Substituting equation (44) into equation (42), and then into equation (40), the following equation is obtained

$$\begin{aligned} c_{li}u_i + \int_\Omega T_{li}u_i d\Gamma = \int_\Gamma U_{li}t_i d\Gamma + \\ \rho \sum_{m=1}^{M} \ddot{\alpha}^m_n \left\{ c_{li}\hat{u}^m_{in} - \int_\Gamma \hat{t}^m_{in} U_{li} d\Gamma + \int_\Gamma T_{li}\hat{u}^m_{in} d\Gamma \right\} \end{aligned} \tag{45}$$

The equation (45) is the basis of dual reciprocity boundary element method. In it can be noted the absence of domain integral.

The traditional procedure to solve the differential equation (43) when the problem is isotropic is to assume the approximation function and compute the corresponding particular solutions. This procedure is quite difficult for anisotropic materials because the anisotropy increases the number of constants in the equilibrium equation. An alternative is to assume a particular solution and find the correspondent approximation function.

This procedure was used by Schclar Schclar [1994] to steady state anisotropic problems and by Albuquerque and Sollero Albuquerque and Sollero [1998] to transient anisotropic problems.

In this work it is used for the displacement particular solution

$$\hat{u}_{mk} = r^3 \delta_{km} \tag{46}$$

where r is the radial vector from the source to the field point and δ_{km} is the Dirac delta.

The corresponding approximation function, obtained by the substitution of equation (46) into equation (43) is given by

$$f_{im} = C_{ijkl} \left\{ 3r \left(r_{,l} r_{,j} \delta_{km} + \delta_{jl} \delta_{km} \right) \right\}. \tag{47}$$

The traction particular solution is given by

$$\hat{t}_{mr} = \hat{\sigma}_{mrs} n_s \tag{48}$$

where the particular stress $\hat{\sigma}_{mrs}$, which is obtained by differentiating the equation (46) and using Hooke's law, is given by

$$\hat{\sigma}_{mrs} = C_{rsjk} \frac{3r^2}{2} (r_{,j} \delta_{km} + r_{,k} \delta_{jm}) \tag{49}$$

In order to solve the elastodynamics problem, the boundary is divided into boundary elements and the displacements and tractions are interpolated in these elements using quadratic shape functions. Then the integral equation (45) can be written in a matrix form as

$$\mathbf{Hu} - \mathbf{Gt} = \rho(\mathbf{H}\hat{\mathbf{u}} - \mathbf{G}\hat{\mathbf{t}})\ddot{\boldsymbol{\alpha}} \tag{50}$$

The coefficient $\ddot{\boldsymbol{\alpha}}$ are computed using the relationship

$$\ddot{\mathbf{u}} = \mathbf{F}\ddot{\boldsymbol{\alpha}} \tag{51}$$

where $\mathbf{F}$ is a matrix whose elements are formed computing the approximation function to every node.

Equation (50) can be written as

$$\mathbf{Hu} - \mathbf{Gt} = \rho(\mathbf{H}\hat{\mathbf{u}} - \mathbf{G}\hat{\mathbf{t}})\mathbf{E}\ddot{\mathbf{u}} \tag{52}$$

where $\mathbf{E} = \mathbf{F}^{-1}$.

Equation (52) can be written as

$$\mathbf{M}\ddot{\mathbf{u}} + \mathbf{Hu} = \mathbf{Gt} \tag{53}$$

where

$$\mathbf{M} = \rho[\mathbf{G}\hat{\mathbf{t}} - \mathbf{H}\hat{\mathbf{u}}]\mathbf{E} \tag{54}$$

Several time integration schemes have been proposed to compute the acceleration $\ddot{\mathbf{u}}$ as it was reported by Bathe and Wilson Bath and Wilson [1976]. However, it has been found by Loffler and Mansur Loeffler and Mansur [1987] that Houbolt method (Houbolt Houbolt [1950]) is the most appropriated to be used with dual reciprocity boundary element method. Because this, the Houbolt method was chosen to proceed the time integration of equation (52). Following Houbolt expression, the acceleration in the instant $\tau + \Delta\tau$ is approximated by

$$\ddot{\mathbf{u}}_{\tau+\Delta\tau} = \frac{1}{\Delta\tau^2}(2\mathbf{u}_{\tau+\Delta\tau} - 5\mathbf{u}_\tau + 4\mathbf{u}_{\tau-\Delta\tau} - \mathbf{u}_{t-2\Delta t}) \tag{55}$$

which can be used to write equation (52) as

$$\mathbf{Bu} = \mathbf{Gt} + \frac{1}{\Delta\tau^2}\mathbf{Mu}_b \tag{56}$$

where $\mathbf{u} = \mathbf{u}_{\tau+\Delta\tau}$, $\mathbf{t} = \mathbf{t}_{\tau+\Delta\tau}$,

$$\mathbf{B} = \left[\frac{2}{\Delta\tau^2}\mathbf{M} + \mathbf{H}\right], \tag{57}$$

and $\mathbf{u}_b = 5\mathbf{u}_\tau - 4\mathbf{u}_{\tau-\Delta\tau} + \mathbf{u}_{\tau-2\Delta\tau}$.

The time step $\Delta\tau$ should be chosen taking into account the material properties and the mesh used. In this work, considering the non-dimensional number

$$\beta = \sqrt{\frac{E_{\max}}{\rho}}\frac{\Delta\tau}{l_{\min}}, \tag{58}$$

where $E_{\max}$ is the value of the biggest Young modulus, and $l_{\min}$ is the length of the smallest boundary element, the time step is chosen so that

$$\beta \geq 0.4716 \tag{59}$$

.

2.7 Numerical Results

2.7.1 Infinity long strip

The first problem to be treated is an infinite long strip (Figure 1) subjected to a step load function applied at time $\tau_o = 0$ (Figure 2). A state of plane stress is assumed with load $\sigma_o = 1$ N. The material is considered quasi-isotropic with the following properties: Young's Moduli $E_1 = 10.6667\ 10^4$ Pa and $E_2 = 10.68\ 10^4$ Pa, Poisson's ratio $\nu_{12} = 0.3333$, shear stress modulus $G_{12} = 4\ \ 10^4$ Pa, and density $\rho = 1$ Kg/m^3.

The mesh used has 12 equal quadratic boundary elements (Figure 3). The results are computed without any internal point and with 3 internal points (Figure 3). The time step used was $\Delta\tau = 7.22\ 10^{-4}$s ($\beta = 0.4716$ for the quasi-isotropic case).

The vertical displacement at the mid point of the free edge are plotted in Figure 4 and the normal tractions at the base mid point are plotted in Figure 5, when using 0 and 3 internal points. The results show good agreement with the exact solution. Although in this problem the use of internal points causes slightly differences in the solution, in many cases the use of internal points are necessary to improve the results and it will be adopted in all other problems treated in this work.

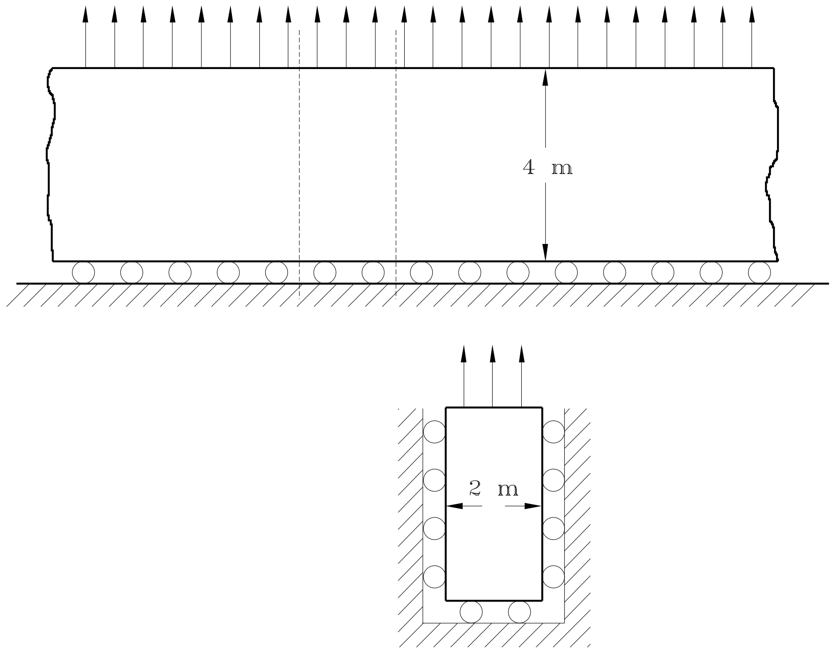

Figure 1: Infinity long strip under an uniform step load.

The same problem is treated now varying the ratio between the Young's Moduli E_1 and E_2 ($R = E_2/E_1$, where E_1 and all other material constants are maintained with a constant value).

Figures 6 and 7 show the results to three different values of R to the vertical displacement to a node in the top and the normal traction to a node in the bottom of the strip, respectively. In these orthotropic cases, analytical solutions were not found in the literature. However the results are the expected ones: the bigger the value of R, the more rigid is the strip, the smaller are the displacements and the higher are the frequencies. In all the cases the results are stable even after many cycles.

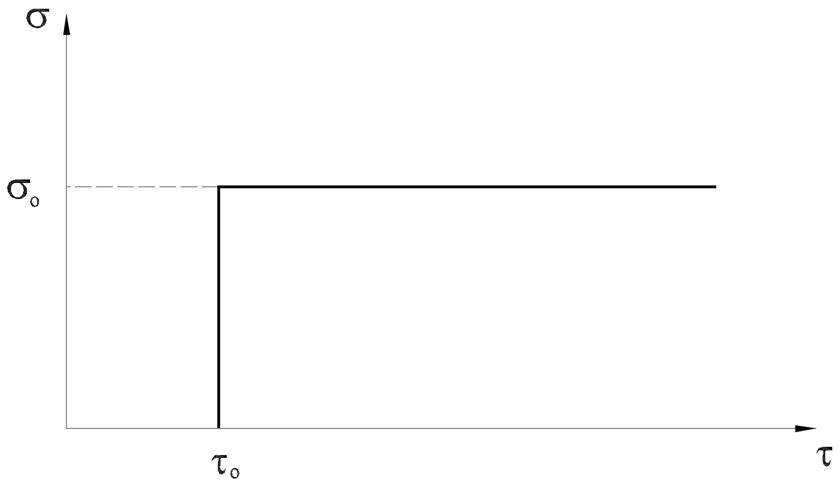

Figure 2: Step load function.

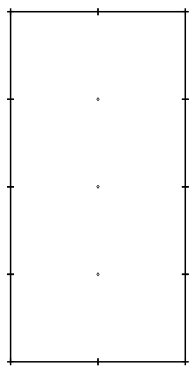

Figure 3: Boundary element mesh and internal points to a part of the infinity strip.

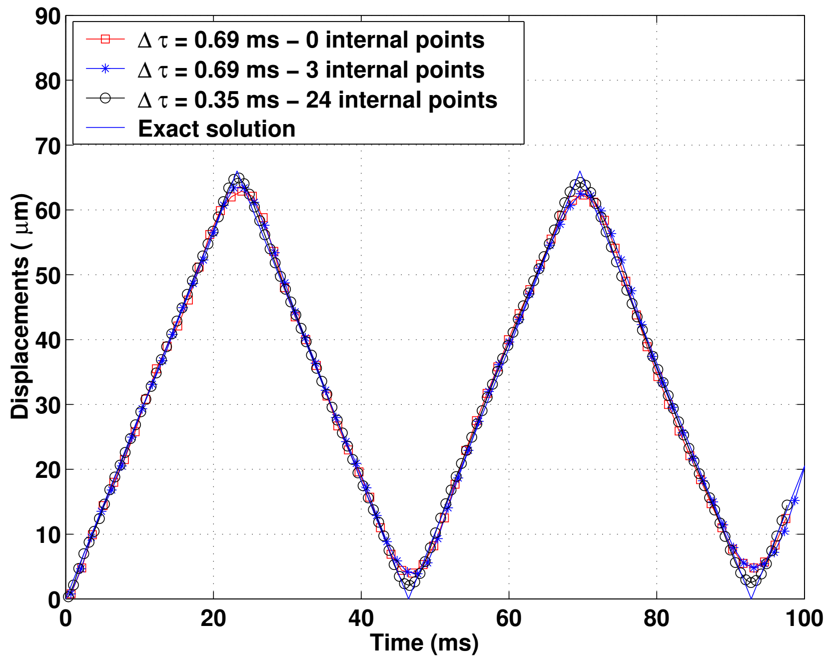

Figure 4: Vertical displacements for a node at mid point of the quasi-isotropic infinity long strip free edge.

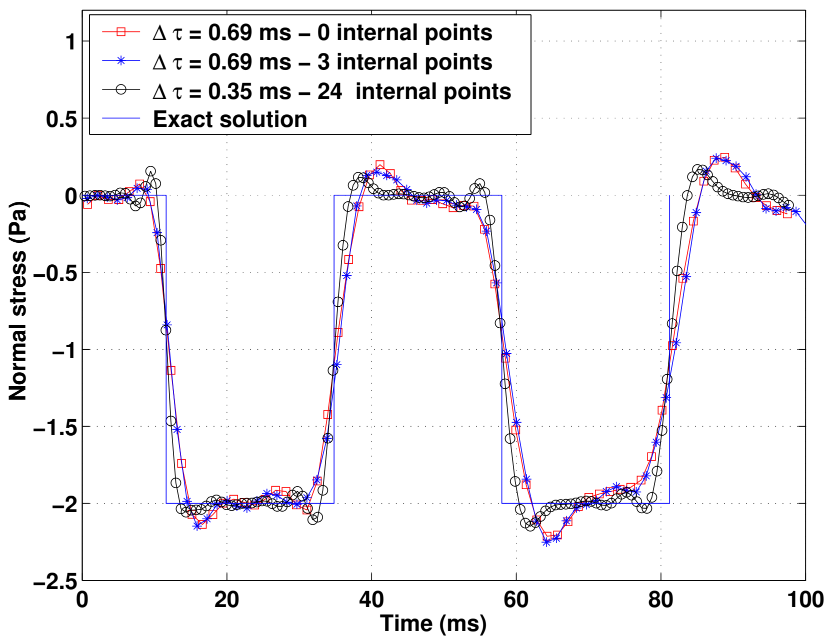

Figure 5: Normal tractions for a node at mid point of the quasi-isotropic infinity long strip base edge.

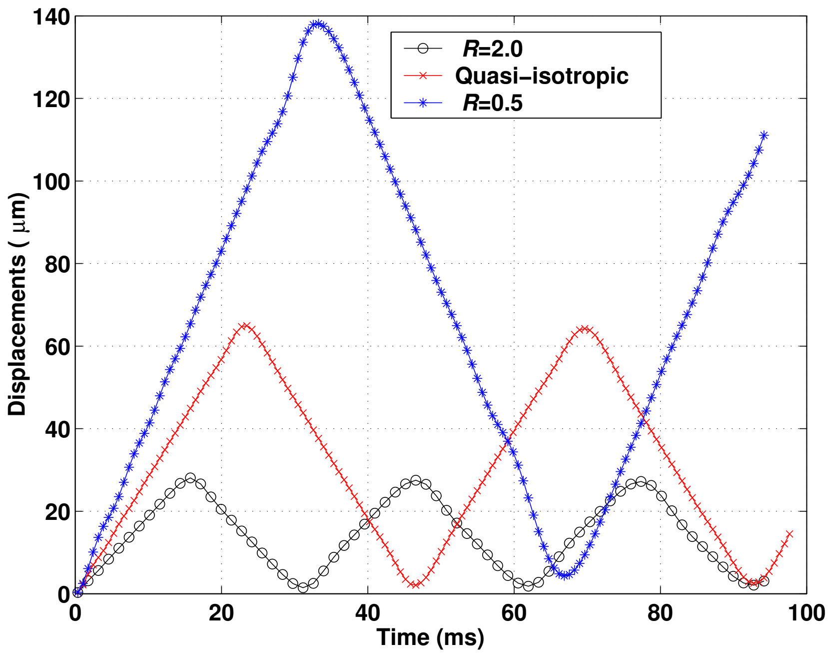

Figure 6: Vertical displacements for a node at mid point of the infinity long strip free edge considering three different Young's Modulus ratios.

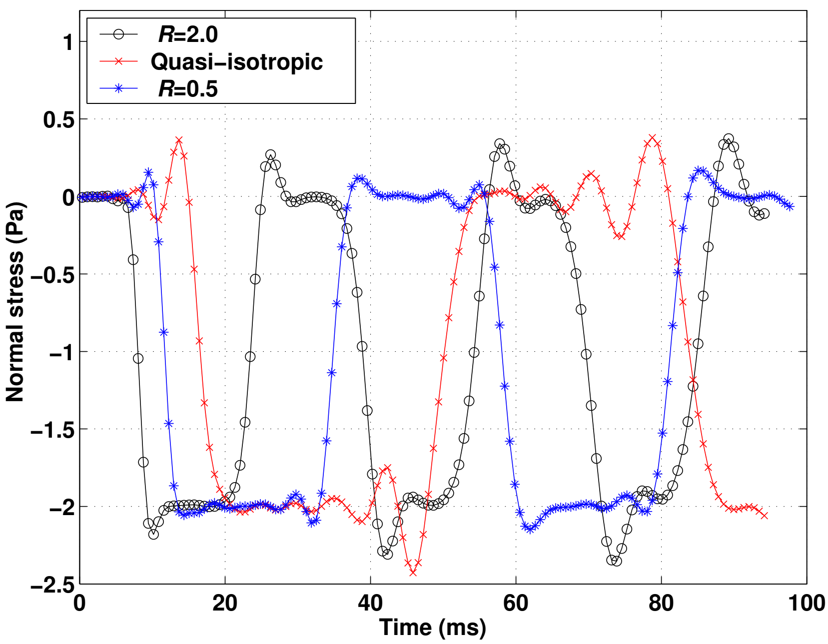

Figure 7: Normal tractions for a node at mid point of the infinity long strip base edge considering three different Young's Modulus ratios.

3 Theory of bending of anisotropic thin plate

A plate is a structural element defined by two flat parallel surfaces (Figure 8) where loads are transversely applied. The distance between these two surfaces defines the thickness of the plate, which is small when compared to other plate dimensions.

Considering its material properties, a plate can be either anisotropic, with different properties in different directions, or isotropic, with equal properties in all directions. Depending on its thickness, a plate can be considered either a thin or a thick plate. In this work, formulations will be developed for anisotropic thin plates.

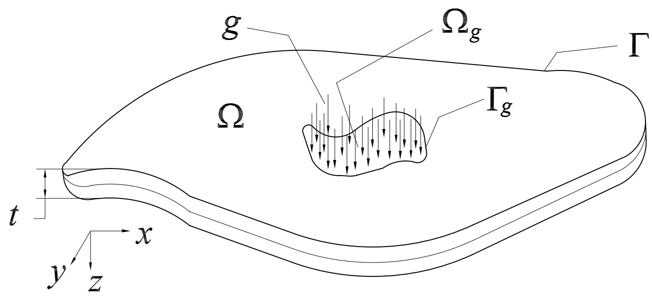

Figure 8: Thin plate.

The theory of anisotropic thin plates bending is based on the following assumptions Lekhnitskii [1968]:

1. Straight sections, which in the undeformed state are normal to its middle surface, remain straight and normal to the deformed middle surface after loading;

2. Normal stress σ_z in cross sections parallel to the middle plane is small if compared with stresses in the transverse cross section, i.e., σ_x, σ_y, τ_{xy}.

3.1 Basic relations for anisotropic plates

Consider a plate element following the assumptions previously defined. Figure 9 shows this element with a stress state acting on it and a distributed load applied on its area. Integrating stress components along the plate thickness, we can define moments and loads (Figure 10):

$$m_x = \int_{-t/2}^{t/2} \sigma_x z dz, \tag{60}$$

$$m_y = \int_{-t/2}^{t/2} \sigma_y z dz, \tag{61}$$

$$m_{xy} = \int_{-t/2}^{t/2} \tau_{xy} z dz, \tag{62}$$

$$m_{yx} = \int_{-t/2}^{t/2} \tau_{yx} z dz, \tag{63}$$

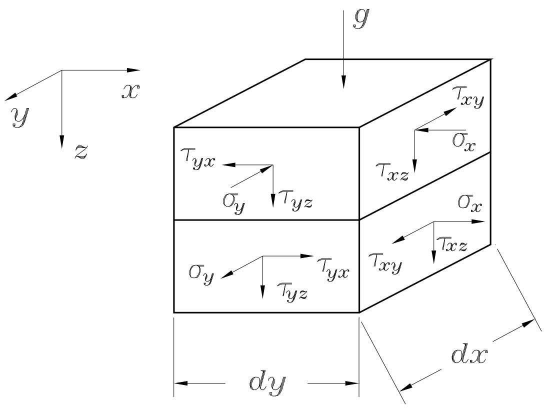

Figure 9: Stresses in a plate element

$$q_x = \int_{-t/2}^{t/2} \tau_{xz} dz, \tag{64}$$

and

$$q_y = \int_{-t/2}^{t/2} \tau_{yz} dz. \tag{65}$$

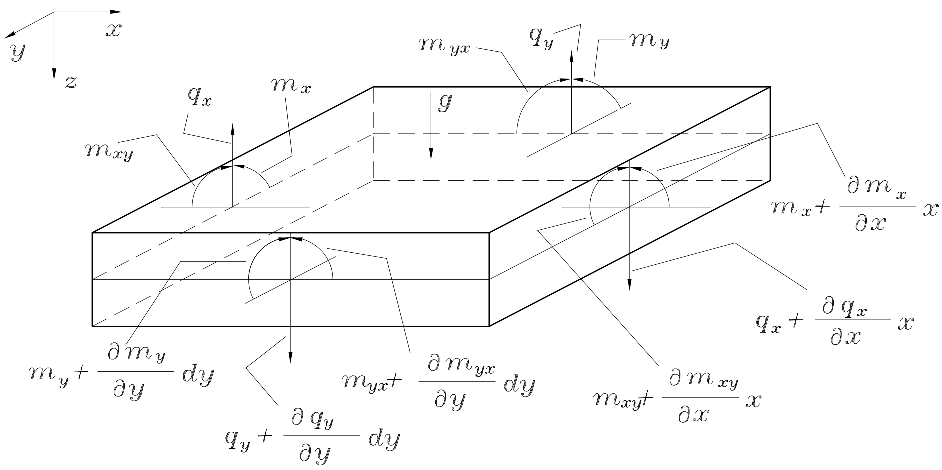

Figure 10: Loads and moments in a plate element

From equilibrium of forces and moments, we can write:

$$\frac{\partial q_x}{\partial x} + \frac{\partial q_y}{\partial y} + g = 0, \tag{66}$$

$$\frac{\partial m_x}{\partial x} + \frac{\partial m_{yx}}{\partial y} - q_x = 0, \tag{67}$$

$$\frac{\partial m_y}{\partial y} + \frac{\partial m_{xy}}{\partial x} - q_y = 0. \tag{68}$$

Solving equations (67) and (68) for q_x and q_y, respectively, substituting in equation (66), and considering symmetry of moments ($m_{xy} = m_{yx}$), we have:

$$\frac{\partial^2 m_x}{\partial x^2} + 2\frac{\partial^2 m_{xy}}{\partial x \partial y} + \frac{\partial^2 m_y}{\partial y^2} = -g. \tag{69}$$

Consider the initial and final position of a plate element given by $abcd$ parallel to the middle plane with sides ab and ad parallel to x and y axes, respectively, at a distance z from the middle plane (Figure 11).

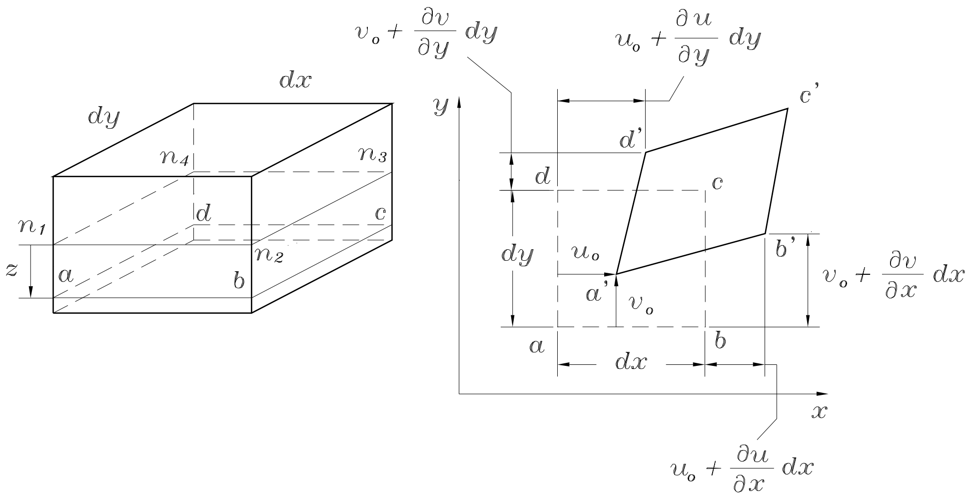

Figure 11: Deformation in a plate element.

Assuming that, during plate bending, points a, b, c, and d, move to a', b', c', and d', calling u_o and v_o displacement components of point a in x and y direction (Figure 11), respectively, the displacement of a point b in the x direction is given by:

$$b'_x - b_x = u_o + \frac{\partial u}{\partial x} dx. \tag{70}$$

So, the increment in the length dx in x direction is given by:

$$\Delta dx = \frac{\partial u}{\partial x} dx, \tag{71}$$

and strain in x direction is given by:

$$\varepsilon_x = \frac{\Delta dx}{dx} = \frac{\partial u}{\partial x}. \tag{72}$$

In a similar way, we can write:

$$\varepsilon_y = \frac{\partial v}{\partial y}, \tag{73}$$

$$\gamma_{xy} = \frac{\partial u}{\partial y} + \frac{\partial v}{\partial x}. \tag{74}$$

Figure 12 shows initial and final positions of a plate section, parallel to xz plane, which contains points a, b, n_1, and n_2. The rotation of element an_1, initially placed in vertical position, is equal to $\frac{\partial w}{\partial x}$ (Figure 12). So, the displacement of a point in x direction, at a distance z from middle surface can be written as:

$$u = -z\frac{\partial w}{\partial x}. \tag{75}$$

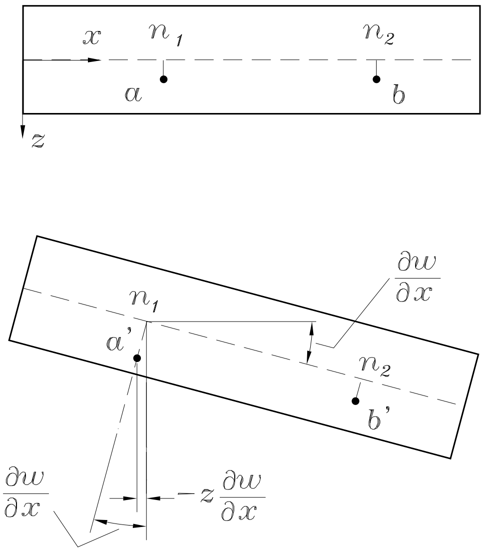

Figure 12: Initial and final position of an element plate abn_1n_2.

Following similar procedure, the displacement of a point in y direction is given by:

$$v = -z\frac{\partial w}{\partial y}. \tag{76}$$

Substituting equations (75) and (76) into equations (72), (73), and (74), we can write:

$$\begin{aligned} \varepsilon_x &= -z\frac{\partial^2 w}{\partial x^2}, \\ \varepsilon_y &= -z\frac{\partial^2 w}{\partial x^2}, \\ \gamma_{xy} &= -2z\frac{\partial^2 w}{\partial x \partial y}. \end{aligned} \tag{77}$$

The constitutive equations for anisotropic material is given by (Lekhnitskii Lekhnitskii [1968]):

$$\begin{aligned} \varepsilon_x &= a_{11}\sigma_x + a_{12}\sigma_y + a_{16}\tau_{xy}, \\ \varepsilon_y &= a_{12}\sigma_x + a_{22}\sigma_y + a_{26}\tau_{xy}, \\ \gamma_{xy} &= a_{16}\sigma_x + a_{26}\sigma_y + a_{66}\tau_{xy}. \end{aligned} \tag{78}$$

Substituting equations (77) into equations (78), we obtain:

$$\begin{aligned}
\sigma_x &= -z\left(B_{11}\frac{\partial^2 w}{\partial x^2}+B_{12}\frac{\partial^2 w}{\partial y^2}+2B_{16}\frac{\partial^2 w}{\partial x\partial y}\right),\\
\sigma_y &= -z\left(B_{12}\frac{\partial^2 w}{\partial x^2}+B_{22}\frac{\partial^2 w}{\partial y^2}+2B_{26}\frac{\partial^2 w}{\partial x\partial y}\right),\\
\tau_{xy} &= -z\left(B_{16}\frac{\partial^2 w}{\partial x^2}+B_{26}\frac{\partial^2 w}{\partial y^2}+2B_{66}\frac{\partial^2 w}{\partial x\partial y}\right),
\end{aligned} \tag{79}$$

where B_{ij} are constants given by:

$$\begin{aligned}
B_{11} &= \frac{1}{\Delta}\left(a_{22}a_{66}-a_{26}^2\right), & B_{22} &= \frac{1}{\Delta}\left(a_{11}a_{66}-a_{16}^2\right),\\
B_{12} &= \frac{1}{\Delta}\left(a_{16}a_{26}-a_{12}a_{66}\right), & B_{66} &= \frac{1}{\Delta}\left(a_{11}a_{22}-a_{12}^2\right),\\
B_{16} &= \frac{1}{\Delta}\left(a_{12}a_{26}-a_{22}a_{16}\right), & B_{26} &= \frac{1}{\Delta}\left(a_{12}a_{16}-a_{11}a_{26}\right),
\end{aligned} \tag{80}$$

and

$$\Delta = \begin{vmatrix} a_{11} & a_{12} & a_{16}\\ a_{12} & a_{22} & a_{26}\\ a_{16} & a_{26} & a_{66}\end{vmatrix}. \tag{81}$$

Substituting equation (79) into equation (77) and integrating, we have:

$$\begin{aligned}
m_x &= -\left(D_{11}\frac{\partial^2 w}{\partial x^2}+D_{12}\frac{\partial^2 w}{\partial y^2}+2D_{16}\frac{\partial^2 w}{\partial x\partial y}\right),\\
m_y &= -\left(D_{12}\frac{\partial^2 w}{\partial x^2}+D_{22}\frac{\partial^2 w}{\partial y^2}+2D_{26}\frac{\partial^2 w}{\partial x\partial y}\right),\\
m_{xy} &= -\left(D_{16}\frac{\partial^2 w}{\partial x^2}+D_{26}\frac{\partial^2 w}{\partial y^2}+2D_{66}\frac{\partial^2 w}{\partial x\partial y}\right),
\end{aligned} \tag{82}$$

where

$$D_{ij} = B_{ij}\frac{t^3}{12}. \tag{83}$$

Substituting equation (82) into equations (67) and (68), we can write:

$$\begin{aligned}
q_x &= \left[D_{11}\frac{\partial^3 w}{\partial x^3}+3D_{16}\frac{\partial^3 w}{\partial x^2\partial y}+(D_{12}+2D_{66})\frac{\partial^3 w}{\partial x\partial y^2}+D_{26}\frac{\partial^3 w}{\partial y^3}\right],\\
q_y &= \left[D_{16}\frac{\partial^3 w}{\partial x^3}+(D_{12}+2D_{66})\frac{\partial^3 w}{\partial x^2\partial y}+3D_{26}\frac{\partial^3 w}{\partial x\partial y^2}+D_{22}\frac{\partial^3 w}{\partial y^3}\right].
\end{aligned} \tag{84}$$

Equation (69) can be rewritten using equations (82) as:

$$D_{11}\frac{\partial^4 w}{\partial x^4}+4D_{16}\frac{\partial^4 w}{\partial x^3\partial y}+2(D_{12}+D_{66})\frac{\partial^4 w}{\partial x^2\partial y^2}+4D_{26}\frac{\partial^4 w}{\partial x\partial y^3}+D_{22}\frac{\partial^4 w}{\partial y^4}=g. \quad (85)$$

General solution to w in equation (85) depends on μ_1, μ_2, $\bar{\mu}_1$, and $\bar{\mu}_2$ roots of characteristic equation given by:

$$D_{22}\mu^4+4D_{26}\mu^3+2(D_{12}+2D_{66})\mu^2+4D_{16}\mu+D_{11}=0. \quad (86)$$

Roots of this equation, as shown by Lekhnitskii Lekhnitskii [1968], are always complex for homogeneous material. The complex roots $\mu_1 = d_1 + e_1 i$ and $\mu_2 = d_2 + e_2 i$ are known as deflexion complex parameters. In general, these roots are different complex numbers.

A general expression for the deflexion has the form:

1. in case of different complex parameters ($\mu_1 \neq \mu_2$):

$$w = w_o + 2\mathrm{Re}[w_1(z_1) + w_2(z_2)]. \quad (87)$$

2. in case of equal complex parameters ($\mu_1 = \mu_2$):

$$w = w_o + 2\mathrm{Re}[w_1(z_1) + \bar{z}_1 w_2(z_1)]. \quad (88)$$

where w_o is a particular solution of equation (85) that depends on the distributed load q in the plate surface, $w_1(z_1)$ and $w_2(z_2)$ are arbitrary analytic functions of complex variable $z_1 = x + \mu_1 y$ and $z_2 = x + \mu_2 y$.

Based on equations (82) and (84), general expressions for forces and moments can be obtained as (for the case $\mu_1 \neq \mu_2$):

$$\begin{aligned}
m_x &= m_x^o - 2\mathrm{Re}[p_1 w''(z_1) + p_2 w''(z_2)],\\
m_y &= m_y^o - 2\mathrm{Re}[q_1 w''(z_1) + q_2 w''(z_2)],\\
m_{xy} &= m_{xy}^o - 2\mathrm{Re}[r_1 w''(z_1) + r_2 w''(z_2)],\\
q_x &= q_x^o - 2\mathrm{Re}[\mu_1 s_1 w'''(z_1) + \mu_2 s_2 w'''(z_2)],\\
q_y &= q_y^o - 2\mathrm{Re}[s_1 w'''(z_1) + s_2 w'''(z_2)]. \quad (89)
\end{aligned}$$

where m_x^o, m_y^o, m_{xy}^o, q_x^o, and q_y^o are moments and shear forces corresponding to function w_o computed from equations (82) and (84). The other constants are given by:

$$p_1 = D_{11} + D_{12}\mu_1^2 + 2D_{16}\mu_1, \qquad p_2 = D_{11} + D_{12}\mu_2^2 + 2D_{16}\mu_2,$$

$$q_1 = D_{12} + D_{22}\mu_1^2 + 2D_{26}\mu_1, \qquad q_2 = D_{12} + D_{22}\mu_2^2 + 2D_{26}\mu_2,$$

$$r_1 = D_{16} + D_{26}\mu_1^2 + 2D_{66}\mu_1, \qquad p_2 = D_{16} + D_{26}\mu_2^2 + 2D_{66}\mu_2,$$

$$s_1 = \frac{D_{11}}{\mu_1} + 3D_{16} + D_{12} + D_{66}\mu_1 + D_{26}\mu_1^2, \tag{90}$$

$$s_2 = \frac{D_{11}}{\mu_2} + 3D_{16} + D_{12} + D_{66}\mu_2 + D_{26}\mu_2^2,$$

$$s_1 - r_1 = \frac{p_1}{\mu_1}, \qquad s_2 - r_2 = \frac{p_2}{\mu_2},$$

$$s_1 + r_1 = -q_1\mu_1, \qquad s_2 + r_2 = -q_2\mu_2.$$

Similar expressions can be obtained for the case where $\mu_1 = \mu_2$. However, this case will not be shown in this work as in general anisotropic problems μ_1 is different from μ_2.

3.2 Computation of bending stiffness in an arbitrary direction

Considering that stiffness bending constants of a plate in a x, y, z coordinate system are given by D_{ij} $(i, j = 1, 2, 6)$ and in a x', y', z' coordinate system, rotated α with respect to the first coordinate system, are given by D'_{ij} $(i, j = 1, 2, 6)$, the equation relating these constants, as shown by Lekhnitskii Lekhnitskii [1968], are given by:

$$D'_{11} = D_{11}\cos^4\phi + 2(D_{12} + 2D_{66})\sin^2\phi\cos^2\phi + D_{22}\sin^4\phi +$$
$$2(D_{16}\cos^2\phi + D_{26}\sin^2\phi)\sin 2\phi, \tag{91}$$

$$D'_{22} = D_{11}\sin^4\phi + 2(D_{12} + 2D_{66})\sin^2\phi\cos^2\phi + D_{22}\cos^4\phi +$$
$$2(D_{16}\sin^2\phi + D_{26}\cos^2\phi)\sin 2\phi, \tag{92}$$

$$D'_{12} = D_{12} + [D_{11} + D_{22} - 2(D_{12} + 2D_{66})]\sin^2\phi\cos^2\phi +$$
$$(D_{26} - D_{16})\cos 2\phi\sin 2\phi, \tag{93}$$

$$D'_{66} = D_{66} + [D_{11} + D_{22} - 2(D_{12} + 2D_{66})] \sin^2\phi \cos^2\phi +$$

$$(D_{26} - D_{16}) \cos 2\phi \sin 2\phi, \tag{94}$$

$$D'_{16} = \frac{1}{2}[D_{22} \sin^2\phi - D_{11} \cos^2\phi + (D_{12} + 2D_{66}) \cos 2\phi] \sin 2\phi +$$

$$D_{16} \cos^2\phi(\cos^2\phi - 3\sin^2\phi) + D_{26} \sin^2\phi(3\cos^2\phi - \sin^2\phi), \tag{95}$$

$$D'_{26} = \frac{1}{2}[D_{22} \cos^2\phi - D_{11} \sin^2\phi + (D_{12} + 2D_{66}) \cos 2\phi] \sin 2\phi +$$

$$D_{16} \sin^2\phi(\cos^2\phi - 3\sin^2\phi) + D_{26} \cos^2\phi(3\cos^2\phi - \sin^2\phi). \tag{96}$$

The stress components σ_n and τ_{ns}, normal and shear stress, respectively, are related with stress σ_x, σ_y, and τ_{xy} by:

$$\sigma_n = \sigma_x \cos^2\alpha + \sigma_y \sin^2\alpha + 2\tau_{xy} \sin\alpha \cos\alpha, \tag{97}$$

$$\tau_{ns} = (\sigma_y - \sigma_x) \sin\alpha \cos\alpha + \tau_{xy}(\cos^2\alpha - \sin^2\alpha). \tag{98}$$

The components of moment, initially written considering axis x and y, can now be rewritten in a generic coordinate system n, s (Paiva Paiva [1987]). The bending moments referring to directions n and s are given by:

$$m_n = m_x \cos^2\alpha + m_y \sin^2\alpha + 2m_{xy} \sin\alpha \cos\alpha, \tag{99}$$

$$m_{ns} = (m_y - m_x) \sin\alpha \cos\alpha + m_{xy}(\cos^2\alpha - \sin^2\alpha). \tag{100}$$

Similarly, q_n, the shear force in the n axis, can be written as:

$$q_n ds = q_x ds \cos\alpha + q_y ds \sin\alpha, \tag{101}$$

or

$$q_n = q_x \cos\alpha + q_y \sin\alpha. \tag{102}$$

In order to solve the plate differential equation (85), it is necessary to impose boundary conditions to displacement w and its derivative $\partial w/\partial n$. Kirchhoff Kirchhoff [1950] has shown that the boundary conditions of shear force q_n and twisting moment m_{ns} can be written as one single boundary condition given by:

$$V_n = q_n + \frac{\partial m_{ns}}{\partial s}. \tag{103}$$

The other loading boundary condition is the moment m_n.

3.3 Boundary element method for bending problems of anisotropic plates

3.3.1 Boundary integral equations

Using Betti theorem, we can relate two states of stress-deformation of a linear material as:

$$\int_{\Omega} \sigma_{ij}^{*}\varepsilon_{ij}d\Omega = \int_{\Omega} \sigma_{ij}\varepsilon_{ij}^{*}d\Omega. \tag{104}$$

Writing the right hand side of equation (104) in von Karman's notation, we have:

$$\int_{\Omega} \sigma_{ij}\varepsilon_{ij}^{*}d\Omega = \int_{\Omega} \left(\sigma_x\varepsilon_x^{*} + \sigma_y\varepsilon_y^{*} + \sigma_z\varepsilon_z^{*} + \tau_{xy}\gamma_{xy}^{*} + \tau_{xz}\gamma_{xz}^{*} + \tau_{yz}\gamma_{yz}^{*}\right) d\Omega. \tag{105}$$

Neglecting stresses normal to the plate, equation (105) is given by:

$$\int_{\Omega} \sigma_{ij}\varepsilon_{ij}^{*}d\Omega = \int_{\Omega} \left(\sigma_x\varepsilon_x^{*} + \sigma_y\varepsilon_y^{*} + \tau_{xy}\gamma_{xy}^{*}\right) d\Omega. \tag{106}$$

Substituting equations (77) and (78) into equation (106), we can write the first term of the integral in the right hand side of equation (106) as:

$$\int_{\Omega} \sigma_x\varepsilon_x^{*}d\Omega = \int_{\Omega} \left[\int_z \left(B_{11}\frac{\partial^2 w}{\partial x^2} + B_{12}\frac{\partial^2 w}{\partial y^2} + 2B_{16}\frac{\partial^2 w}{\partial x\partial y}\right)\left(z\frac{\partial^2 w}{\partial x^2}\right) dz\right] d\Omega. \tag{107}$$

Integrating (107) throughout the thickness of the plate, we have:

$$\int_{\Omega} \sigma_x\varepsilon_x^{*}d\Omega = \int_{\Omega} \left(D_{11}\frac{\partial^2 w}{\partial x^2} + D_{12}\frac{\partial^2 w}{\partial y^2} + 2D_{16}\frac{\partial^2 w}{\partial x\partial y}\right)\frac{\partial^2 w}{\partial x^2}d\Omega = -\int_{\Omega} m_x\frac{\partial^2 w}{\partial x^2}d\Omega. \tag{108}$$

In order to obtain equations of the boundary element method, it is necessary to transform domain integrals into boundary integrals.

Consider two functions $f(x)$ and $g(x)$. The derivative of their product can be written as:

$$\frac{\partial}{\partial x}[f(x)g(x)] = \frac{\partial f(x)}{\partial x}g(x) + \frac{\partial g(x)}{\partial x}f(x). \tag{109}$$

Using the derivative property (109) in equation (108), we can write:

$$\int_{\Omega} \sigma_x\varepsilon_x^{*}d\Omega = -\int_{\Omega} \left[\frac{\partial}{\partial x}\left(m_x\frac{\partial w^{*}}{\partial x}\right) - \frac{\partial w^{*}}{\partial x}\frac{\partial m_x}{\partial x}\right] d\Omega. \tag{110}$$

Using Green theorem, equation (110) can be written as:

$$\int_{\Omega} \sigma_x\varepsilon_x^{*}d\Omega = -\int_{\Gamma} m_x\frac{\partial w^{*}}{\partial x}\cos\alpha d\Gamma + \int_{\Omega} \frac{\partial w^{*}}{\partial x}\frac{\partial m_x}{\partial x}d\Omega. \tag{111}$$

Applying the derivative property (109) in the second right hand side term of equation (111), we have:

$$\int_\Omega \sigma_x \varepsilon_x^* d\Omega = -\int_\Gamma m_x \frac{\partial w^*}{\partial x} \cos\alpha d\Gamma + \int_\Omega \left[\frac{\partial}{\partial x} \left(w^* \frac{\partial m_x}{\partial x} \right) - w^* \frac{\partial^2 m_x}{\partial x^2} \right] d\Omega. \quad (112)$$

After using Green theorem, we can write:

$$\int_\Omega \sigma_x \varepsilon_x^* d\Omega = \int_\Gamma \left(-m_x \frac{\partial w^*}{\partial x} \cos\alpha + w^* \frac{\partial m_x}{\partial x} \cos\alpha \right) d\Gamma - \int_\Omega w^* \frac{\partial^2 m_x}{\partial x^2} d\Omega. \quad (113)$$

Following similar procedure, we can show that:

$$\int_\Omega \sigma_y \varepsilon_y^* d\Omega = \int_\Gamma \left(-m_y \frac{\partial w^*}{\partial y} \sin\alpha + w^* \frac{\partial m_y}{\partial y} \sin\alpha \right) d\Gamma - \int_\Omega w^* \frac{\partial^2 m_y}{\partial y^2} d\Omega, \quad (114)$$

and

$$\int_\Omega \tau_{xy} \gamma_{xy}^* d\Omega = \int_\Gamma \left(-m_{xy} \frac{\partial w^*}{\partial y} \cos\alpha - m_{xy} \frac{\partial w^*}{\partial x} \sin\alpha + w^* \frac{\partial m_{xy}}{\partial x} \sin\alpha + \right.$$
$$\left. w^* \frac{\partial m_{xy}}{\partial y} \cos\alpha \right) d\Gamma - \int_\Omega 2w^* \frac{\partial^2 m_{xy}}{\partial x \partial y} d\Omega. \quad (115)$$

Thus, equation (106) is written as:

$$\int_\Omega \sigma_{ij} \varepsilon_{ij}^* d\Omega = -\int_\Gamma \left(m_x \frac{\partial w^*}{\partial x} \cos\alpha + m_y \frac{\partial w^*}{\partial y} \sin\alpha + m_{xy} \frac{\partial w^*}{\partial y} \cos\alpha + \right.$$
$$\left. m_{xy} \frac{\partial w^*}{\partial x} \sin\alpha \right) d\Gamma + \int_\Gamma w^* \left[\cos\alpha \left(\frac{\partial m_x}{\partial x} + \frac{\partial m_{xy}}{\partial y} \right) \sin\alpha \left(\frac{\partial m_y}{\partial y} + \frac{\partial m_{xy}}{\partial x} \right) \right] d\Gamma -$$
$$\int_\Omega w^* \left(\frac{\partial^2 m_x}{\partial x^2} + 2\frac{\partial^2 m_{xy}}{\partial x \partial y} + \frac{\partial^2 m_y}{\partial y^2} \right) d\Omega. \quad (116)$$

Substituting equations (67) and (68) and using equation (102), equation (116) can be written as:

$$\int_\Omega \sigma_{ij} \varepsilon_{ij}^* d\Omega = -\int_\Gamma \left(m_x \frac{\partial w^*}{\partial x} \cos\alpha + m_y \frac{\partial w^*}{\partial y} \sin\alpha + m_{xy} \frac{\partial w^*}{\partial y} \cos\alpha + \right.$$
$$\left. m_{xy} \frac{\partial w^*}{\partial x} \sin\alpha \right) d\Gamma + \int_\Gamma w^* q_n d\Gamma + \int_\Omega g w^* d\Omega. \quad (117)$$

From the relation between two coordinate systems (x, y) and (n, s), we have:

$$\frac{\partial w^*}{\partial x} = \frac{\partial w^*}{\partial n} \cos\alpha - \frac{\partial w^*}{\partial s} \sin\alpha,$$
$$\frac{\partial w^*}{\partial y} = \frac{\partial w^*}{\partial n} \sin\alpha + \frac{\partial w^*}{\partial s} \cos\alpha. \quad (118)$$

Substituting equations (118) into equation (117), we have:

$$\int_\Omega \sigma_{ij}\varepsilon^*_{ij}d\Omega = -\int_\Gamma \left[m_x\cos\alpha\left(\frac{\partial w^*}{\partial n}\cos\alpha - \frac{\partial w^*}{\partial s}\sin\alpha\right) + \right.$$
$$m_y\sin\alpha\left(\frac{\partial w^*}{\partial n}\sin\alpha + \frac{\partial w^*}{\partial s}\cos\alpha\right) + m_{xy}\cos\alpha\left(\frac{\partial w^*}{\partial n}\sin\alpha + \frac{\partial w^*}{\partial s}\cos\alpha\right) +$$
$$\left. m_{xy}\sin\alpha\left(\frac{\partial w^*}{\partial n}\cos\alpha - \frac{\partial w^*}{\partial s}\sin\alpha\right)\right] d\Gamma + \int_\Gamma w^* q_n d\Gamma + \int_\Omega g w^* d\Omega. \qquad (119)$$

After some algebraic manipulations, equation (119) can be rewritten as:

$$\int_\Omega \sigma_{ij}\varepsilon^*_{ij}d\Omega = -\int_\Gamma \left\{\frac{\partial w^*}{\partial n}\left(m_x\cos^2\alpha + m_y\sin^2\alpha + 2m_{xy}\sin\alpha\cos\alpha\right) + \right.$$
$$\left.\frac{\partial w^*}{\partial s}\left[m_{xy}\left(\cos^2\alpha - \sin^2\alpha\right) + (m_y - m_x)\sin\alpha\cos\alpha\right]\right\} d\Gamma +$$
$$\int_\Gamma w^* q_n d\Gamma + \int_\Omega g w^* d\Omega. \qquad (120)$$

Substituting equations (99) and (100) into equation (120), we have:

$$\int_\Omega \sigma_{ij}\varepsilon^*_{ij}d\Omega = -\int_\Gamma \left(m_n\frac{\partial w^*}{\partial n} + m_{ns}\frac{\partial w^*}{\partial s} - q_n w^*\right) d\Gamma + \int_\Omega g w^* d\Omega. \qquad (121)$$

Computing the second term of the first integral in the right hand side of equation (121), we have:

$$\int_\Gamma m_{ns}\frac{\partial w^*}{\partial s}d\Gamma = m_{ns}w^*\Big|_{\Gamma_1}^{\Gamma_2} - \int_\Gamma \frac{\partial m_{ns}}{\partial s}w^* d\Gamma, \qquad (122)$$

where Γ_1 and Γ_2 are coordinates of ends of the boundary where the integration is being carried out.

In the case of a closed boundary without corner, i.e., the function that describes the boundary curve and its derivative are continuous, the first term in the right hand side of equation (122) vanishes. In the case where there are corners, equation (122) can be written as:

$$\int_\Gamma m_{ns}\frac{\partial w^*}{\partial s}d\Gamma = -\sum_{i=1}^{N_c} R_{c_i} w^*_{c_i} - \int_\Gamma \frac{\partial m_{ns}}{\partial s}w^* d\Gamma, \qquad (123)$$

where

$$R_{c_i} = m^+_{ns_i} - m^-_{ns_i}, \qquad (124)$$

and the terms w_{c_i}, $m^+_{ns_i}$, $m^-_{ns_i}$ are values of displacements and twisting moments after and before the i corner of the plate, N_c are the total number of boundary corners (Paiva Paiva [1987]).

From equation (121) and (123), we can write:

$$\int_\Omega \sigma_{ij}\varepsilon^*_{ij} d\Omega = \int_\Gamma \left(q_n w^* - m_n \frac{\partial w^*}{\partial n} + \frac{\partial m_{ns}}{\partial s} w^* \right) d\Gamma + \sum_{i=1}^{N_c} R_{c_i} w^*_{c_i} + \int_\Omega g w^* d\Omega. \quad (125)$$

From equations (125) and (103), we have:

$$\int_\Omega \sigma_{ij}\varepsilon^*_{ij} d\Omega = \int_\Gamma \left(V_n w^* - m_n \frac{\partial w^*}{\partial n} \right) d\Gamma + \sum_{i=1}^{N_c} R_{c_i} w^*_{c_i} + \int_\Omega g w^* d\Omega. \quad (126)$$

Following a similar procedure to that used to obtain equation (126), the left hand side of equation (104) can be written as:

$$\int_\Omega \sigma^*_{ij}\varepsilon_{ij} d\Omega = \int_\Gamma \left(V^*_n w - m_n \frac{\partial w^*}{\partial n} \right) d\Gamma + \sum_{i=1}^{N_c} R^*_{c_i} w_{c_i} + \int_\Omega g^* w d\Omega. \quad (127)$$

Substituting equations (126) and (127) into equation (104), we can write:

$$\int_\Gamma \left(V_n w^* - m_n \frac{\partial w^*}{\partial n} \right) d\Gamma + \sum_{i=1}^{N_c} R_{c_i} w^*_{c_i} + \int_\Omega g w^* d\Omega =$$
$$\int_\Gamma \left(V^*_n w - m^*_n \frac{\partial w}{\partial n} \right) d\Gamma + \sum_{i=1}^{N_c} R^*_{c_i} w_{c_i} + \int_\Omega g^* w d\Omega. \quad (128)$$

Equation (128) relates two states of an elastic material. In order to apply this equation to solve bending problems, we need to consider one of states as known and other as the state which stands for the problem which we want to analyse. To obtain a boundary integral equation, the known state is chosen so that the domain integral given by

$$\int_\Omega g^* w d\Omega \quad (129)$$

vanishes. Using the properties of Dirac delta function $\delta(P,Q)$, so that integral $g^* = \delta(P,q)$, integral (129) is written as:

$$\int_\Omega \delta(P,Q) w(P) d\Omega(P) = w(Q), \quad (130)$$

where Q is the point where the load is applied, known as source point, and P is the point where the deflexion is observed, known as field point.

The state corresponding to a linear material under loading of a Dirac delta function is known as fundamental state and the variables of equation (128) related to this state (w^*, V^*_n and m^*_n) are known as fundamental solutions which are computed analytically from the differential equation (85).

Considering the state ”*” as the fundamental state, equation (128) can be written as:

$$Kw(Q) + \int_{\Gamma} \left[V_n^*(Q,P)w(P) - m_n^*(Q,P)\frac{\partial w(P)}{\partial n} \right] d\Gamma(P) + \sum_{i=1}^{N_c} R_{c_i}^*(Q,P)w_{c_i}(P) -$$
$$\int_{\Gamma} \left[V_n(P)w^*(Q,P) - m_n(P)\frac{\partial w^*}{\partial n}(Q,P) \right] d\Gamma(P) + \sum_{i=1}^{N_c} R_{c_i}(P)w_{c_i}^*(Q,P) +$$
$$\int_{\Omega} g(P)w^*(Q,P)d\Omega. \tag{131}$$

The constant K is introduced in order to consider that the Dirac delta function can be applied in the domain, in the boundary, or outside the domain. If the Dirac delta function is applied in a point where the boundary is smooth, than $K = 1/2$.

Variables of equation (131) are displacements $w(P)$, rotations $\partial w(P)/\partial n$, moments $m_n(P)$, and loads $V_n(P)$. For a given boundary condition, some of these variables are known. In order to have an equal number of equations and unknown variables, it is necessary to write an integral equation corresponding to the derivative of displacement $w(q)$ in relation to a cartesian coordinate system fixed in the source point, i.e., the point where the Dirac delta of the fundamental state is applied. The axis directions of this coordinate system are coincident with normal and tangent to the boundary directions in the source point.

For a particular case where the source point is placed in a point where the boundary is smooth, the boundary equation is given by (Paiva Paiva [1987]):

$$\frac{1}{2}\frac{\partial w(Q)}{\partial n_1} + \int_{\Gamma} \left[\frac{\partial V^*}{\partial n_1}(Q,P)w(P) - \frac{\partial m_n^*}{\partial n_1}(Q,P)\frac{\partial w}{\partial n}(P) \right] d\Gamma(P) +$$
$$\sum_{i=1}^{N_c} \frac{\partial R_{c_i}^*}{\partial n_1}(Q,P)w_{c_i}(P) = \int_{\Gamma} \left\{ V_n(P)\frac{\partial w^*}{\partial n_1}(Q,P) - m_n(P)\frac{\partial}{\partial n_1}\left[\frac{\partial w^*}{\partial n}(Q,P) \right] \right\} d\Gamma(P) +$$
$$\sum_{i=1}^{N_c} R_{c_i}(P)\frac{\partial w_{c_i}^*}{\partial n_1}(Q,P) + \int_{\Omega} g(P)\frac{\partial w^*}{\partial n_1}(Q,P)d\Omega. \tag{132}$$

It is important to say that it is possible to use only equation (131) in a boundary element formulation by using as source points the boundary nodes and an equal number of points external to the domain of the problem.

3.4 Fundamental solutions for bending problems in anisotropic materials

The fundamental solution is an essential part of the boundary element method. Fundamental solutions for anisotropic plates utilize complex variable theory following groundwork laid by Lekhnitskii Lekhnitskii [1968]. Mossakowski Mossakowski [1955] presented a solution for a point force on an infinite plate using complex parameters of the firs kind, and Suchar Suchar [1964] presented the solutions for a point force and point moment in terms of complex parameters of second kind. Lamattina Lamattina [1997] derived a more general solution for the point force using the same mapping functions as

Mossakowski Mossakowski [1955]. Lamatina *et al.* Lamattina et al. [1998] presented a comparison between three fundamental solutions and discussed the differences between these solutions.

The transversal displacement plate bending fundamental solution is computed by placing the non-homogeneous term of the differential equation (85) equal to a concentrated force given by a Dirac delta function $\delta(Q,P)$, i.e.,

$$\Delta\Delta w^*(Q,P) = \delta(Q,P), \tag{133}$$

where $\Delta\Delta(.)$ is the differential operator:

$$\Delta\Delta(.) = \frac{D_{11}}{D_{22}}\frac{\partial^4(.)}{\partial x^4} + 4\frac{D_{16}}{D_{22}}\frac{\partial^4(.)}{\partial^3 \partial y} + \frac{2(D_{12}+2D_{66})}{D_{22}}\frac{\partial^4(.)}{\partial x^2 \partial y^2} + 4\frac{D_{26}}{D_{22}}\frac{\partial^4(.)}{\partial x \partial y^3} + \frac{\partial^4(.)}{\partial y^4}. \tag{134}$$

As shown by Shi and Bezine [1988], the transversal displacement fundamental solution is given by:

$$w^*(\rho,\theta) = \frac{1}{8\pi}\left\{C_1 R_1(\rho,\theta) + C_2 R_2(\rho,\theta) + C_3\left[S_1(\rho,\theta) - S_2(\rho,\theta)\right]\right\}, \tag{135}$$

where

$$\rho = [(x-x_o)^2 + (y-y_o)^2]^{1/2}, \tag{136}$$

x and y are the coordinates of the field point P, x_o and y_o are coordinates of the source point Q,

$$\theta = \arctan\frac{y-y_o}{x-x_o}, \tag{137}$$

$$C_1 = \frac{(d_1-d_2)^2 - (e_1^2 - e_2^2)}{GHe_1}, \tag{138}$$

$$C_2 = \frac{(d_1-d_2)^2 + (e_1^2 - e_2^2)}{GHe_2}, \tag{139}$$

$$C_3 = \frac{4(d_1-d_2)}{GH}, \tag{140}$$

$$G = (d_1-d_2)^2 + (e_1+e_2)^2, \tag{141}$$

$$H = (d_1-d_2)^2 + (e_1-e_2)^2, \tag{142}$$

$$
\begin{aligned}
R_i &= \rho^2 \left[(\cos\theta + d_i \sin\theta)^2 - e_i^2 \sin^2\theta\right] \times \\
&\left\{ \log\left[\frac{\rho^2}{a^2}\left((\cos\theta + d_i \sin\theta)^2 + e_i^2 \sin^2\theta\right)\right] - 3 \right\} - \\
&4\rho^2 e_i \sin\theta \left(\cos\theta + d_i \sin\theta\right) \arctan\frac{e_i \sin\theta}{\cos\theta + d_i \sin\theta}, \qquad (143)
\end{aligned}
$$

and

$$
\begin{aligned}
S_i &= \rho^2 e_i \sin\theta \left(\cos\theta + d_i \sin\theta\right) \times \\
&\left\{ \log\left[\frac{\rho^2}{a^2}\left((\cos\theta + d_i \sin\theta)^2 + e_i^2 \sin^2\theta\right)\right] - 3 \right\} + \\
&\rho^2 \left[(\cos\theta + d_i \sin\theta)^2 - e_i^2 \sin^2\theta\right] \arctan\frac{e_i \sin\theta}{\cos\theta + d_i \sin\theta}. \qquad (144)
\end{aligned}
$$

The repeated index i in the terms of R_i and S_i does not imply summation. The coefficient a is an arbitrary constant taken as $a = 1$.

Other fundamental solutions are given by:

$$
m_n^* = -\left(f_1 \frac{\partial^2 w^*}{\partial x^2} + f_2 \frac{\partial^2 w^*}{\partial x \partial y} + f_3 \frac{\partial^2 w^*}{\partial y^2} \right), \qquad (145)
$$

$$
R_{c_i}^* = -\left(g_1 \frac{\partial^2 w^*}{\partial x^2} + g_2 \frac{\partial^2 w^*}{\partial x \partial y} + g_3 \frac{\partial^2 w^*}{\partial y^2} \right), \qquad (146)
$$

$$
\begin{aligned}
V_n^* &= -\left(h_1 \frac{\partial^3 w^*}{\partial x^3} + h_2 \frac{\partial^3 w^*}{\partial x^2 \partial y} + h_3 \frac{\partial^3 w^*}{\partial x \partial y^2} + h_4 \frac{\partial^3 w^*}{\partial y^3} \right) - \\
&\frac{1}{\bar{R}} \left(h_5 \frac{\partial^2 w^*}{\partial x^2} + h_6 \frac{\partial^2 w^*}{\partial x \partial y} + h_7 \frac{\partial^2 w^*}{\partial y^2} \right). \qquad (147)
\end{aligned}
$$

where $\bar{R}$ is the curvature radius at a smooth point of the boundary Γ. Other constants are defined as:

$$f_1 = D_{11}n_x^2 + 2D_{16}n_xn_y + D_{12}n_y^2, \tag{148}$$

$$f_2 = 2(D_{16}n_x^2 + 2D_{66}n_xn_y + D_{26}n_y^2), \tag{149}$$

$$f_3 = D_{12}n_x^2 + 2D_{26}n_xn_y + D_{22}n_y^2, \tag{150}$$

$$g_1 = (D_{12} - D_{11})\cos\beta\sin\beta + D_{16}(\cos^2\beta - \sin^2\beta), \tag{151}$$

$$g_2 = 2(D_{26} - D_{16})\cos\beta\sin\beta + 2D_{66}(\cos^2\beta - \sin^2\beta), \tag{152}$$

$$g_3 = (D_{22} - D_{12})\cos\beta\sin\beta + D_{26}(\cos^2\beta - \sin^2\beta), \tag{153}$$

$$h_1 = D_{11}n_x(1 + n_y^2) + 2D_{16}n_y^3 - D_{12}n_xn_y^2, \tag{154}$$

$$h_2 = 4D_{16}n_x + D_{12}n_y(1 + n_x^2) + 4D_{66}n_y^3 - D_{11}n_x^2n_y - 2D_{26}n_xn_y^2, \tag{155}$$

$$h_3 = 4D_{26}n_y + D_{12}n_x(1 + n_y^2) + 4D_{66}n_x^3 - D_{22}n_xn_y^2 - 2D_{16}n_x^2n_y, \tag{156}$$

$$h_4 = D_{22}n_y(1 + n_x^2) + 2D_{26}n_x^3 - D_{12}n_x^2n_y, \tag{157}$$

$$h_5 = (D_{12} - D_{11})\cos 2\beta - 4D_{16}\sin 2\beta, \tag{158}$$

$$h_6 = 2(D_{26} - D_{16})\cos 2\beta - 4D_{66}\sin 2\beta, \tag{159}$$

$$h_7 = (D_{22} - D_{12})\cos 2\beta - 4D_{26}\sin 2\beta, \tag{160}$$

and β is the angle between the global coordinate system xy and a coordinate system ns in which their axis directions are parallels to vectors $\mathbf{n}$ and $\mathbf{s}$, normal and tangent, respectively, to the boundary in the field point Q. The derivatives of the transversal displacement fundamental solution can be expressed by linear combination of derivatives of functions R_i and S_i. For example:

$$\frac{\partial^2 w^*}{\partial y^2} = \frac{1}{8\pi}\left[C_1\frac{\partial^2 R_1}{\partial y^2} + C_2\frac{\partial^2 R_2}{\partial y^2} + C_3\left(\frac{\partial^2 S_1}{\partial y^2} - \frac{\partial^2 S_2}{\partial y^2}\right)\right]. \tag{161}$$

The derivatives of R_i and S_i are given by:

$$\begin{aligned}
\frac{\partial R_i}{\partial x} &= 2r\left(\cos\theta + d_i\sin\theta\right)\left\{\log\left[\frac{r^2}{a^2}\left((\cos\theta + d_i\sin\theta)^2 + e_i^2\sin^2\theta\right)\right] - 2\right\} - \\
&\quad 4re_i\sin\theta\arctan\frac{e_i\sin\theta}{\cos\theta + d_i\sin\theta}, \qquad (162)\\
\frac{\partial R_i}{\partial y} &= 2r\left[d_i\left(\cos\theta + d_i\sin\theta\right) - e_i^2\sin\theta\right]\times \\
&\quad \left\{\log\left[\frac{r^2}{a^2}\left((\cos\theta + d_i\sin\theta)^2 + e_i^2\sin^2\theta\right)\right] - 2\right\} - \\
&\quad 4re_i\left(\cos\theta + 2d_i\sin\theta\right)\arctan\frac{e_i\sin\theta}{\cos\theta + d_i\sin\theta}, \qquad (163)\\
\frac{\partial^2 R_i}{\partial x^2} &= 2\log\left\{\frac{r^2}{a^2}\left[(\cos\theta + d_i\sin\theta)^2 + e_i^2\sin^2\theta\right]\right\} \qquad (164)\\
\frac{\partial^2 R_i}{\partial x\partial y} &= 2d_i\log\left\{\frac{r^2}{a^2}\left[(\cos\theta + d_i\sin\theta)^2 + e_i^2\sin^2\theta\right]\right\} - \\
&\quad 4e_i\arctan\frac{e_i\sin\theta}{\cos\theta + d_i\sin\theta}, \qquad (165)\\
& \qquad (166)
\end{aligned}$$

$$\begin{aligned}
\frac{\partial^2 R_i}{\partial y^2} &= 2\left(d_i^2 - e_i^2\right)\log\left\{\frac{r^2}{a^2}\left[(\cos\theta + d_i\sin\theta)^2 + e_i^2\sin^2\theta\right]\right\} - \\
&\quad 8d_ie_i\arctan\frac{e_i\sin\theta}{\cos\theta + d_i\sin\theta}, \qquad (167)\\
\frac{\partial^3 R_i}{\partial x^3} &= \frac{4\left(\cos\theta + d_i\sin\theta\right)}{r\left[(\cos\theta + d_i\sin\theta)^2 + e_i^2\sin^2\theta\right]}, \qquad (168)\\
\frac{\partial^3 R_i}{\partial x^2\partial y} &= \frac{4\left[d_i\left(\cos\theta + d_i\sin\theta\right) + e_i^2\sin\theta\right]}{r\left[(\cos\theta + d_i\sin\theta)^2 + e_i^2\sin^2\theta\right]}, \qquad (169)\\
\frac{\partial^3 R_i}{\partial x\partial y^2} &= \frac{4\left[\left(d_i^2 - e_i^2\right)\cos\theta + \left(d_i^2 + e_i^2\right)d_i\sin\theta\right]}{r\left[(\cos\theta + d_i\sin\theta)^2 + e_i^2\sin^2\theta\right]}, \qquad (170)\\
& \qquad (171)
\end{aligned}$$

$$\frac{\partial^3 R_i}{\partial y^3} = \frac{4\left[d_i\left(d_i^2-3e_i^2\right)\cos\theta+\left(d_i^4-e_i^4\right)\sin\theta\right]}{r\left[\left(\cos\theta+d_i\sin\theta\right)^2+e_i^2\sin^2\theta\right]}, \tag{172}$$

$$\frac{\partial^4 R_i}{\partial x^4} = -\frac{4\left[\left(\cos\theta+d_i\sin\theta\right)^2-e_i^2\sin^2\theta\right]}{r^2\left[\left(\cos\theta+d_i\sin\theta\right)^2+e_i^2\sin^2\theta\right]^2}, \tag{173}$$

$$\frac{\partial^4 R_i}{\partial x^3\partial y} = -\frac{4}{r^2}\left\{\frac{d_i}{\left(\cos\theta+d_i\sin\theta\right)^2+e_i^2\sin^2\theta}+\frac{2e_i^2\sin\theta\cos\theta}{\left[\left(\cos\theta+d_i\sin\theta\right)^2+e_i^2\sin^2\theta\right]^2}\right\}, \tag{174}$$

$$\frac{\partial^4 R_i}{\partial x^2\partial y^2} = -\frac{4}{r^2}\left\{\frac{\left(d_i^2+e_i^2\right)}{\left(\left(\cos\theta+d_i\sin\theta\right)^2+e_i^2\sin^2\theta\right)}-\frac{2e_i^2\cos^2\theta}{\left[\left(\cos\theta+d_i\sin\theta\right)^2+e_i^2\sin^2\theta\right]^2}\right\}, \tag{175}$$

$$\tag{176}$$

$$\frac{\partial^4 R_i}{\partial x\partial y^3} = -\frac{4}{r^2}\left\{\frac{d_i\left(d_i^2+e_i^2\right)}{\left(\left(\cos\theta+d_i\sin\theta\right)^2+e_i^2\sin^2\theta\right)}-\frac{2e_i^2\cos\theta\left(2d_i\cos\theta+\left(d_i^2+e_i^2\right)\sin\theta\right)}{\left[\left(\cos\theta+d_i\sin\theta\right)^2+e_i^2\sin^2\theta\right]^2}\right\}, \tag{177}$$

$$\frac{\partial^4 R_i}{\partial y^4} = -\frac{4}{r^2}\left\{\frac{\left(d_i^4-e_i^4\right)}{\left(\cos\theta+d_i\sin\theta\right)^2+e_i^2\sin^2\theta}-\frac{2e_i^2\cos\theta\left[\left(3d_i^2-e_i^2\right)\cos\theta+2d_i\left(d_i^2+e_i^2\right)\sin\theta\right]}{\left[\left(\cos\theta+d_i\sin\theta\right)^2+e_i^2\sin^2\theta\right]^2}\right\}, \tag{178}$$

$$\tag{179}$$

$$\begin{aligned}
\frac{\partial S_i}{\partial x} &= re_i \sin\theta \left\{ \log\left[\frac{r^2}{a^2} \left((\cos\theta + d_i \sin\theta)^2 + e_i^2 \sin^2\theta \right) \right] - 2 \right\} + \\
& 2r \left(\cos\theta + d_i \sin\theta \right) \arctan \frac{e_i \sin\theta}{\cos\theta + d_i \sin\theta}, \qquad (180) \\
\frac{\partial S_i}{\partial y} &= re_i \left(\cos\theta + 2d_i \sin\theta \right) \left\{ \log\left[\frac{r^2}{a^2} \left((\cos\theta + d_i \sin\theta)^2 + e_i^2 \sin^2\theta \right) \right] - 2 \right\} + \\
& 2r \left[d_i \left(\cos\theta + d_i \sin\theta \right) - e_i^2 \sin\theta \right] \arctan \frac{e_i \sin\theta}{\cos\theta + d_i \sin\theta}, \qquad (181) \\
\frac{\partial^2 S_i}{\partial x^2} &= 2 \arctan \frac{e_i \sin\theta}{\cos\theta + d_i \sin\theta}, \qquad (182) \\
\frac{\partial^2 S_i}{\partial x \partial y} &= e_i \log \left\{ \frac{r^2}{a^2} \left[(\cos\theta + d_i \sin\theta)^2 + e_i^2 \sin^2\theta \right] \right\} + \\
& 2d_i \arctan \frac{e_i \sin\theta}{\cos\theta + d_i \sin\theta}, \qquad (183) \\
& \qquad (184)
\end{aligned}$$

$$\begin{aligned}
\frac{\partial^2 S_i}{\partial y^2} &= 2d_i e_i \log \left\{ \frac{r^2}{a^2} \left[(\cos\theta + d_i \sin\theta)^2 + e_i^2 \sin^2\theta \right] \right\} + \\
& 2 \left(d_i^2 - e_i^2 \right) \arctan \frac{e_i \sin\theta}{\cos\theta + d_i \sin\theta}, \qquad (185) \\
\frac{\partial^3 S_i}{\partial x^3} &= -\frac{2e_i \sin\theta}{r \left[(\cos\theta + d_i \sin\theta)^2 + e_i^2 \sin^2\theta \right]}, \qquad (186) \\
\frac{\partial^3 S_i}{\partial x^2 \partial y} &= \frac{2e_i \cos\theta}{r \left[(\cos\theta + d_i \sin\theta)^2 + e_i^2 \sin^2\theta \right]}, \qquad (187) \\
\frac{\partial^3 S_i}{\partial x \partial y^2} &= \frac{2e_i \left[2d_i \left(\cos\theta + d_i \sin\theta \right) - (d_i^2 - e_i^2) \sin\theta \right)}{r \left[(\cos\theta + d_i \sin\theta)^2 + e_i^2 \sin^2\theta \right]}, \qquad (188) \\
\frac{\partial^3 S_i}{\partial y^3} &= \frac{2e_i \left[(3d_i^2 - e_i^2) \cos\theta + 2d_i \left(d_i^2 + e_i^2 \right) \sin\theta \right]}{r \left((\cos\theta + d_i \sin\theta)^2 + e_i^2 \sin^2\theta \right]}, \qquad (189) \\
& \qquad (190)
\end{aligned}$$

$$
\begin{aligned}
\frac{\partial^4 S_i}{\partial x^4} &= \frac{4e_i \sin\theta\left(\cos\theta + d_i \sin\theta\right)}{r^2\left[\left(\cos\theta + d_i\sin\theta\right)^2 + e_i^2\sin^2\theta\right]^2}, && (191)\\
\frac{\partial^4 S_i}{\partial x^3 \partial y} &= \frac{2e_i}{r^2}\left\{\frac{1}{\left(\cos\theta + d_i\sin\theta\right)^2 + e_i^2\sin^2\theta} - \right.\\
&\left.\frac{2\cos\theta\left(\cos\theta + d_i\sin\theta\right)}{\left[\left(\cos\theta + d_i\sin\theta\right)^2 + e_i^2\sin^2\theta\right]^2}\right\}, && (192)\\
\frac{\partial^4 S_i}{\partial x^2 \partial y^2} &= -\frac{4e_i\cos\theta\left[d_i\left(\cos\theta + d_i\sin\theta\right) + e_i^2\sin\theta\right]}{r^2\left[\left(\cos\theta + d_i\sin\theta\right)^2 + e_i^2\sin^2\theta\right]^2}, && (193)\\
\frac{\partial^4 S_i}{\partial x \partial y^3} &= -\frac{2e_i}{r^2}\left\{\frac{\left(d_i^2 + e_i^2\right)}{\left(\cos\theta + d_i\sin\theta\right)^2 + e_i^2\sin^2\theta} + \right.\\
&\left.\frac{2\left(d_i^2 + e_i^2\right)\cos\theta\left(\cos\theta + d_i\sin\theta\right) - 4e_i^2\cos^2\theta}{\left[\left(\cos\theta + d_i\sin\theta\right)^2 + e_i^2\sin^2\theta\right]^2}\right\}, && (194)\\
& && (195)
\end{aligned}
$$

$$
\begin{aligned}
\frac{\partial^4 S_i}{\partial y^4} &= -\frac{4e_i}{r^2}\left\{\frac{d_i\left(d_i^2 + e_i^2\right)}{\left(\cos\theta + d_i\sin\theta\right)^2 + e_i^2\sin^2\theta} + \right.\\
&\left.\frac{\cos\theta\left[d_i\left(d_i^2 - 3e_i^2\right)\cos\theta + \left(d_i^4 - e_i^4\right)\sin\theta\right]}{\left[\left(\cos\theta + d_i\sin\theta\right)^2 + e_i^2\sin^2\theta\right]^2}\right\}. && (196)
\end{aligned}
$$

As it can be seen, derivatives of R_i and S_i present weak ($\log r$), strong ($1/r$), and hyper ($1/r^2$) singularities that will need special attention during their integration in boundary element kernels.

3.5 Transformation of domain integrals into boundary integrals in anisotropic plate bending problems

As it can be seen in equations (131) and (132), there are domain integrals in the formulation due to the distributed load in the domain. These integrals can be computed in the domain by direct integration in the area Ω_g (see Figure 8). However, the boundary element formulation loses its main feature that is the boundary only discretization. In this work, domain integrals which come from distributed loads are transformed into boundary integrals by an exact transformation.

Consider the plate of Figure 8, under loading g, applied in an area Ω_g. Assuming that loading g has a linear distribution $(Ax + By + C)$ in the area Ω_g, the domain integral can be written as:

$$\int_{\Omega_g} g w^* d\Omega = \int_{\Omega_g} (Ax + By + C) w^* \rho d\rho d\theta \tag{197}$$

or

$$\int_{\Omega_g} g w^* d\Omega = \int_{\theta}\int_0^r (Ax + By + C) w^* \rho d\rho d\theta, \tag{198}$$

where r is the value of ρ in a point of boundary Γ_g.

Defining F^* as the following integral:

$$F^* = \int_0^r (Ax + By + C) w^* \rho d\rho, \tag{199}$$

we can write:

$$\int_{\Omega_g} g w^* d\Omega = \int_{\theta} F^* d\theta. \tag{200}$$

Considering an infinitesimal angle $d\theta$ (Figure 13), the relation between the arch length $rd\theta$ and the infinitesimal boundary length $d\Gamma$, can be written as:

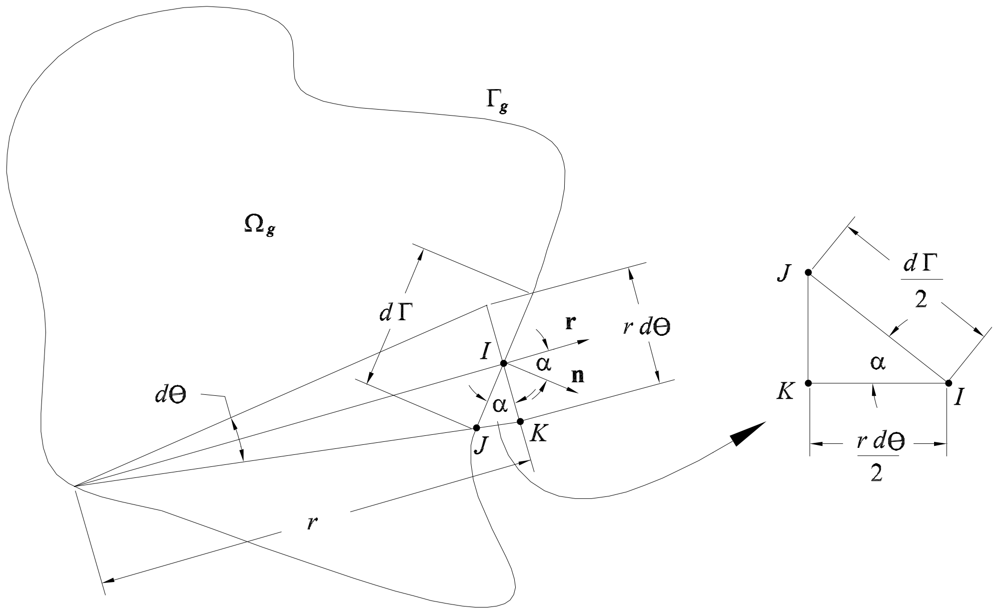

Figure 13: Transformation of domain integral into boundary integral.

$$\cos\alpha = \frac{r\frac{d\theta}{2}}{\frac{d\Gamma}{2}}, \tag{201}$$

or

$$d\theta = \frac{\cos\alpha}{r} d\Gamma. \tag{202}$$

Using the properties of internal product of unity vectors $\mathbf{n}$ and $\mathbf{r}$, indicated in Figure 13, we can write:

$$d\theta = \frac{\mathbf{n}.\mathbf{r}}{r} d\Gamma. \tag{203}$$

Finally, substituting equation (203) into equation (200), the domain integral of equation (131) can be written as a boundary integral given by:

$$\int_{\Omega_g} g w^* d\Omega = \int_{\Gamma_g} \frac{F^*}{r} \mathbf{n}.\mathbf{r} d\Gamma. \tag{204}$$

Provided that

$$x = \rho \cos\theta \tag{205}$$

and

$$y = \rho \sin\theta, \tag{206}$$

the integral F^* can be written as:

$$F^* = \int_0^r \frac{1}{8\pi} (A\rho\cos\theta + B\rho\sin\theta + C) \left[C_1 R_1 + C_2 R_2 + C_3 (S_1 - S_2)\right] \rho d\rho, \tag{207}$$

where C_1, C_2, and C_3 are given by equations (138), (139), (140), respectively. Equation (207) can be rewritten as:

$$\begin{aligned} F^* \quad = \quad & \frac{1}{8\pi} \left\{ (A\cos\theta + B\sin\theta) \int_0^r \rho^2 \left[C_1 R_1 + C_2 R_2 + C_3 (S_1 - S_2)\right] d\rho + \right. \\ & \left. C \int_0^r \rho \left[C_1 R_1 + C_2 R_2 + C_3 (S_1 - S_2)\right] d\rho \right\}. \end{aligned} \tag{208}$$

Following similar procedure to obtain equation (204), the domain term of equation (132) can be written as:

$$\int_{\Omega_g} g \frac{\partial w^*}{\partial n_1} d\Omega = \int_\theta \frac{G^*}{r} \text{n.r} d\Gamma, \tag{209}$$

where

$$G^* = \int_0^r (Ax + By + C) \frac{\partial w^*}{\partial n_1} \rho d\rho \tag{210}$$

or

$$\begin{aligned} G^* = \frac{1}{8\pi} & \left\{ (A\cos\theta + B\sin\theta) \int_0^r \rho^2 \left[C_1 \frac{\partial R_1}{\partial n_1} + C_2 \frac{\partial R_2}{\partial n_1} + \right.\right. \\ C_3 & \left.\left. \left(\frac{\partial S_1}{\partial n_1} - \frac{\partial S_2}{\partial n_1} \right) \right] d\rho + C \int_0^r \rho \left[C_1 \frac{\partial R_1}{\partial n_1} + C_2 \frac{\partial R_2}{\partial n_1} + C_3 \left(\frac{\partial S_1}{\partial n_1} - \frac{\partial S_2}{\partial n_1} \right) \right] d\rho \right\}. \end{aligned} \tag{211}$$

As it can be seen, equations (208) and (211) are not θ dependent. By analytical integration, we can obtain:

$$\begin{aligned}\int_0^r R_i \rho d\rho &= \frac{r^4}{16}\left\{-16 e_i \arctan\frac{e_i \sin\theta}{\cos\theta + d_i \sin\theta}\sin\theta\left(\cos\theta + d_i\sin\theta\right) - \right.\\ &\left[-7 + 2\log\frac{r^2\left(e_i^2\sin^2\theta + \left(\cos\theta + d_i\sin\theta\right)^2\right)}{a^2}\right]\times\\ &\left.\left[-1 - d_i^2 + e_i^2 + \left(-1 + d_i^2 - e_i^2\right)\cos 2\theta - 2d_i\sin 2\theta\right]\right\}, \qquad (212)\end{aligned}$$

$$\begin{aligned}\int_0^r S_i \rho d\rho &= \frac{r^4}{16}\left\{2e_i\left[-7 + 2\log\frac{r^2\left(e_i^2\sin^2\theta + \left(\cos\theta + d_i\sin\theta\right)^2\right)}{a^2}\right]\times\right.\\ &\sin\theta\left(\cos\theta + d_i\sin\theta\right) + 2\arctan\frac{e_i\sin\theta}{\cos\theta + d_i\sin\theta}\times\\ &\left.\left[1 + d_i^2 - e_i^2 + \left(1 - d_i^2 + e_i^2\right)\cos 2\theta + 2d_i\sin 2\theta\right]\right\}, \qquad (213)\end{aligned}$$

(214)

$$\int_0^r R_i \rho^2 d\rho = \frac{r^5}{50}\left\{-40 e_i \arctan\frac{e_i \sin\theta}{\cos\theta + d_i \sin\theta}\sin\theta\left(\cos\theta + d_i\sin\theta\right) - \left[-17 + 5\log\frac{r^2\left(e_i^2\sin^2\theta + (\cos\theta + d_i\sin\theta)^2\right)}{a^2}\right]\times \left[-1 - d_i^2 + e_i^2 + \left(-1 + d_i^2 - e_i^2\right)\cos 2\theta - 2d_i\sin 2\theta\right]\right\}, \tag{215}$$

$$\int_0^r S_i \rho^2 d\rho = \frac{r^5}{50}\left\{2e_i\left[-17 + 5\log\frac{r^2\left(e_i^2\sin^2\theta + (\cos\theta + d_i\sin\theta)^2\right)}{a^2}\right]\times \sin\theta\left(\cos\theta + d_i\sin\theta\right) + 5\arctan\frac{e_i\sin\theta}{\cos\theta + d_i\sin\theta}\times \left[1 + d_i^2 - e_i^2 + \left(1 - d_i^2 + e_i^2\right)\cos 2\theta + 2d_i\sin 2\theta\right]\right\}, \tag{216}$$

$$\int_0^r \frac{\partial R_i}{\partial x}\rho d\rho = \frac{2r^3}{9}\left\{-6e_i\arctan\frac{e_i\sin\theta}{\cos\theta + d_i\sin\theta}\sin\theta + \left[-8 + 3\log\frac{r^2\left(e_i^2\sin^2\theta + (\cos\theta + d_i\sin\theta)^2\right)}{a^2}\right]\left(\cos\theta + d_i\sin\theta\right)\right\}, \tag{217}$$

$$\tag{218}$$

$$\int_0^r \frac{\partial R_i}{\partial y}\rho d\rho = \frac{2r^3}{9}\left\{-6e_i\arctan\frac{e_i\sin\theta}{\cos\theta + d_i\sin\theta}\left(\cos\theta + 2d_i\sin\theta\right) + \left[-8 + 3\log\frac{r^2\left(e_i^2\sin^2\theta + (\cos\theta + d_i\sin\theta)^2\right)}{a^2}\right]\left[d_i\cos\theta + \left(d_i^2 - e_i^2\right)\sin\theta\right]\right\}, \tag{219}$$

$$\int_0^r \frac{\partial S_i}{\partial x}\rho d\rho = \frac{r^3}{9}\left\{e_i\left[-8 + 3\log\frac{r^2\left(e_i^2\sin^2\theta + (\cos\theta + d_i\sin\theta)^2\right)}{a^2}\right]\sin\theta + 6\arctan\frac{e_i\sin\theta}{\cos\theta + d_i\sin\theta}\left(\cos\theta + d_i\sin\theta\right)\right\}, \tag{220}$$

$$\tag{221}$$

$$\int_0^r \frac{\partial S_i}{\partial y}\rho d\rho = \frac{r^3}{9}\left\{e_i\left[-8+3\log\frac{r^2\left(e_i^2\sin^2\theta+(\cos\theta+d_i\sin\theta)^2\right)}{a^2}\right]\times\right.$$
$$\left.(\cos\theta+2d_i\sin\theta)-6\arctan\frac{e_i\sin\theta}{\cos\theta+d_i\sin\theta}\left[d_i\cos\theta+\left(d_i^2-e_i^2\right)\sin\theta\right]\right\}, \tag{222}$$

$$\int_0^r \frac{\partial R_i}{\partial x}\rho^2 d\rho = \frac{r^4}{4}\left\{-4e_i\arctan\frac{e_i\sin\theta}{\cos\theta+d_i\sin\theta}\sin\theta+\right.$$
$$\left.\left[-5+2\log\frac{r^2\left(e_i^2\sin^2\theta+(\cos\theta+d_i\sin\theta)^2\right)}{a^2}\right](\cos\theta+d_i\sin\theta)\right\}, \tag{223}$$

$$\int_0^r \frac{\partial R_i}{\partial y}\rho^2 d\rho = \frac{r^4}{4}\left\{-4e_i\arctan\frac{e_i\sin\theta}{\cos\theta+d_i\sin\theta}(\cos\theta+2d_i\sin\theta)+\right.$$
$$\left.\left[-5+2\log\frac{r^2\left(e_i^2\sin^2\theta+(\cos\theta+d_i\sin\theta)^2\right)}{a^2}\right]\left[d_i\cos\theta+\left(d_i^2-e_i^2\right)\sin\theta\right]\right\}, \tag{224}$$

$$\int_0^r \frac{\partial S_i}{\partial x}\rho^2 d\rho = \frac{r^4}{8}\left\{e_i\left[-5+2\log\frac{r^2\left(e_i^2\sin^2\theta+(\cos\theta+d_i\sin\theta)^2\right)}{a^2}\right]\sin\theta+\right.$$
$$\left.4\arctan\frac{e_i\sin\theta}{\cos\theta+d_i\sin\theta}(\cos\theta+d_i\sin\theta)\right\}, \tag{225}$$
$$\tag{226}$$

$$\int_0^r \frac{\partial S_i}{\partial y}\rho^2 d\rho = \frac{r^4}{8}\left\{e_i\left[-5+2\log\frac{r^2\left(e_i^2\sin^2\theta+(\cos\theta+d_i\sin\theta)^2\right)}{a^2}\right]\right.$$
$$\left.(\cos\theta+2d_i\sin\theta)+4\arctan\frac{e_i\sin\theta}{\cos\theta+d_i\sin\theta}\left[d_i\cos\theta+\left(d_i^2-e_i^2\right)\sin\theta\right]\right\}. \tag{227}$$

Although in this work the domain loads are considered as uniformly distributed or linearly distributed, the procedure presented in this section can be extended to other higher order loads.

3.6 Matrix equation

In order to compute unknown boundary variables, the boundary Γ is discretized in N_e straight elements and the boundary variables w, $\partial w/\partial n$, m_n, and V_n are assumed constant along each element. Taking a node d as the source point, equations (131) and (132) can be written in a matrix form as:

$$\frac{1}{2}\left\{\begin{array}{c} w^{(d)} \\ \\ \frac{\partial w^{(d)}}{\partial n_1} \end{array}\right\} + \sum_{i=1}^{N_e}\left(\left[\begin{array}{cc} h_{11}^{(i,d)} & h_{12}^{(i,d)} \\ h_{21}^{(i,d)} & h_{22}^{(i,d)} \end{array}\right]\left\{\begin{array}{c} w^{(i)} \\ \frac{\partial w^{(i)}}{\partial n} \end{array}\right\}\right) =$$
$$\sum_{i=1}^{N_e}\left(\left[\begin{array}{cc} g_{11}^{(i,d)} & g_{12}^{(i,d)} \\ g_{21}^{(i,d)} & g_{22}^{(i,d)} \end{array}\right]\left\{\begin{array}{c} V_n^{(i)} \\ m_n^{(i)} \end{array}\right\}\right) + \sum_{i=1}^{N_c}\left(\left\{\begin{array}{c} R_1^{(i,d)} \\ R_2^{(i,d)} \end{array}\right\} w_c^{(i)}\right) +$$
$$\sum_{i=1}^{N_c}\left(\left\{\begin{array}{c} c_1^{(i,d)} \\ c_2^{(i,d)} \end{array}\right\} R_c^{(i)}\right) + \left\{\begin{array}{c} P_1^{(d)} \\ P_2^{(d)} \end{array}\right\} \tag{228}$$

Terms of equation (228) are integrals given by:

$$h_{11}^{(i,d)} = \int_{\Gamma_i} V_n^* d\Gamma, \qquad h_{12}^{(i,d)} = -\int_{\Gamma_i} m_n^* d\Gamma, \tag{229}$$

$$h_{21}^{(i,d)} = \int_{\Gamma_i} \frac{\partial V_n^*}{\partial n_1} d\Gamma, \qquad h_{22}^{(i,d)} = -\int_{\Gamma_i} \frac{\partial m_n^*}{\partial n_1} d\Gamma, \tag{230}$$

$$g_{11}^{(i,d)} = \int_{\Gamma_i} w^* d\Gamma, \qquad g_{12}^{(i,d)} = -\int_{\Gamma_i} \frac{\partial w^*}{\partial n} d\Gamma, \tag{231}$$

$$g_{21}^{(i,d)} = \int_{\Gamma_i} \frac{\partial w^*}{\partial n_1} d\Gamma, \qquad g_{22}^{(i,d)} = -\int_{\Gamma_i} \frac{\partial}{\partial n_1}\frac{\partial m_n^*}{\partial n} d\Gamma, \tag{232}$$

$$c_1^{(i,d)} = w_{ci}^*, \qquad c_2^{(i,d)} = \frac{\partial w_{ci}^*}{\partial n_1}, \tag{233}$$

$$R_1^{(i,d)} = R_{ci}^*, \qquad R_2^{(i,d)} = \frac{\partial R_{ci}^*}{\partial n_1}, \tag{234}$$

$$P_1^{(d)} = \int_\Omega g w^* d\Omega, \qquad P_2^{(d)} = \int_\Omega g \frac{\partial w}{\partial n_1} d\Omega. \tag{235}$$

Matrix equation (228) has two equations and $2N_e + N_c$ unknown variables. In order to obtain a solvable linear system, the source point is placed successively in each boundary node ($d = 1, ..., N_e$) as well as in each corner node ($d = N_e + 1, ..., N_e + N_c$). It is worth noting that while both equations, (131) and (132), are used for each boundary node (providing the first $2N_e$ equations), only the equation (131) is used for each corner (providing other N_c equations). So, the following matrix equation is obtained:

$$\left[\begin{array}{cc} \mathbf{H}' & \mathbf{R}' \\ \mathbf{H}'' & \mathbf{R}'' \end{array}\right]\left\{\begin{array}{c} \mathbf{w}_{bn} \\ \mathbf{w}_c \end{array}\right\} = \left[\begin{array}{cc} \mathbf{G}' & \mathbf{C}' \\ \mathbf{G}'' & \mathbf{C}'' \end{array}\right]\left\{\begin{array}{c} \mathbf{V}_{bn} \\ \mathbf{V}_c \end{array}\right\} + \left\{\begin{array}{c} \mathbf{P}_{bn} \\ \mathbf{P}_c \end{array}\right\} \tag{236}$$

where $\mathbf{w}_{bn}$ contains the transversal displacement and the rotation of each boundary node, $\mathbf{V}_{bn}$ contains the shear force and the twisting moment of each boundary node, $\mathbf{P}_{bn}$ contains the domain integral for each boundary node, $\mathbf{w}_c$ contains the transversal displacement of each corner, and $\mathbf{V}_c$ contains the corner reaction of each corner, $\mathbf{P}_c$ contains the domain integral for each corner. Terms $\mathbf{H}'$, $\mathbf{C}'$, $\mathbf{R}'$, and $\mathbf{G}'$ are matrices which contain the respective terms of equation (228) written to the N_e boundary nodes; $\boldsymbol{\gamma}$ is the vector that contains coefficients γ^m. Terms $\mathbf{H}''$, $\mathbf{C}''$, $\mathbf{R}''$, and $\mathbf{G}''$ are matrices which contain the respective first line terms of equation (228) written to N_c corners.

Equation (236) can be rewritten as:

$$\mathbf{H}\mathbf{w} = \mathbf{G}\mathbf{V} + \mathbf{P} \tag{237}$$

where

$$\mathbf{H} = \begin{bmatrix} \mathbf{H}' & \mathbf{R}' \\ \mathbf{H}'' & \mathbf{R}'' \end{bmatrix} \tag{238}$$

$$\mathbf{w} = \begin{Bmatrix} \mathbf{w}_{bn} \\ \mathbf{w}_c \end{Bmatrix} \tag{239}$$

$$\mathbf{G} = \begin{bmatrix} \mathbf{G}' & \mathbf{C}' \\ \mathbf{G}'' & \mathbf{C}'' \end{bmatrix} \tag{240}$$

$$\mathbf{V} = \begin{Bmatrix} \mathbf{V}_{bn} \\ \mathbf{V}_c \end{Bmatrix} \tag{241}$$

$$\mathbf{P} = \begin{Bmatrix} \mathbf{P}_{bn} \\ \mathbf{P}_c \end{Bmatrix} \tag{242}$$

Applying boundary conditions, equation (236) can be rearranged as

$$\mathbf{A}\mathbf{x} = \mathbf{b} \tag{243}$$

which can be solved by standard procedure for linear systems.

3.7 Quadratic Elements

In order to increase the convergency of results to the formulation presented here, quadratic elements were implemented. As the formulation has integrals with singular integrands, these integrals need to be computed in the Cauchy sense, in the case of strong singularities, or Hadamard sense, in the case of hyper singularities. Integration in the Hadamard sense demands Holder's continuity in the nodes. Because this, discontinuous elements are strongly recommended. In this work, discontinuous quadratic elements with nodes placed at $\xi = -2/3$, $\xi = 0$, and $\xi = +2/3$ (Figure 14) were implemented. The shape functions for these elements are given by:

$$N_1 = \xi \left(\frac{9}{8}\xi - \frac{3}{4} \right); \quad (244)$$

$$N_2 = \left(1 - \frac{3}{2}\xi \right) \left(1 + \frac{3}{2}\xi \right); \quad (245)$$

$$N_3 = \xi \left(\frac{9}{8}\xi + \frac{3}{4} \right). \quad (246)$$

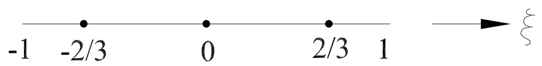

Figure 14: Discontinuous quadratic boundary element.

3.8 Transformation of domain integrals into boundary integrals for unknown body forces

3.8.1 Dual reciprocity method

The procedure presented in section 3.5 to transform domain integrals into boundary integral is suitable when body forces are constants or functions of coordinates x and y coordinates along the domain. When these body forces are functions of deflexion w, as in dynamic problems for example, the exact transformation is no longer useful. In this case, approaches as the dual reciprocity method is very suitable. The dual reciprocity formulation for anisotropic plate bending problems is presented in this section.

Consider that the term b of equation (131) is approximated over the domain as a sum of the M products between radial basis functions f^m and unknown coefficients γ^m, that is:

$$b(P) = \sum_{m=1}^{M} \gamma^m f^m. \quad (247)$$

for approximation functions based on pure radial basis function, or

$$b(P) = \sum_{m=1}^{M} \gamma_m f_m + ax + by + c \quad (248)$$

with

$$\sum_{m=1}^{M} \gamma_m x_m = \sum_{m=1}^{M} \gamma_m y_m = \sum_{m=1}^{M} \gamma_m = 0 \quad (249)$$

for approximation functions based on radial basis function combined with augmentation functions.

Thus, the domain integral of equation (131) can be written as:

$$P_1(Q) = \int_{\Omega_g} b(P) w^*(Q,P) d\Omega = \sum_{m=1}^{M} \gamma^m \int_{\Omega_g} f^m w^*(Q) d\Omega. \tag{250}$$

Particular solutions $\hat{w}$ can be obtained by solving the following differential equation:

$$D_{11}\frac{\partial^4 \hat{w}}{\partial x^4} + 4D_{16}\frac{\partial^4 \hat{w}}{\partial x^3 \partial y} + 2(D_{12}+D_{66})\frac{\partial^4 \hat{w}}{\partial x^2 \partial y^2} + 4D_{26}\frac{\partial^4 \hat{w}}{\partial x \partial y^3} + D_{22}\frac{\partial^4 \hat{w}}{\partial y^4} = f. \tag{251}$$

The reciprocal relation between the fundamental solution and the particular solution can be written as:

$$\begin{aligned} &K\hat{w}(Q) + \int_\Gamma \left[V_n^*(Q,P)\hat{w}(P) - m_n^*(Q,P)\frac{\partial \hat{w}(P)}{\partial n} \right] d\Gamma(P) + \sum_{i=1}^{N_c} R_{c_i}^*(Q,P)\hat{w}_{c_i}(P) = \\ &\int_\Gamma \left[\hat{V}_n(P) w^*(Q,P) - \hat{m}_n(P)\frac{\partial w^*}{\partial n}(Q,P) \right] d\Gamma(P) + \sum_{i=1}^{N_c} \hat{R}_{c_i}(P) w_{c_i}^*(Q,P) + \\ &\int_\Omega f(P) w^*(Q,P) d\Omega. \end{aligned} \tag{252}$$

Substituting equation (252) into equation (250), we have:

$$\begin{aligned} P_1(Q) = \int_\Omega g w^* d\Omega = \sum_{m=1}^{M} \gamma_n^m \Bigg\{ & K\hat{w}(Q) + \int_\Gamma \left[V_n^*(Q,P)\hat{w}(P) - m_n^*(Q,P)\frac{\partial \hat{w}(P)}{\partial n} \right] d\Gamma(P) + \\ & \sum_{i=1}^{N_c} R_{c_i}^*(Q,P)\hat{w}_{c_i}(P) - \int_\Gamma \left[V_n(P) w^*(Q,P) - \hat{m}_n(P)\frac{\partial w^*}{\partial n}(Q,P) \right] d\Gamma(P) + \\ & \sum_{i=1}^{N_c} \hat{R}_{c_i}(P) w_{c_i}^*(Q,P) \Bigg\}. \end{aligned} \tag{253}$$

Following the same procedure, the domain integral of equation (132) can be approximated as:

$$P_2(Q) = \int_{\Omega_g} b \frac{\partial w^*(Q,P)}{\partial n_1} d\Omega = \sum_{m=1}^{M} \gamma^m \int_{\Omega_g} f^m \frac{\partial w^*(Q)}{\partial n_1} d\Omega, \tag{254}$$

Using the dual reciprocity boundary element method, the integral P_2, given by the sum of domain integrals (254), is transformed into a sum of boundary integrals.

Following the same procedure to obtain equation (253), equation (254) can be written as:

$$P_2(Q) = \int_{\Omega_g} b(P) \frac{\partial w^*(Q,P)}{\partial n_1} d\Omega = \sum_{m=1}^{M} \gamma_n^m \left\{ \frac{1}{2} \frac{\partial \hat{w}(Q)}{\partial n_1} + \int_\Gamma \left[\frac{\partial V^*}{\partial n_1}(Q,P)\hat{w}(P) - \right.\right.$$
$$\left. \frac{\partial m_n^*}{\partial n_1}(Q,P) \frac{\partial \hat{w}}{\partial n}(P) \right] d\Gamma(P) + \sum_{i=1}^{N_c} \frac{\partial R^* c_i}{\partial n_1}(Q,P)\hat{w}_{c_i}(P) -$$
$$\int_\Gamma \left\{ \hat{V}_n(P) \frac{\partial w^*}{\partial n_1}(Q,P) - \hat{m}_n(P) \frac{\partial}{\partial n_1} \left[\frac{\partial w^*}{\partial n_1}(Q,P) \right] \right\} d\Gamma(P) -$$
$$\left. \sum_{i=1}^{N_c} R_{c_i}(P) \frac{\partial w_{c_i}^*}{\partial n_1}(Q,P) \right\}. \tag{255}$$

Equations (253) and (255) are the basis of the dual reciprocity boundary element method for bending problems. As it can be seen, the domain integral where transformed in a sum of boundary integrals.

Particular solutions need to satisfy the equilibrium equation (251). The traditional solution procedure to solve the differential equation (251), when the problem is isotropic, is to assume an approximation function, $f = 1 + r$ for example, and compute the correspondent particular solutions. This procedure is quite difficult to apply to anisotropic materials, as the anisotropy increases the number of constants in the equilibrium equation. An alternative approach is to assume a particular solution $\hat{w}$ and evaluate the corresponding approximation function f. This approach was proposed by Schclar Schclar [1994] for anisotropic three dimensional problems and later it was used by different researchers in different anisotropic problems Albuquerque et al. [2002, 2003a,b, 2004], Kogl and Gaul [2000a,b, 2003].

Here it is used for the particular solution:

$$\hat{w} = c\ r^5, \tag{256}$$

where c is an arbitrary constant. The approximation function f is computed by equation (251) using the derivatives of particular solution (256). Other particular solutions are given by:

$$\hat{m}_n = -\left(f_1 \frac{\partial^2 \hat{w}}{\partial x^2} + f_2 \frac{\partial^2 \hat{w}}{\partial x \partial y} + f_3 \frac{\partial^2 \hat{w}}{\partial y^2} \right), \tag{257}$$

$$\hat{R}_{c_i} = -\left(g_1 \frac{\partial^2 \hat{w}}{\partial x^2} + g_2 \frac{\partial^2 \hat{w}}{\partial x \partial y} + g_3 \frac{\partial^2 \hat{w}}{\partial y^2} \right), \tag{258}$$

$$\hat{V}_n = -\left(h_1 \frac{\partial^3 \hat{w}}{\partial x^3} + h_2 \frac{\partial^3 \hat{w}}{\partial x^2 \partial y} + h_3 \frac{\partial^3 \hat{w}}{\partial x \partial y^2} + h_4 \frac{\partial^3 \hat{w}}{\partial y^3} \right) - \frac{1}{R} \left(h_5 \frac{\partial^2 \hat{w}}{\partial x^2} + h_6 \frac{\partial^2 \hat{w}}{\partial x \partial y} + h_7 \frac{\partial^2 \hat{w}}{\partial y^2} \right). \tag{259}$$

Although the particular solutions are given by known expressions, they are approximated in the boundary by the same shape functions used in the approximation of the unknown variables. So, discretizing the boundary in boundary elements, equations (253) and (255) can be written in a matrix form as:

$$\mathbf{P} = \left[\mathbf{H}\hat{\mathbf{w}} - \mathbf{G}\hat{\mathbf{V}}\right]\boldsymbol{\gamma} \tag{260}$$

where

$$\hat{\mathbf{w}} = \left\{ \begin{array}{c} \hat{\mathbf{w}}_{bn} \\ \hat{\mathbf{w}}_{c} \end{array} \right\}, \tag{261}$$

$$\hat{\mathbf{V}} = \left\{ \begin{array}{c} \hat{\mathbf{V}}_{bn} \\ \hat{\mathbf{V}}_{c} \end{array} \right\}, \tag{262}$$

$\hat{\mathbf{w}}_{bn}$ contains the displacement and rotation particular solutions to each boundary node, $\hat{\mathbf{V}}_{bn}$ contains the shear force and the twisting moment particular solutions for each boundary node, $\hat{\mathbf{V}}_{bn}$ contains the displacement particular solution for each corner, and $\hat{\mathbf{V}}_{c}$ contains the corner reaction particular solution for each corner.

Defining

$$\mathbf{S} = \left[\mathbf{H}\hat{\mathbf{w}} - \mathbf{G}\hat{\mathbf{V}}\right] \tag{263}$$

Equation (260) can be rewritten as:

$$\mathbf{P} = \mathbf{S}\boldsymbol{\gamma} \tag{264}$$

Equation (247) can be written in a matrix form, considering all source points, as:

$$\mathbf{b} = \mathbf{F}\boldsymbol{\gamma} \tag{265}$$

Thus, $\boldsymbol{\gamma}$ can be computed as:

$$\boldsymbol{\gamma} = \mathbf{F}^{-1}\mathbf{b} \tag{266}$$

Terms P_1 of equation (250) and P_2 of equation (254) can be written in a matrix form, considering all source points, as:

$$\mathbf{P} = \mathbf{S}\mathbf{F}^{-1}\mathbf{b} \tag{267}$$

For free vibration dynamic problems, the body force vector is given by:

$$\mathbf{b} = \varrho h \omega^2 \mathbf{w} \tag{268}$$

where ϱ is the material density, h is the plate thickness, and ω is the circular frequency of vibration.

So, equation (267) can be written as:

$$\mathbf{P} = \omega^2 \varrho h \mathbf{S}\mathbf{F}^{-1}\mathbf{w} \tag{269}$$

or

$$\mathbf{P} = \omega^2 \mathbf{M}\mathbf{w} \tag{270}$$

where $\mathbf{M}$ is the mass matrix given by:

$$\mathbf{M} = \varrho h \mathbf{S}\mathbf{F}^{-1} \tag{271}$$

Finally, equation (237) for dynamic problems can be written as:

$$\mathbf{H}\mathbf{w} = \mathbf{G}\mathbf{V} + \omega^2 \mathbf{M}\mathbf{w} \tag{272}$$

3.9 The radial integration method

The domain integral of equation (250) can be written as:

$$P_1(Q) = \sum_{m=1}^{M} \gamma^m \int_{\Omega_g} f^m w^*(Q,P) \rho d\rho d\theta \tag{273}$$

or

$$P_1(Q) = \sum_{m=1}^{M} \gamma^m \int_{\theta} \int_0^r f^m w^*(Q,P) \rho d\rho d\theta, \tag{274}$$

where r is the value of ρ in a point of the boundary Γ_g (see Figure 13).

Defining $F^m(Q)$ as the following integral:

$$F^m(Q) = \int_0^r f^m w^*(Q,P) \rho d\rho, \tag{275}$$

we can write:

$$P_1(Q) = \sum_{m=1}^{M} \gamma^m \int_{\theta} F^m(Q) d\theta. \tag{276}$$

Considering an infinitesimal angle $d\theta$ (Figure 13), the relation between the arch length $rd\theta$ and the infinitesimal boundary length $d\Gamma$, can be written as:

$$\cos\alpha = \frac{r\frac{d\theta}{2}}{\frac{d\Gamma}{2}}, \tag{277}$$

or

$$d\theta = \frac{\cos\alpha}{r} d\Gamma. \tag{278}$$

where α is the angle between unity vectors $\mathbf{r}$ and $\mathbf{n}$.

Using the inner product properties of the unity vectors $\mathbf{n}$ and $\mathbf{r}$, showed in Figure 13, we can write:

$$d\theta = \frac{\mathbf{n}.\mathbf{r}}{r} d\Gamma. \tag{279}$$

Finally, substituting equation (279) into equation (276), the domain integral of equation (131) can be written as a boundary integral given by:

$$P_1(Q) = \sum_{m=1}^{M} \gamma^m \int_{\Gamma_g} \frac{F^m(Q)}{r} \mathbf{n}.\mathbf{r} d\Gamma. \tag{280}$$

Following similar procedure to obtain equation (280), the domain term of equation (254) can be written as:

$$P_2(Q) = \int_{\Omega_g} b \frac{\partial w^*(Q,P)}{\partial n_1} d\Omega = \sum_{m=1}^{M} \gamma^m \int_{\Gamma_g} \frac{G^m(Q)}{r} \mathbf{n}.\mathbf{r} d\Gamma, \tag{281}$$

where

$$G^m(Q) = \int_0^r f^m \frac{\partial w^*(Q,P)}{\partial n_1} \rho d\rho. \tag{282}$$

So, the domain integrals of matrix equation (228) can be written as

$$\left\{ \begin{array}{c} P_1^{(d)} \\ P_2^{(d)} \end{array} \right\} = \sum_{m=1}^{M} \gamma^m \sum_{i=1}^{N_e} \left\{ \begin{array}{c} p_1^{(d,m)} \\ p_2^{(d,m)} \end{array} \right\} \tag{283}$$

where

$$p_1^{(d,m)} = \int_{\Gamma_i} \frac{F^{(d,m)}}{r} \mathbf{n}.\mathbf{r} d\Gamma, \qquad p_2^{(d,m)} = \int_{\Gamma_i} \frac{G^{(d,m)}}{r} \mathbf{n}.\mathbf{r} d\Gamma. \tag{284}$$

In this work, the approximation functions f^m are radial basis function written in terms of R, where R is the distance between the centre S of the radial basis function and the integration point P (Figure 15). From Figure 15, we can write:

$$R = \sqrt{\rho^2 + l^2 - 2\rho l \cos\beta}, \tag{285}$$

where l is the vector from S to Q, and β is the angle between ρ and l.

As already mentioned, the RIM is more time-consuming than the DRM since integrals given by equations (275) and (282) cannot be computed analytically for the majority of the approximation fuctions. For example, if $f^m = R$, equation (275) is written as:

$$F^m(Q) = \int_0^r c_1 \sqrt{\rho^2 + l^2 - 2\rho l \cos\beta}\, \ln(c_2\rho)\rho^3 d\rho, \tag{286}$$

where c_1 and c_2 are coefficients that don't depend on ρ. The integral of equation (286) cannot be computed analytically. The numerical integration of these integrals needs to be performed accurately, what demands an expressive number of integration points. In this work the numerical integration is carried out using Gauss quadrature with 10 integration points.

The most interesting advantage of the RIM over the DRM is that the approximation function can be freely chosen. As shown by Paiva et al. [2004], the choice of the approximation function in the DRM is restricted to the analytical computation of the particular solution $\hat{w}$ of the equation (251).

In this work, in order to compare the RIM and the DRM, the same approximation function is used in both methods. This approximation function is given by equation (251) when the particular solution is given by equation (256).

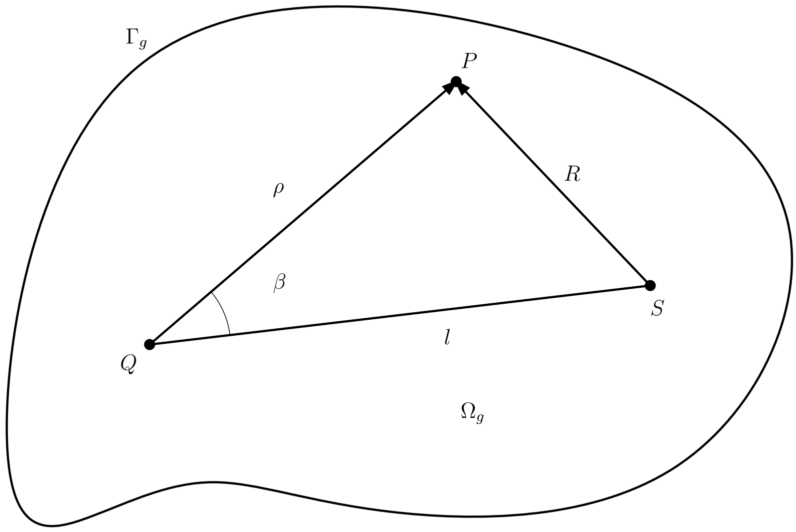

Figure 15: Positions of points in the domain.

3.9.1 Numerical results

A plate under a uniformely distributed load

In order to compare the accuracy of the RIM and the DRM, these methods were first applied to a problem with a known domain load. In this case, domain integrals given by equations (250) and (254) can be exactly computed, as shown by equations (204) and (209)

We considered a square plate of side length $a = 1$ m and thickness $h = 0.01$ m. The material is orthotropic and its material properties are: $E_x = 2.068 \times 10^{11}$ Pa, $E_y = E_x/15$, $\nu_{xy} = 0.3$, $G_{xy} = 6.055 \times 10^8$ Pa. The plate is under a uniformly distributed load $q = 1 \times 10^4$ Pa applied along its domain (Figure 16) and simply supported along its four edges. The plate was discretized with a mesh of 40 constant boundary elements and 64 internal points as shown in Figure 17.

Tables 1 and 2 show the values of domain integrals P_1 and P_2, respectively, computed by the exact transformation, the DRM, and the RIM.

As can be seen, the DRM and the RIM have good agreement with the exact integration for the term P_1 in all nodes. For the term P_2, at some nodes near corners errors for the DRM are greater than 10%. Errors in these nodes remain around 10% even for more refined mesh. The reason for large errors to compute P_2 at some nodes by the DRM might be owing to the use of constant elements to approximate particular solutions at the boundary. Although the particular solutions are given by analytical expressions, in the DRM they are approximated at the boundary by the same shape functions used to approximate physical variables w, $\partial w/\partial n$, V_n, and m_n. Instead of this, in the RIM, domain integrals that contain approximation functions are exact transformed into boundary integrals. However, in the most part of time, these boundary integrals need to be computed numerically, making the RIM more time-consuming than the DRM.

Table 1: Domain integral P_1 computed by the exact transformation, the DRM, and the RIM.

Node	Exact transformation	DRM		RIM	
	P_1 ($10^{-5}\times$ m)	P_1 ($10^{-5}\times$ m)	Error (%)	P_1 ($10^{-5}\times$ m)	Error (%)
1	0.4212	0.4190	0.53	0.4205	0.18
2	0.3824	0.3814	0.25	0.3817	0.18
3	0.3524	0.3516	0.21	0.3518	0.16
4	0.3320	0.3313	0.19	0.3314	0.18
5	0.3216	0.3210	0.18	0.3210	0.18
11	0.4570	0.4559	0.24	0.4561	0.18
12	0.4700	0.4691	0.19	0.4692	0.18
13	0.4722	0.4714	0.18	0.4714	0.18
14	0.4701	0.4693	0.18	0.4693	0.18
15	0.4680	0.4672	0.18	0.4672	0.18

Table 2: Domain integral P_2 computed by the exact transformation, the DRM, and the RIM.

Node	Exact transformation	DRM		RIM	
	P_2 ($10^{-5}\times$ rad)	P_2 ($10^{-5}\times$ rad)	Error (%)	P_2 ($10^{-5}\times$ rad)	Error (%)
1	-0.2832	-0.2549	10.0151	-0.2827	0.18
2	-0.2120	-0.2130	0.48	-0.2116	0.18
3	-0.1568	-0.1555	0.82	-0.1565	0.21
4	-0.1192	-0.1184	0.69	-0.1189	0.21
5	-0.1002	-0.0995	0.66	-0.0999	0.25
11	0.5086	0.5119	0.64	0.5078	0.16
12	0.5816	0.5815	0.03	0.5807	0.16
13	0.6381	0.6376	0.09	0.6372	0.16
14	0.6763	0.6756	0.118	0.6752	0.15
15	0.6954	0.6946	0.11	0.6944	0.15

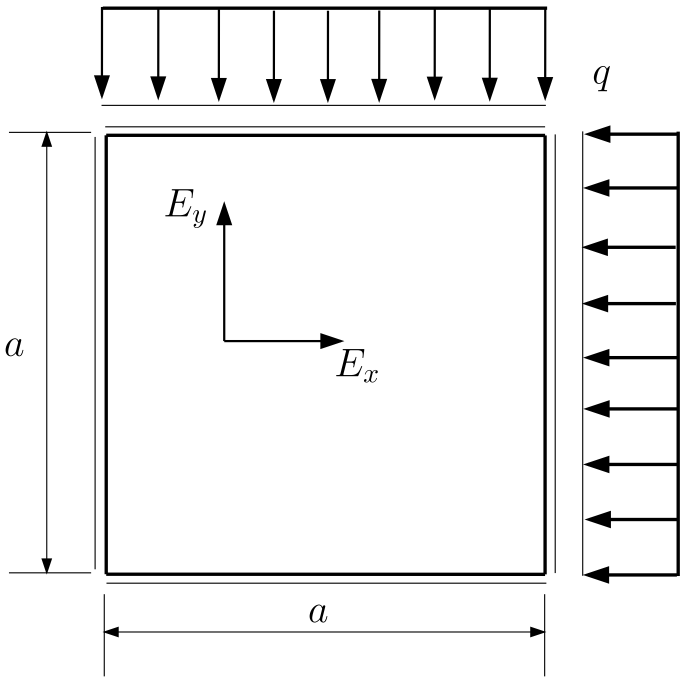

Figure 16: Orthotropic square plate with simply-supported edges under uniformly distributed load.

3.10 Modal analysis

In order to transform equation (272) in an eigenproblem, the boundary is divided into Γ_1 and Γ_2 (Figure 18), where Γ_1 stands for constrained degrees of freedom and Γ_2 stands for free degrees of freedom. Thus, equation (272) can be written as:

$$\begin{bmatrix} \mathbf{H_{11}} & \mathbf{H_{12}} \\ \mathbf{H_{21}} & \mathbf{H_{22}} \end{bmatrix} \begin{Bmatrix} \mathbf{w_1} \\ \mathbf{w_2} \end{Bmatrix} - \begin{bmatrix} \mathbf{G_{11}} & \mathbf{G_{12}} \\ \mathbf{G_{21}} & \mathbf{G_{22}} \end{bmatrix} \begin{Bmatrix} \mathbf{V_1} \\ \mathbf{V_2} \end{Bmatrix} = \omega^2 \begin{bmatrix} \mathbf{M_{11}} & \mathbf{M_{12}} \\ \mathbf{M_{21}} & \mathbf{M_{22}} \end{bmatrix} \begin{Bmatrix} \mathbf{w_1} \\ \mathbf{w_2} \end{Bmatrix}, \tag{287}$$

where indices 1 and 2 stand for boundaries Γ_1 and Γ_2, respectively.

As $\mathbf{w_1} = \mathbf{0}$ and $\mathbf{V_2} = \mathbf{0}$, equation (287) can be written as:

$$\begin{aligned} \mathbf{H_{12}w_2} - \mathbf{G_{11}V_1} &= \omega^2 \mathbf{M_{12}w_2}, \\ \mathbf{H_{22}w_2} - \mathbf{G_{21}V_1} &= \omega^2 \mathbf{M_{22}w_2} \end{aligned} \tag{288}$$

or

$$\hat{\mathbf{H}}\mathbf{w_2} = \omega^2 \hat{\mathbf{M}}\mathbf{w_2}, \tag{289}$$

where $\hat{\mathbf{H}}$ and $\hat{\mathbf{M}}$ are given by:

$$\begin{aligned} \hat{\mathbf{H}} &= \mathbf{H_{22}} - \mathbf{G_{21}G_{11}^{-1}H_{12}}, \\ \hat{\mathbf{M}} &= \mathbf{M_{22}} - \mathbf{G_{21}G_{11}^{-1}M_{12}}. \end{aligned} \tag{290}$$

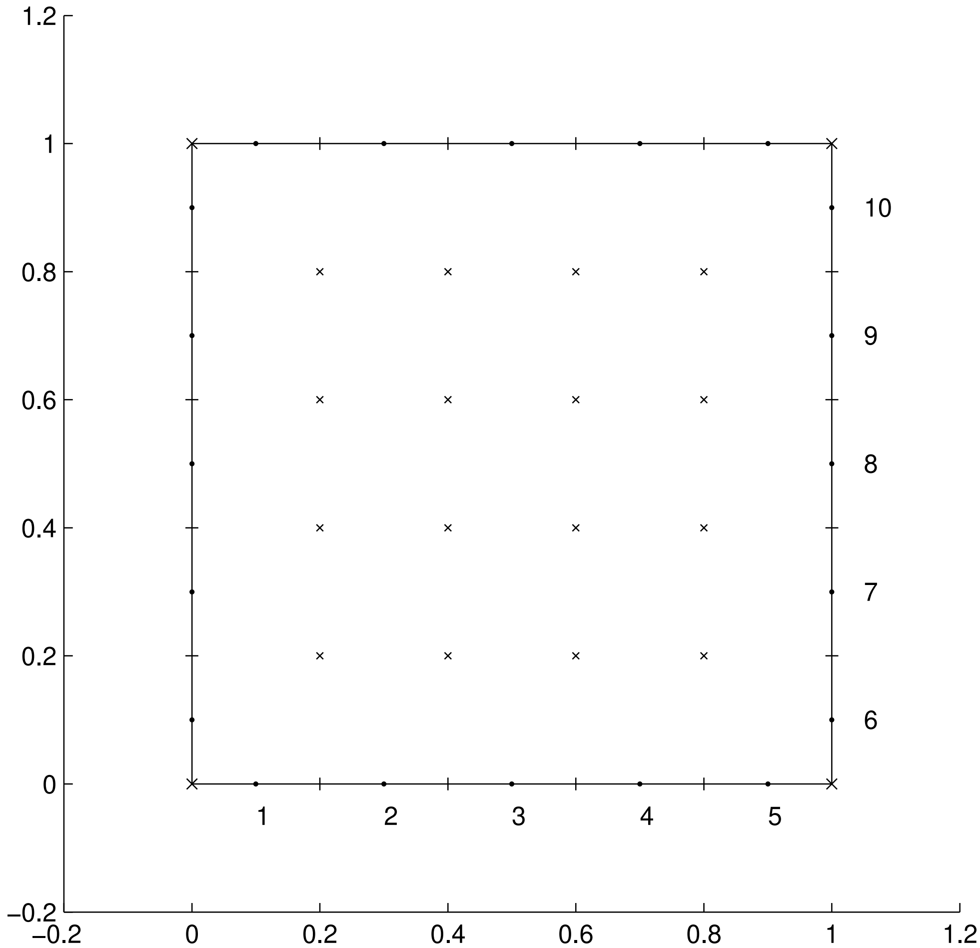

Figure 17: Boundary elements and internal points for the square plate.

The matrix equation (289) can be rewritten as an eigenproblem

$$\mathbf{A}\mathbf{w_2} = \lambda \mathbf{w_2}, \tag{291}$$

where

$$\mathbf{A} = \hat{\mathbf{H}}^{-1}\hat{\mathbf{M}}, \tag{292}$$

λ is the eigenvalue that can be written as:

$$\lambda = \frac{1}{\omega^2}, \tag{293}$$

and $\mathbf{w_2}$ is the eigenvector that is equivalent to the vibration mode shape of the plate.

Provided that $\mathbf{A}$ is nosymmetric, eigenvalues and eigenvectors of equation (291) can be found using standard numerical procedures for nonsymmetric matrices.

3.10.1 Numerical results

Square plate with clampled edges

The problem to be analysed in this section is a square plate of side length $a = 1$ m and thickness $h = 0.01$ m. The material is orthotropic and its material properties are:

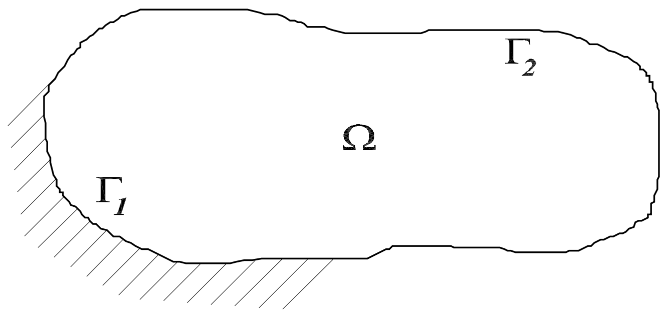

Figure 18: Domain with constrained and free degrees of freedom.

$E_1 = 118.3 \times 10^9$ Pa, $E_2 = 236.6 \times 10^9$ Pa, $G_{12} = 236.6 \times 10^9$ Pa, $\nu_{12} = 0.415$, and $\rho = 1900$ kg/m^3.

The plate has its four edges clamped. The problem was discretized by 44 constant boundary elements of equal lengths and 121 internal points (Figure 19).

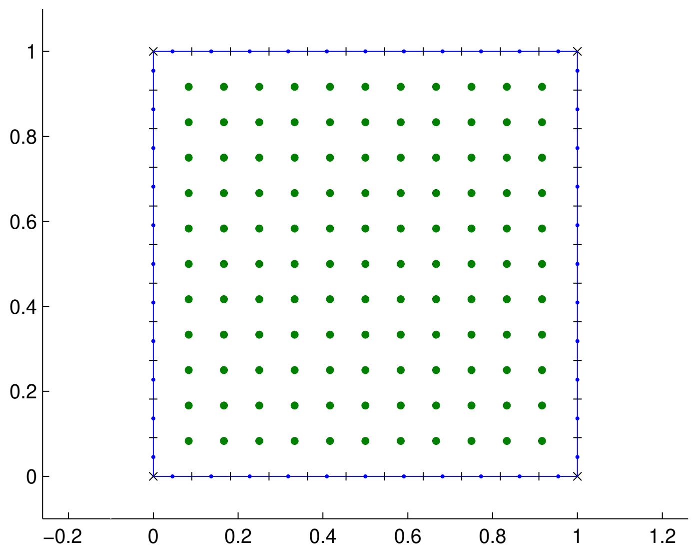

Figure 19: Boundary element mesh and internal points (44 constant boundary elements and 121 internal points).

Table 3 shows the first five natural frequencies computed by the dual reciprocity boundary element method compared to the first five frequencies computed by the finite element method using a commercial code with a very fine mesh (6400 rectangular eight node elements). As it can be seen, all results are in good agreement.

Rectangular plate with free and simply supported edges

Consider a rectangular plate with width $b = 350$ mm, length $a = 450$ mm, and thickness $h = 2.1$ mm (Figure 20). The plate is orthotropic with the following material properties: E_x = 120 GPa, E_y = 10 GPa, G_{xy} = 4.8 GPa, ν_{12} = 0.3 and ϱ = 1510 kg/m^3.

Two meshes were used: a) 28 constant boundary elements and 77 internal points (Figure 21); and b) 72 constant boundary elements and 391 internal points (Figure 22).

Table 3: Natural frequencies for the orthotropic plate with clamped edges computed by the dual reciprocity boundary element method (DRM) and by the finite element method (FEM).

Mode number	Natural frequency (Hz)		Difference (%)
	DRM	FEM	
1	165.82	165.72	0.061
2	303.74	302.95	0.260
3	367.14	367.15	0.003
4	510.94	507.33	0.712
5	524.88	515.75	1.771

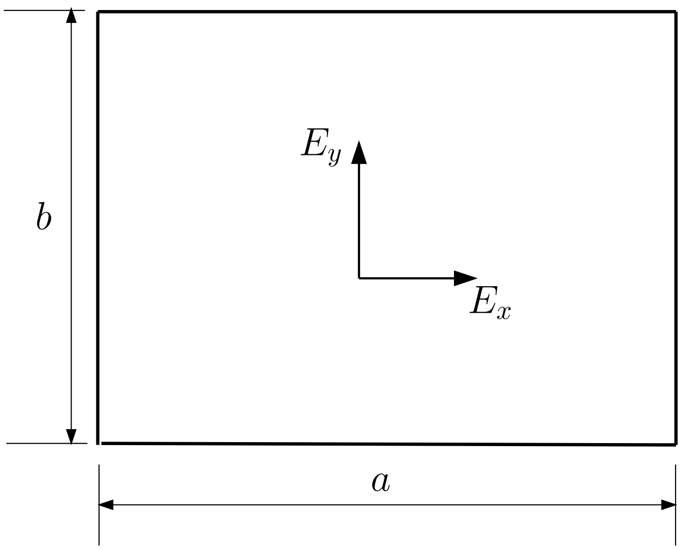

Figure 20: Orthotropic rectangular plate.

Results for the simply supported edges were compared to the exact solution presented by Gibson [1994] while for free edges where compared to the finite element method using a commercial code with a very fine mesh (6400 rectangular eight node elements).

Table 4 and 5 show the first five natural frequencies of plate with free edges computed by the dual reciprocity boundary element method with the mesh given by Figures 21 and 22, respectively, compared to the first five frequencies computed by the finite element method. As can be seen, all results are in good agreement. It also can be seen that there is a convergency to the finite element results as the discretization and number of internal node increses.

Tables 6 and 7 show the first five natural frequencies of plate with simply supported edges computed by the dual reciprocity boundary element method with meshes shown in Figures 21 and 22, respectively, compared to the exact solution presented by Gibson [1994]. As can be seen, all results are in good agreement, excepeted for the second mode. Results converges to the exact solution as the discretization and number of internal points increases.

Dual reciprocity boundary element method $\times$ radial integration method for modal analysis

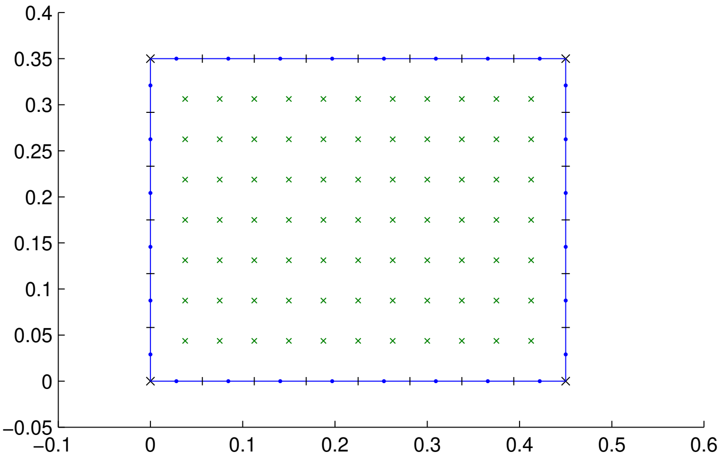

Figure 21: Boundary element mesh and internal points (28 constant boundary elements and 77 internal points).

Table 4: Natural frequencies for the orthotropic plate with free edges computed by the dual reciprocity boundary element method (DRM) and by the finite element method (FEM). 28 boundary elements and 77 internal points.

Mode number	Natural frequency (Hz) DRM	Natural frequency (Hz) FEM	Difference (%)
1	24.6222	25.4970	3.4310
2	45.9983	45.3480	1.4340
3	66.2378	68.7790	3.6947
4	90.3550	95.2470	5.1361
5	101.2286	107.6100	5.9301

Now the dual reciprocity boundary element method and the radial integration method are applied in the analysis of a problem in that body forces are unknown. Consider a rectangular plate with free edges and width $b = 350$ mm, length $a = 450$ mm, and thickness $h = 2.1$ mm (Figure 20). The plate is orthotropic with the following material properties: E_x = 120 GPa, E_y = 10 GPa, G_{xy} = 4.8 GPa, ν_{12} = 0.3 and ϱ = 1510 kg/m^3.

This plate was analysed using a mesh of 66 constant boundary elements and 63 internal points as shown in Figure 23.

Table 8 shows the first five natural frequencies computed by the finite element method (FEM), the dual reciprocity boundary element method (DRM), and the radial integration method (RIM), and the respective relative differences between the last two methods and the FEM. The finite element mesh has 150 (15×10) quadrilateral finite elements (8 nodes per element). As it can be seen, the agreement of the RIM and the DRM with the FEM is similar when the same approximation function is used. The numerical integration used in the RIM is the Gauss quadrature with 10 points. There is the possibility of improve

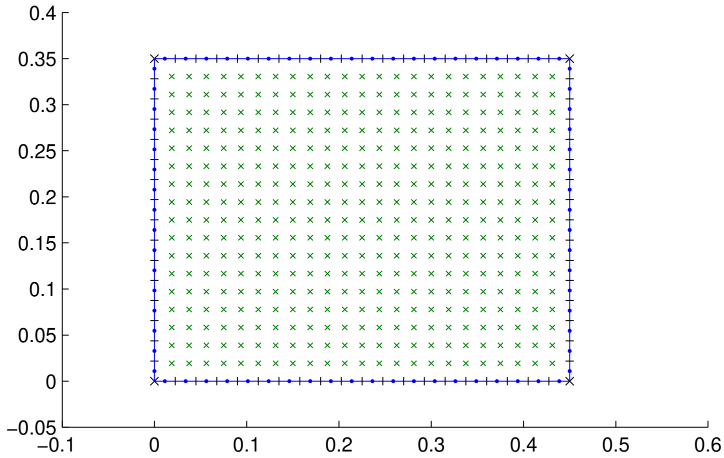

Figure 22: Boundary element mesh and internal points (72 constant boundary elements and 391 internal points).

Table 5: Natural frequencies for the orthotropic plate with free edges computed by the dual reciprocity boundary element method (DRM) and by the finite element method (FEM). 72 boundary elements and 391 internal points.

Mode number	Natural frequency (Hz) DRM	FEM	Difference (%)
1	24.7545	25.4970	2.9122
2	44.9061	45.3480	0.9744
3	69.2577	68.7790	0.6960
4	96.8308	95.2470	1.6628
5	101.4698	107.6100	5.7060

accuracy of the numerical integration by using more integration points. The price of the gain in the accuracy is a larger computation time. However, this analysis is out of the scope of this article and will be treated in future works.

3.11 Buckling analysis

Demand by an accurate stability analysis of anisotropic materials has increase with the increasing use of composite materials in engineering projects. In general, composites panels are very light structures that present high stiffness and strength. However, due to their slenderness, buckling is one of the main concern during their design.

The boundary element method (BEM) has provided a powerful solution to the field of plate buckling. Syngellakis and Elzein Syngellakis and Elzein [1994] presented a boundary element solution of the plate buckling based on Kirchhoff theory under any combination of loadings and support conditions. Nerantzaki and Katsidelakis Nerantzaki

Table 6: Natural frequencies for the orthotropic plate with supported edges computed by the dual reciprocity boundary element method (DRM) compared to the exact solution. 28 boundary elements and 77 internal points.

Mode number	Natural frequency (Hz)		Error (%)
	DRM	Exact solution	
1	50.8502	52.7700	3.6381
2	118.6346	103.2800	14.8669
3	169.5112	176.5700	3.9978
4	216.9047	199.8300	8.5446
5	228.1276	211.0900	8.0713

Table 7: Natural frequencies for the orthotropic plate with supported edges computed by the dual reciprocity boundary element method (DRM) compared to exact solution. 72 boundary elements and 391 internal points.

Mode number	Natural frequency (Hz)		Error (%)
	DRM	Exact solution	
1	51.5836	52.7700	2.2482
2	110.6339	103.2800	7.1204
3	171.3100	176.5700	2.9790
4	205.2756	199.8300	2.7251
5	212.4413	211.0900	0.6402

and Katsikadelis [1996] developed a boundary element method for buckling analysis of plates with variable thickness. Elastic buckling analysis of plates using boundary elements can also be found in Lin et al. [1999]. Buckling analysis of shear deformable isotropic plates was presented in Purbolaksono and Aliabadi [2005]. To the best of author's knowledge, the only work that presents a boundary element formulation applied to non-isotropic plates is due to Shi [1990] who presented an orthotropic formulation with a domain discretization.

In this paper, a boundary element formulation for the stability analysis of general anisotropic plates with no domain discretization is presented. Classical plate bending and plane elasticity formulations are used and the domain integrals due to body forces

Table 8: Natural frequencies computed by the FEM, the DRM and the RIM.

Mode shape	FEM	DRM		RIM	
	$\omega/(2\pi)$ (Hz)	$\omega/(2\pi)$ (Hz)	Difference (%)	$\omega/(2\pi)$ (Hz)	Difference (%)
1	25.50	24.64	3.38	24.3932	4.34
2	45.35	45.03	0.71	45.5682	0.48
3	68.78	68.69	0.13	67.3678	2.05
4	95.25	98.06	2.95	94.6026	0.68
5	107.61	100.93	6.21	106.3381	1.18

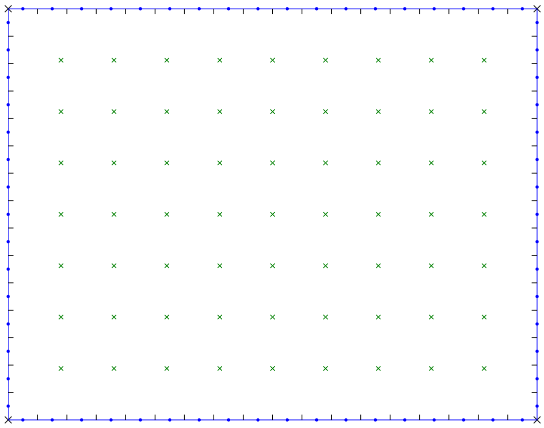

Figure 23: Boundary elements and internal points for the rectangular plate.

are transformed into boundary integrals using the radial integration method. Numerical results are presented to assess the accuracy of the method. Buckling coefficients computed using the proposed formulation are in good agreement with results available in literature.

3.11.1 Boundary integral equations

In the absence of body forces, the governing equation of the anisotropic thin plate buckling is given by:

$$N_{ij,j} = 0, \tag{294}$$

$$D_{11}u_{3,1111} + 4D_{16}u_{3,1112} + 2(D_{12} + D_{66})u_{3,1122} + 4D_{26}u_{3,1222} + D_{22}u_{3,2222} = N_{ij}u_{3,ij}, \tag{295}$$

where $i, j, k = 1, 2$; u_k is the displacement in directions x_1 and x_2, u_3 stands for the displacement in the normal direction of the plate surface; N_{ij} are the in-plane stress components, D_{11}, D_{22}, D_{66}, D_{12}, D_{16}, and D_{26} are the anisotropic thin plate stiffness constants.

The boundary integral equation for in-plane displacements, obtained by applying reciprocity and Green theorems at equation (294), is given by Aliabadi [2002]:

$$c_{ij}u_j(Q) + \int_\Gamma t^*_{ik}(Q,P)u_k(P)d\Gamma(P) = \int_\Gamma u^*_{ik}(Q,P)t_k(P)d\Gamma(P) \tag{296}$$

where $t_i = N_{ij}n_j$ is the traction in the boundary of the plate in the plane $x_1 - x_2$, and n_j is the normal at the boundary point; P is the field point; Q is the source point; and asterisks denote fundamental solutions. The anisotropic plane elasticity fundamental solutions can be found, for example, in Sollero and Aliabadi [1993]. The constant c_{ij} is introduced in order to take into account the possibility that the point Q can be placed in the domain, on the boundary, or outside the domain.

The in-plane stress resultants at a point $Q \in \Omega$ are written as:

$$c_{ik}N_{kj}(Q) + \int_{\Gamma} S^{*}_{ikj}(Q,P)u_k(P)d\Gamma(P) = \int_{\Gamma} D^{*}_{ijk}(Q,P)t_k(P)d\Gamma(P) \tag{297}$$

where D_{ikj} and S_{ikj} are linear combinations of the plane-elasticity fundamental solutions.

The integral equation for the plate buckling formulation, obtained by applying reciprocity and Green theorems at equation (295), is given by:

$$\begin{aligned} &Ku_3(Q) + \int_{\Gamma} \left[V^{*}_{n}(Q,P)w(P) - m^{*}_{n}(Q,P)\frac{\partial w(P)}{\partial n} \right] d\Gamma(P) + \sum_{i=1}^{N_c} R^{*}_{c_i}(Q,P)u_{3_{ci}}(P) \\ &= \sum_{i=1}^{N_c} R_{c_i}(P)u^{*}_{3_{ci}}(Q,P) + \int_{\Gamma} \left[V_n(P)u^{*}_{3}(Q,P) - m_n(P)\frac{\partial u^{*}_{3}}{\partial n}(Q,P) \right] d\Gamma(P) \\ &+\lambda \left[\int_{\Omega} u_3 N_{ij} u^{*}_{3,ij}\, d\Omega + \int_{\Gamma} \left(t_i u^{*}_{3} u_{3,i} - t_i u_3 u^{*}_{3,i} \right) d\Gamma \right], \end{aligned} \tag{298}$$

where $\frac{\partial()}{\partial n}$ is the derivative in the direction of the outward vector $\mathbf{n}$ that is normal to the boundary Γ; m_n and V_n are, respectively, the normal bending moment and the Kirchhoff equivalent shear force on the boundary Γ; R_c is the thin-plate reaction of corners; $u^{*}_{3_{ci}}$ is the transverse displacement of corners; λ is the critical load factor; the constant K is introduced in order to take into account the possibility that the point Q can be placed in the domain, on the boundary, or outside the domain. As in the previous equation, an asterisk denotes a fundamental solution. Fundamental solutions for anisotropic thin plates can be found, for example, in Albuquerque et al. [2006].

A second integral equation is necessary in order to obtain the thin plate buckling boundary element formulation. This equation is given by:

$$\begin{aligned} &K\frac{\partial u_3}{\partial m}(Q) + \int_{\Gamma} \left[\frac{\partial V^{*}_{n}}{\partial m}(Q,P)w(P) - \frac{\partial M^{*}_{n}}{\partial m}(Q,P)\frac{\partial w(P)}{\partial n} \right] d\Gamma(P) + \sum_{i=1}^{N_c} \frac{\partial R^{*}_{c_i}}{\partial m}(Q,P)u_{3_{ci}}(P) \\ &= \sum_{i=1}^{N_c} R_{c_i}(P)\frac{\partial u^{*}_{3_{ci}}}{\partial m}(Q,P) + \int_{\Gamma} \left[V_n(P)\frac{\partial u^{*}_{3}(Q,P)}{\partial m} - m_n(P)\frac{\partial^2 u^{*}_{3}}{\partial n \partial m}(Q,P) \right] d\Gamma(P) \\ &+\lambda \left[\int_{\Omega} u_3 N_{ij} \frac{\partial u^{*}_{3,ij}}{\partial m}\, d\Omega + \int_{\Gamma} \left(t_i u^{*}_{3} \frac{\partial u_{3,i}}{\partial m} - t_i u_3 \frac{\partial u^{*}_{3,i}}{\partial m} \right) d\Gamma \right], \end{aligned} \tag{299}$$

where $\frac{\partial()}{\partial m}$ is the derivative in the direction of the outward vector $\mathbf{m}$ that is normal to the boundary Γ at the source point Q.

As can be seen in equations (298) and (299), domain integrals arise in the formulation owing to the contribution of in-plane stresses to the out of plane direction. In order to transform these integrals into boundary integrals, consider that a body force b is approximated over the domain Ω as a sum of M products between approximation functions f_m and unknown coefficients γ_m, as given by equation (247).

Body forces of integral equations (298) and (299) depend on displacements. So, following the procedure presented by Albuquerque *et al.* Albuquerque et al. [2007], domain integrals that come from these body forces can be transformed into boundary integrals.

3.11.2 Matrix Equations

After the discretization of equations (298) and (299) into boundary elements and collocation of the source points in all boundary nodes, a linear system is generated. It is worth notice that the only loads considered in the linear buckling equations are that related to the in-plane stress N_{ij} and tractions t_i that are multiplied by the critical load factor λ. This means that all the known values of u_3, $\partial u_3/\partial n$, M_n, V_n, w_{ci}, R_{ci} (boundary conditions) are set to zero.

Dividing the boundary into Γ_1 and Γ_2 (Figure 18), this linear system can be written in the same way of equaition (287).

3.11.3 Numerical results

The numerical results are presented in terms of the dimensionless parameter K_{cr} which is given by:

$$K_{cr} = \frac{N_{cr} a^2}{D_{22}} \tag{300}$$

where N_{cr} is the critical load ($N_{cr} = \lambda \times$ the applied load) and a is the edge length of the square plate.

Consider a square graphite/epoxy plate under different boundary conditions. The thickness of the plate is h = 0.01 m. The material properties are: elastic moduli E_1 = 181 GPa and E_2 = 10.3 GPa, Poisson ratio $\nu_{12} = 0.28$, and shear modulus $G_{12} = 7.17$ GPa.

The mesh used has 28 quadratic discontinuous boundary elements of the same length (7 per edge) and 49 (7 $\times$ 7) uniformly distributed internal points.

The plate is under uniformly uniaxial compression and the critical load parameter K_{cr} is computed considering all edges simply-supported (SSSS), all edges clamped (CCCC), and two edges clamped and two edges simply supported (CSCS). In the last case, the two edges where the load is applied are simply supported and the two remaining edges are clamped. The results are shown in Table 9 together with results obtained by Shi [1990] using a boundary element formulation with domain discretization and the analytical solution presented by Lekhnitskii [1968].

As it can be seen, there is a good agreement between the results obtained in this work and those presented in literature.

4 Shallow Shells

4.1 Introduction

The demand for construction of advanced aerospace, automotive, and marine structures has increased the interest in composite laminated shells. Some requirements, as for example high strength-to-weight ratio, good resistance to corrosion, as well as long fatigue

Table 9: Critical load parameter K_{cr} for a graphite/epoxy plate with different boundary conditions.

Case	B. Conditions	Loads	This work	Shi [1990]	Lekhnitskii [1968]
1	SSSS	$N_1 \neq 0$	130.82	–	129.78
2	SSSS	$N_2 \neq 0$	71.53	71.36	69.46
3	CCCC	$N_1 \neq 0$	493.70	481.21	–
4	CCCC	$N_2 \neq 0$	168.27	168.16	–
5	CSCS	$N_1 \neq 0$	161.47	163.24	162.03
6	CSCS	$N_2 \neq 0$	146.47	143.89	141.33
7	SSSS	$N_{12} \neq 0$	417.44		

life, cannot be obtained with the use of metallic or any other engineering materials except composites. Other requirements, as aerodynamic profile and good stealth characteristics demand curved structures or shell like structures.

The DRM has been shown as a powerful technique to transform domain integrals into boundary integrals and it has been extensively applied in many different formulation for this purpose. In this technique, the domain terms are approximated using a finite series expansion involving proposed approximation functions and coefficients to be determined. In order to accomplish the transformation, it is necessary to compute particular solutions for the governing differential equation, considering the approximation function as the non-homogeneous term. It is quite suitable for potential problems as well as for isotropic structures. However, when it is applied to anisotropic structures, the complexity of the differential equation become quite difficult, or even impossible, to compute the particular solutions for many chosen approximation functions.

An alternative approach to overcome the main drawback of the DRM, that is the lack of free choice of the approximation function, is the radial integration method (RIM). This method was proposed by Gao Gao [2002] and its use has been extended for the anisotropic thin plate formulation by Albuquerque *et al.* Albuquerque et al. [2006, 2007]. As in the DRM, the RIM also approximate the domain terms by a sum of approximation functions and coefficients to be determined. However, the RIM doesn't demand the computation of any particular solution, what become this technique specially suitable for anisotropic formulations.

In this chapter, a boundary element formulation for anisotropic shallow shells with no domain discretization is presented. Classical plate bending and plane elasticity formulations are coupled and effects of curvature are treated as body forces. The domain integrals due to body forces are transformed into boundary integrals using the radial integration method. Numerical results are presented to assess the accuracy of the method. Displacements computed using the proposed formulation are in good agreement with results available in literature. For the best of authors knowledge, there is no paper in the literature for anisotropic shells using the coupling of plate bending and plane elasticity formulations.

4.2 Boundary integral equations

Consider a shallow shell of an anisotropic elastic material with the mid-surface being described by $z = z(x_1, x_2)$ as shown in Figure 24. The base-plane of the shell is defined by a domain Ω in the plane x_1, x_2 whose boundary is given by Γ.

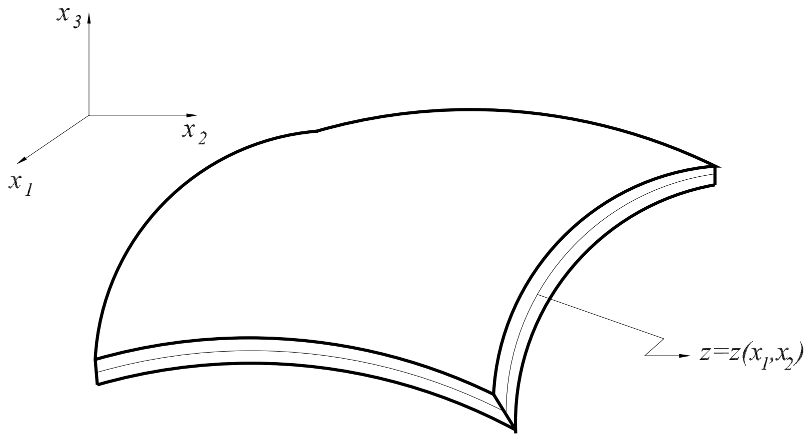

Figure 24: Shallow shell.

As shown by Reissner, the equilibrium equation for this structure can be written as:

$$N_{ij,j} + q_i = 0, \tag{301}$$

$$D_{11}w_{,1111} + 4D_{16}w_{,1112} + 2(D_{12} + D_{66})w_{,1122} + 4D_{26}w_{,1222} + D_{22}w_{,2222} + \frac{N_{ij}}{R_{ij}} = q_3, \tag{302}$$

where $i, j, k = 1, 2$; N_{ij} are membrane forces applied in the shell; D_{11}, D_{22}, D_{66}, D_{12}, D_{16}, and D_{26} are the flexural rigidities of the anisotropic plate w stands for the displacement in the normal direction of the shell surface; q_i are domain loads applied in directions of axis x_1 and x_2, q_3 is the domain load applied in direction of axis x_3; and

$$R_{ij} = \frac{-1}{z_{,ij}} \tag{303}$$

are the radii of curvature of the undeformed shell.

Using equilibrium equations of isotropic shallow shells, the reciprocity relation, and the Green theorem, Zhang and Atluri Zhang and Atluri [1986] derived integral equations that can be divided in terms of plane elasticity and plate bending formulations. These formulations are coupled by the domain integrals that arise in equations. Plane elasticity integral equations (membrane equations) are given by:

$$
\begin{aligned}
& c_{ij}u_j + \int_\Gamma t^*_{ik}(Q,P)u_k(P)d\Gamma(P) \\
& = \int_\Gamma u^*_{ik}(Q,P)t_k(P)d\Gamma(P) \\
& + \int_\Omega C\kappa_{kj}wu^*_{ik,j}(Q,P)d\Omega \\
& + \int_\Omega u^*_{ik}(Q,P)q_k(P)d\Omega(P),
\end{aligned} \tag{304}
$$

where u_k is the displacement in directions x_1 and x_2, $t_i = N_{ij}n_j$, P is the field point; Q is the source point. The constant c_{ij} is introduced in order to take into account the possibility that the point Q can be placed in the domain, on the boundary, or outside the domain. The symbol * stands for fundamental solutions (see Aliabadi, Aliabadi [2002]). Constant κ_{kj} depends on the curvature radii R_{kj} of the shallow shell.

The plate bending integral equation is given by:

$$
\begin{aligned}
& Kw(Q) \\
& + \int_\Gamma \left[V^*_n(Q,P)w(P) - m^*_n(Q,P)\frac{\partial w(P)}{\partial n} \right] d\Gamma(P) \\
& + \sum_{i=1}^{N_c} R^*_{c_i}(Q,P)w_{ci}(P) = \sum_{i=1}^{N_c} R^*_{c_i}(P)w_{ci}(Q,P) \\
& + \int_\Omega q_3(P)w^*(Q,P)\, d\Omega \\
& + \int_\Gamma \left[V_n(P)w^*(Q,P) - m_n(P)\frac{\partial w^*}{\partial n}(Q,P) \right] d\Gamma(P) \\
& + \int_\Gamma C\kappa_{ij}n_ju_i(P)w^*(Q,P)\, d\Gamma(P) \\
& + \int_\Omega C\frac{\kappa_{ij}}{\rho_{ij}}w^*(Q,P)w(P)\, d\Omega \\
& + \int_\Omega \left[C\kappa_{ij}(P)w^*(Q,P) \right]_{,j} u_i(P)\, d\Omega,
\end{aligned} \tag{305}
$$

where $\frac{\partial()}{\partial n}$ is the derivative in the direction of the outward vector $\mathbf{n}$ that is normal to the boundary Γ; m_n and V_n are, respectively, the normal bending moment and the Kirchhoff equivalent shear force on the boundary Γ; R_c is the thin-plate reaction of corners; w_{ci} is the transverse displacement of corners; q_3 is the domain force in the transversal direction; K is a constant equivalent to c_{ij} of equation (304).

In order to have an equal number of equations and unknowns, it is necessary to write an integral equation corresponding to the derivative of the displacement $w(Q)$ in relation to the unity vector $\mathbf{m}$ that is normal to the boundary in the source point Q. This equation is given by:

$$
\begin{aligned}
&K\frac{\partial w}{\partial m}(Q)\\
&+\int_{\Gamma}\left[\frac{\partial V_n^*(Q,P)}{\partial m}w(P)-\frac{\partial m_n^*(Q,P)}{\partial m}\frac{\partial w(P)}{\partial n}\right]d\Gamma(P)\\
&+\sum_{i=1}^{N_c}\frac{\partial R_{c_i}^*(Q,P)}{\partial m}w_{ci}(P)=\sum_{i=1}^{N_c}\frac{\partial R_{c_i}(P)^*}{\partial m}w_{ci}(Q,P)\\
&+\int_{\Omega}q_3(P)\frac{\partial w^*(Q,P)}{\partial m}\,d\Omega\\
&+\int_{\Gamma}\left[V_n(P)\frac{\partial w^*(Q,P)}{\partial m}-m_n(P)\frac{\partial^2 w^*}{\partial n\partial m}(Q,P)\right]d\Gamma(P)\\
&+\int_{\Gamma}C\kappa_{ij}n_ju_i(P)\frac{\partial w^*(Q,P)}{\partial m}\,d\Gamma(P)\\
&+\int_{\Omega}C\frac{\kappa_{ij}}{\rho_{ij}}\frac{\partial w^*(Q,P)}{\partial m}w(P)\,d\Omega\\
&+\int_{\Omega}\left[C\kappa_{ij}(P)\frac{\partial w^*(Q,P)}{\partial m}\right]_{,j}u_i(P)\,d\Omega.
\end{aligned}
\tag{306}
$$

As can be seen in equations (304), (305), and (306), domain integrals arise in the formulation owing to the curvature of the shell. These domain integrals are:

$$P_1(Q)=\int_{\Omega}C\kappa_{kj}wu_{ik,j}^*(Q,P)d\Omega, \tag{307}$$

$$P_2(Q)=\int_{\Omega}C\frac{\kappa_{ij}}{\rho_{ij}}w^*(Q,P)w(P)\,d\Omega, \tag{308}$$

$$P_3(Q)=\int_{\Omega}\left[C\kappa_{ij}(P)w^*(Q,P)\right]_{,j}u_i(P)\,d\Omega, \tag{309}$$

$$P_4(Q)=\int_{\Omega}C\frac{\kappa_{ij}}{\rho_{ij}}\frac{\partial w^*(Q,P)}{\partial m}w(P)\,d\Omega, \tag{310}$$

and

$$P_5(Q)=\int_{\Omega}\left[C\kappa_{ij}(P)\frac{\partial w^*(Q,P)}{\partial m}\right]_{,j}u_i(P)\,d\Omega. \tag{311}$$

In order to transform these integrals into boundary integrals, the RIM is used. Details of this method can be found in Albuquerque, Sollero, and Paiva (Albuquerque et al. [2007]). However, for sake of completeness, some steps of the method are repeated here, in the next section.

4.3 The radial integration method

Consider, in a general case, the following domain integration:

$$P(Q) = \int_{\Omega} b(P) v^*(Q,P) d\Omega, \tag{312}$$

where b and v^* are generic body force and fundamental solution, respectively.

The body force is approximated over the domain Ω as a sum of M products between approximation functions f_m and unknown coefficients γ_m, as given by equation (247).

Now, considering that the body force is approximated, for simplicity, by equation (247), the domain integral (312) can be written as:

$$P(Q) = \int_{\Omega} b(P) v^*(Q,P) d\Omega = \sum_{m=1}^{M} \gamma_m \int_{\Omega} f_m v^*(Q,P) d\Omega, \tag{313}$$

that can be transformed into a sum o boundary integrals by using the RIM as already presented in section 3.9.
In a matrix form, we can write:

$$P(Q) = \begin{bmatrix} \int_{\Gamma} \frac{F_1(Q)}{r} \mathbf{n}.\mathbf{r} d\Gamma & \int_{\Gamma} \frac{F_2(Q)}{r} \mathbf{n}.\mathbf{r} d\Gamma & \dots & \int_{\Gamma} \frac{F_M(Q)}{r} \mathbf{n}.\mathbf{r} d\Gamma \end{bmatrix} \begin{Bmatrix} \gamma_1 \\ \gamma_2 \\ \vdots \\ \gamma_M \end{Bmatrix}. \tag{314}$$

To compute γ_m, it is necessary to consider the body force in M points of the domain and of the boundary. In the case of this work, these points are the boundary nodes and some internal points. Thus, equation (247) can be written as:

$$\mathbf{b} = \mathbf{F}\boldsymbol{\gamma}, \tag{315}$$

and $\boldsymbol{\gamma}$ can be computed as:

$$\boldsymbol{\gamma} = \mathbf{F}^{-1}\mathbf{b}. \tag{316}$$

Substituting (316) into equation (314), we have:

$$P(Q) = \begin{bmatrix} \int_{\Gamma} \frac{F_1(Q)}{r} \mathbf{n}.\mathbf{r} d\Gamma & \int_{\Gamma} \frac{F_2(Q)}{r} \mathbf{n}.\mathbf{r} d\Gamma & \dots & \int_{\Gamma} \frac{F_M(Q)}{r} \mathbf{n}.\mathbf{r} d\Gamma \end{bmatrix} \mathbf{F}^{-1}\mathbf{b}. \tag{317}$$

Writing equation (317) for all source points, i.e., all boundary nodes and internal points, we have the following matrix equation:

$$\mathbf{P} = \mathbf{R}\mathbf{F}^{-1}\mathbf{b} = \mathbf{S}\mathbf{b}, \tag{318}$$

where $\mathbf{S} = \mathbf{R}\mathbf{F}^{-1}$, $\mathbf{P}$ is a vector that contains the value of $P(Q)$ in all source points Q, and $\mathbf{R}$ is a matrix that contains the value of integrals of equation (317) when this equation is written for all source points Q.

4.4 Matrix equation

Considering all body forces that appears in equations (296), (298), and (306), the vector $\mathbf{P}$ for these equations are given by:

$$\mathbf{P} = \begin{bmatrix} \mathbf{0} & \mathbf{0} & \mathbf{S}_{bb}^{mc} & \mathbf{S}_{bi}^{mc} & \mathbf{S}_{bc}^{mc} \\ \mathbf{0} & \mathbf{0} & \mathbf{S}_{ib}^{mc} & \mathbf{S}_{ii}^{mc} & \mathbf{S}_{ic}^{mc} \\ \mathbf{S}_{bb}^{p1c} & \mathbf{S}_{bi}^{p1c} & \mathbf{S}_{bb}^{p1} & \mathbf{S}_{bi}^{p1} & \mathbf{S}_{bc}^{p1} \\ \mathbf{S}_{bb}^{p2c} & \mathbf{S}_{bi}^{p2c} & \mathbf{S}_{bb}^{p2} & \mathbf{S}_{bi}^{p2} & \mathbf{S}_{bc}^{p2} \\ \mathbf{S}_{ib}^{p1c} & \mathbf{S}_{ii}^{p1c} & \mathbf{S}_{ib}^{p1} & \mathbf{S}_{ii}^{p2} & \mathbf{S}_{ic}^{p1} \\ \mathbf{S}_{cb}^{p1c} & \mathbf{S}_{ci}^{p1c} & \mathbf{S}_{cb}^{p1} & \mathbf{S}_{ci}^{p1} & \mathbf{S}_{cc}^{p1} \end{bmatrix} \begin{Bmatrix} \mathbf{u}_b \\ \mathbf{u}_i \\ \mathbf{w}_b \\ \mathbf{w}_i \\ \mathbf{w}_c \end{Bmatrix} \tag{319}$$

where the superscript index of matrix $\mathbf{S}$ stands for the type of equation that is being used, i.e., m stands for the membrane equation given by equation (296), $p1$ stands for the first plate equation, given by equation (298), and $p2$ stands for the second plate equation, given by equation (306). The letter c in the superscript index means that these are coupling terms. In matrix $\mathbf{S}$, the first subscript index stands for the location of the source points (b if source points are at a smooth part of the boundary, i if they are in the domain and c if they are at corners). The second subscript index shows where are the body forces that are multiplied by terms of the matrix $\mathbf{S}$. For the second index, the same letters of the first subscript index are used with the same meaning. The right hand side vector has nodal values of the body forces that in this case are given by displacements (all the remaining terms of domain integrals are considered as part of the fundamental solution v^*). The letter $\mathbf{u}$ stands for displacements in the x_1 and x_2 directions and $\mathbf{w}$ stands for displacement in the transversal direction. Subscript indices in the right hand side vector indicate the location of nodes where displacements are computed.

Finally, if the boundary Γ is discretized in boundary elements and equations (296), (298), and (306) is written for all source points, the following matrix equation can be obtained:

$$\begin{bmatrix} \mathbf{H}_{bb}^{m} & \mathbf{0} & \mathbf{0} & \mathbf{0} & \mathbf{0} \\ \mathbf{H}_{ib}^{m} & \mathbf{I} & \mathbf{0} & \mathbf{0} & \mathbf{0} \\ \mathbf{H}_{bb}^{p1c} & \mathbf{0} & \mathbf{H}_{bb}^{p1} & \mathbf{0} & \mathbf{H}_{bc}^{p1} \\ \mathbf{H}_{bb}^{p2c} & \mathbf{0} & \mathbf{H}_{bb}^{p2} & \mathbf{0} & \mathbf{H}_{bc}^{p2} \\ \mathbf{H}_{ib}^{p1c} & \mathbf{0} & \mathbf{H}_{ib}^{p1} & \mathbf{I} & \mathbf{H}_{ic}^{p1} \\ \mathbf{H}_{cb}^{p1c} & \mathbf{0} & \mathbf{H}_{cb}^{p1} & \mathbf{0} & \mathbf{H}_{cc}^{p1} \end{bmatrix} \begin{Bmatrix} \mathbf{u}_b \\ \mathbf{u}_i \\ \mathbf{v}_b \\ \mathbf{w}_i \\ \mathbf{w}_c \end{Bmatrix}$$
$$= \begin{bmatrix} \mathbf{G}_{bb}^{m} & \mathbf{0} & \mathbf{0} \\ \mathbf{G}_{ib}^{m} & \mathbf{0} & \mathbf{0} \\ \mathbf{0} & \mathbf{G}_{bb}^{p1} & \mathbf{G}_{bc}^{p1} \\ \mathbf{0} & \mathbf{G}_{bb}^{p2} & \mathbf{G}_{bc}^{p2} \\ \mathbf{0} & \mathbf{G}_{ib}^{p1} & \mathbf{G}_{ic}^{p1} \\ \mathbf{0} & \mathbf{G}_{cb}^{p1} & \mathbf{G}_{cc}^{p1} \end{bmatrix} \begin{Bmatrix} \mathbf{t}_b \\ \mathbf{p}_b \\ \mathbf{p}_c \end{Bmatrix}$$
$$+ \begin{bmatrix} \mathbf{0} & \mathbf{0} & \mathbf{S}_{bb}^{mc} & \mathbf{S}_{bi}^{mc} & \mathbf{S}_{bc}^{mc} \\ \mathbf{0} & \mathbf{0} & \mathbf{S}_{ib}^{mc} & \mathbf{S}_{ii}^{mc} & \mathbf{S}_{ic}^{mc} \\ \mathbf{S}_{bb}^{p1c} & \mathbf{S}_{bi}^{p1c} & \mathbf{S}_{bb}^{p1} & \mathbf{S}_{bi}^{p1} & \mathbf{S}_{bc}^{p1} \\ \mathbf{S}_{bb}^{p2c} & \mathbf{S}_{bi}^{p2c} & \mathbf{S}_{bb}^{p2} & \mathbf{S}_{bi}^{p2} & \mathbf{S}_{bc}^{p2} \\ \mathbf{S}_{ib}^{p1c} & \mathbf{S}_{ii}^{p1c} & \mathbf{S}_{ib}^{p1} & \mathbf{S}_{ii}^{p2} & \mathbf{S}_{ic}^{p1} \\ \mathbf{S}_{cb}^{p1c} & \mathbf{S}_{ci}^{p1c} & \mathbf{S}_{cb}^{p1} & \mathbf{S}_{ci}^{p1} & \mathbf{S}_{cc}^{p1} \end{bmatrix} \begin{Bmatrix} \mathbf{u}_b \\ \mathbf{u}_i \\ \mathbf{w}_b \\ \mathbf{w}_i \\ \mathbf{w}_c \end{Bmatrix} + \mathbf{q} \tag{320}$$

where $\mathbf{H}$ and $\mathbf{G}$ are influence matrices of the BEM; the vector $\mathbf{v}$ contains transversal displacements and rotations of the nodes (not only transversal displacement as vector $\mathbf{w}$). Vectors $\mathbf{t}$ and $\mathbf{p}$ contain boundary node reactions for membrane and plate equations, respectively. The vector $\mathbf{q}$ is due to the domain load q_i. Domain integrals due to q_i's are transformed exactly into boundary integrals using the procedure presented in Albuquerque, Sollero, Venturini, and Aliabadi (Albuquerque et al. [2007]).

Equation (320) can be written in a more concise form as:

$$\mathbf{Hv} = \mathbf{Gt} + \mathbf{Su} + \mathbf{q} \tag{321}$$

Finally, columns of matrices of equation (321) can be reordered in accordance with boundary conditions and a linear equation system can be obtained where the unknown displacements and reactions can be computed.

4.5 Approximation functions

Two approximation functions are used in this work. The first is a radial basis function that has been used extensively in the DRM and is given by:

$$f_{m_1} = 1 + R. \tag{322}$$

The second is the well known thin plate spline:

$$f_{m_3} = R^2 \log(R), \tag{323}$$

used with the augmentation function given by equations (248) and (249).

4.6 Numerical results

4.6.1 Square spherical shallow shell

In order to assess the accuracy of the proposed formulation, consider a square spherical shallow shell, as shown in Figure 25. The geometry and material properties of the shell are as follow: length of the base edge of the shell a =0.254 m, thickness h = 0.0127 m, curvature radii $R_1 = R_2 = R$ = 2.54 m ($R_{12} = R_{21} = 0$), elastic moduli E_2 = 6.895 GPa and E_1 = $2E_1$, Poisson ratio $\nu_{12} = 0.3$, and shear modulus $G_{12} = E_2/[2(1-\nu_{12})]$. The shell is under a uniformly distributed load in the transversal direction (internal pressure) q_3 = 2.07 MPa ($q_1 = q_2 = 0$).

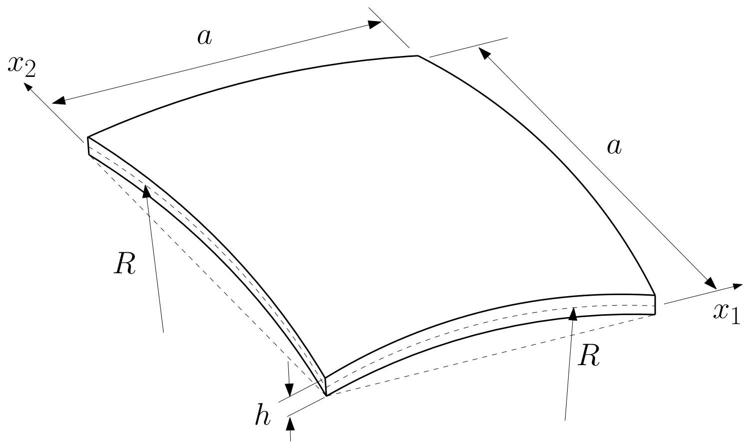

Figure 25: Square spherical shallow shell.

This problem was analysed considering two types of boundary conditions, i.e., clamped and simply-supported. Three meshes were used. Mesh 1 has 12 constant boundary elements and 9 internal points, mesh 2 has 20 boundary elements and 25 internal points, and mesh 3 has 28 boundary elements and 49 internal points. Mesh 3 is shown in Figure 26. All meshes have elements of equal length and uniformly distributed internal points.

Figures 27 and 28 show results for the clamped and simply-supported boundary conditions, respectively, together with meshless results obtained by Sladek et al. Sladek et al. [2007] for the same problems but considering the shell as shear deformable.

As it can be seen, the results for the clamped boundary conditions are in good agreement with the meshless results while for the simply-supported boundary conditions they are slightly lower.

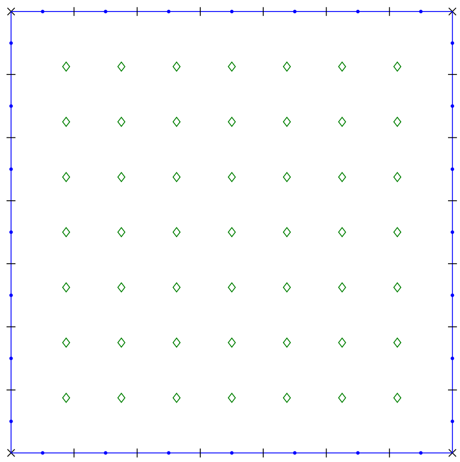

Figure 26: Boundary elements and internal points for the square spherical shallow shell (mesh 3, 28 boundary elements and 49 internal points).

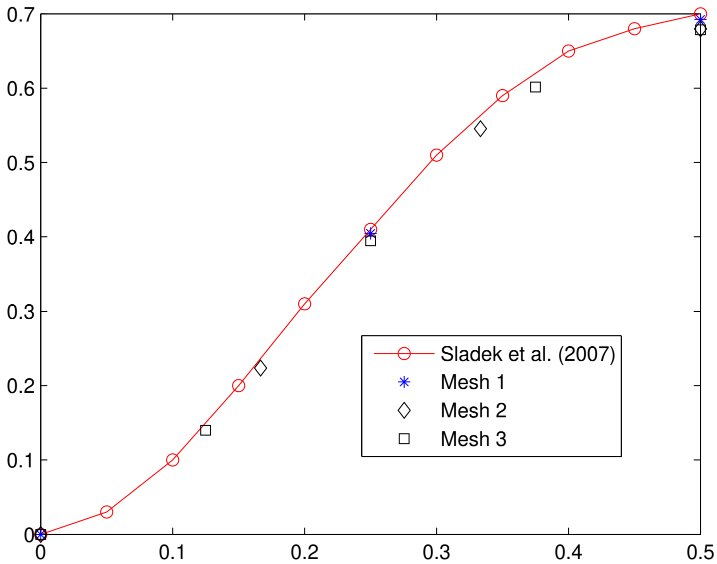

Figure 27: Transversal displacement for the spherical shell with clamped edge.

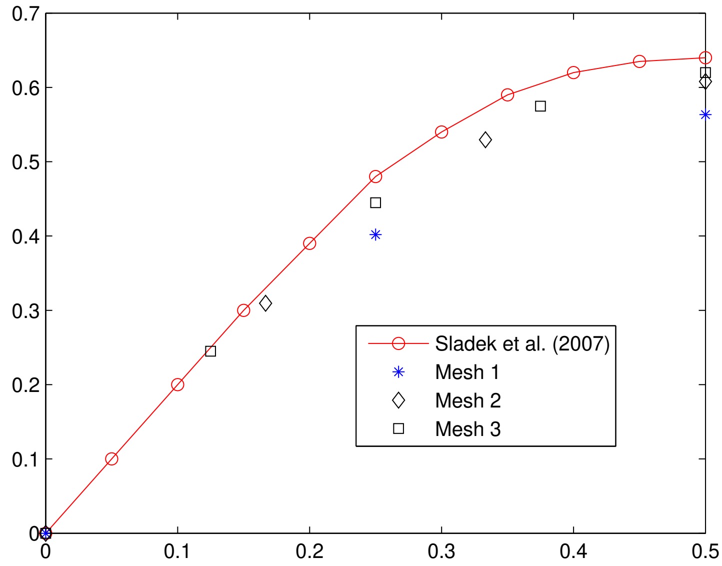

Figure 28: Transversal displacement for the spherical shell with simply-supported edge.

5 Conclusions

5.1 Conclusions

This chapter presented a boundary element formulation for the numerical analysis of static and dynamic problems in laminated composite plates and shallow shells. Two boundary integral equations, for transverse displacement and rotation, were used, and these integral equations were discretized into constant and quadratic boundary elements. For elastostatics, the domain integrals which arise from linearly and uniformly distributed loads were transformed into boundary integrals by an exact radial transformation. Several numerical examples were shown for quasi-isotropic, orthotropic, and general anisotropic materials. The numerical results obtained with the present boundary element technique were compared with results obtained analytically in the form of a series solution and results obtained by the finite element method, and show good agreement.

The use of the dual reciprocity boundary element method (DRM) and the radial integration method (RIM) for problems in which the body forces are unknowns was explored. In both methods body forces are approximated as a sum of the product between radial basis function and unknown coefficients. The main advantage of the RIM over the DRM is that there is no need to compute analytical particular solutions in the former, which allows a free choice of the approximation function for problems of anisotropic materials. As some of the integrals that arises in the formulation cannot be computed analytically, the use of numerical integration becomes the RIM more time-consuming than the DRM. Results have shown that similar accuracy is obtained with the RIM and the DRM when the same approximation function is used for problems of unknown body forces. This is a first work and both methods still demands a lot of research. An important analysis that should be carried out in order to improve the accuracy of the RIM is the use of other approximation functions, such as radial basis functions augmented by polynomials or thin plate splines. However, this analysis was not in the scope of this work.

In the analysis of thin shallow shells, domain integrals are transformed into boundary integrals by the radial integration method. As the radial integration method doesn't demand particular solutions, it is easier to implement than the dual reciprocity boundary element method. Besides, strong singularities in domain integrals are cancelled by the radial integration. Two different approximation functions are used in the radial integration method. Results obtained with both approximation functions are in good agreement with results presented in literature. As in the dual reciprocity method, the accuracy of the method is improved by increasing the number of boundary nodes and internal points. However, different from dual reciprocity and even from other applications of the radial integration method, the use of radial basis function augmented by polynomials hasn't produced significantly changes in results.

References

E. L. Albuquerque and P. Sollero. The boundary element method applied to transient dynamic anisotropic problems. In A. J. Kassab, C. A. Brebbia, and M. Chopra, editors, *Proc. Boundary Element Method XX*, pages 617–624, Orlando - USA, jul 1998.

E. L. Albuquerque, P. Sollero, and M. H. Aliabadi. The boundary element method applied to time dependent problems in anisotropic materials. *International Journal of Solids and Structures*, 39:1405–1422, 2002.

E. L. Albuquerque, P. Sollero, and P. Fedelinski. Dual reciprocity boundary element method in laplace domain applied to anisotropic dynamic crack problems. *Computers and Structures*, 81:1703–1713, 2003a.

E. L. Albuquerque, P. Sollero, and P. Fedelinski. Free vibration analysis of anisotropic material structures using the boundary element method. *Engineering Analysis with Boundary Elements*, 27:977–985, 2003b.

E. L. Albuquerque, P. Sollero, and M. H. Aliabadi. Dual boundary element method for anisotropic dynamic fracture mechanics. *International Journal for Numerical Methods in Engineering*, 59:1187–1205, 2004.

E. L. Albuquerque, P. Sollero, W. Venturini, and M. H. Aliabadi. Boundary element analysis of anisotropic kirchhoff plates. *International Journal of Solids and Structures*, 43:4029–4046, 2006.

E. L. Albuquerque, P. Sollero, and W. P. Paiva. The radial integration method applied to dynamic problems of anisotropic plates. *Communications in Numerical Methods in Engineering*, 23:805–818, 2007.

M. H. Aliabadi. *Boundary element method, the application in solids and structures*. John Wiley and Sons Ltd, New York, 2002.

P. M. Baiz and M. H. Aliabadi. Linear buckling of shear deformable shallow shells by the boundary domain element method. *CMES - Computer Modeling in Engineering and Sciences*, 13:19–34, 2006.

K. Bath and E. L. Wilson. *Numerical methods in finite element analysis*. Prentice-Hall Inc., Englewood Cliffs, New Jersey, 1976.

T. A. Cruse and J. L. Swedlow. Interactive program for analysis and design problems in advanced composites. Technical report, Carnegie-Mellon University, Report AFLM-TR-71-268, 1971.

A. Deb. Boundary elements analysis of anisotropic bodies under thermo mechanical body force loadings. *Computers and Structures*, 58:715–726, 1996.

T. Dirgantara and M. H. Aliabadi. A new boundary element formulation for shear deformable shells analysis. *Int. J. for Numerical Methods in Engn.*, 45:1257–1275, 1999.

X. Gao. The radial integration method for evaluation of domain integrals with boundary only discretization. *Engn. Analysis with Boundary Elements*, 26:905–916, 2002.

R. F. Gibson. *Principles of composite material mechanics*. McGraw Hill, New York, 1994.

J. C. Houbolt. A reccurrence matrix solution for the dynamic response of elastic aircraft. *J. of Aeronautical and Science*, 17:540–550, 1950.

G. Kirchhoff. On the equilibrium and motion of an elastic plate. *J. Math.*, 40:51–58, 1950. In German.

M. Kogl and L. Gaul. A boundary element method for transient piezoelectric analysis. *Engineering Analysis with Boundary Elements*, 24:591–598, 2000a.

M. Kogl and L. Gaul. A 3-d boundary element method for dynamic analysis of anisotropic elastic solids. *CMES - Computational Modelling in Engineering and Science*, 1:27–43, 2000b.

M. Kogl and L. Gaul. Free vibration analysis of anisotropic solids with the boundary element method. *Engineering Analysis with Boundary Elements*, 27:107–114, 2003.

B. Lamattina. *Anisotropic plate bendign analysis using complex variable methods*. PhD thesis, North Carolina State University, Raleigh - USA, 1997.

B. Lamattina, E. C. Klang, and J. W. Eischen. A study of solutions for the anisotropic plate subjected to a concentrated force. *Journal of Applied Mechanics*, 65:273–276, 1998.

S. G. Lekhnitskii. *Anisotropic plates*. Gordon and Breach, New York, 1968.

J. Lin, R. C. Duffield, and H. Shih. Buckling analysis of elastic plates by boundary element method. *Engineering Analysis with Boundary Element*, 23:131–137, 1999.

C. Loeffler and W. J. Mansur. Analysis of time integration schemes for boundary element applications to transient wave propagation problems. In C. A. Brebbia and W. S. Venturini, editors, *Boundary Element techniques: Applications in stress analysis and heat transfer*, pages 105–122, Computational Mechanics Publications, Southhampton, 1987.

P. Lu and O. Mahrenholtz. The fundamental solution for the theory of orthotropic shallow shells involving shear deformation. *Int. J. of Solids and Structures*, 31:913–923, 1994.

J. Mossakowski. Singular solutions of anisotropic plates. *Arch. Mech. Stos.*, 7:97–110, 1955. In Polish.

D. Nardini and C. A. Brebbia. A new approach to free vibration analysis using boundary elements. In *Boundary Element Method in Engineering - IV International Seminar*, 1982.

M. S. Nerantzaki and J. T. Katsikadelis. Buckling of plates with variable thickness, an analog equation solution. *Engineering Analysis with Boundary Element*, 18:149–154, 1996.

A. J. Nowak and A. C. Neves. *The multiple reciprocity boundary element method*. Computational Mechanics Publication, Southampton, 1994.

J. B. Paiva. *Boundary element formulation for plate bending and its aplication in engineering*. PhD thesis, University of São Paulo, São Carlos School of Engineering, 1987. In Portuguese.

W. P. Paiva, P. Sollero, and E. L. Albuquerque. Treatment of hypersingularities in boundary element anisotropic plate bending problems. *Latin American Journal of Solids and Structures*, 1:49–73, 2003.

W. P. Paiva, P. Sollero, E. L. Albuquerque, R. Pavanello, and M. H. Aliabadi. Dynamics of thin anisotropic plates. In *Advances in Boundary Element Techniques V*, 2004.

P. W. Partridge, C. A. Brebbia, and L. C. Wrobel. *The dual reciprocity boundary element method*. Computational Mechanics Publications, Southampton, Boston, 1992.

J. Purbolaksono and M. H. Aliabadi. Buckling analysis of shear deformable plates by boundary element method. *International Journal for Numerical Methods in Engineering*, 62:537–563, 2005.

C. Rajamohan and J. Raamachandran. Bending of anisotropic plates by charge simulation method. *Advances in Engn. Software*, 30:369–373, 1999.

N. A. Schclar. *Anisotropic analysis using boundary elements*. Computational Mechanics Publications, Southampton, Boston, 1994.

G. Shi. Flexural vibration and buckling analysis of orthotropic plates by the boundary element method. *J. of Solids and Structures*, 26:1351–1370, 1990.

G. Shi and G. Bezine. A general boundary integral formulation for the anisotropic plate bending problems. *J. Composite Materials*, 22:694–716, 1988.

J. Sladek, V. Sladek, J. Krivacek, and M. H. Aliabadi. Local boundary integral equations for orthotropic shallow shells. *International Journal of Solids and Structures*, 44:2285–2303, 2007.

P. Sollero and M. H. Aliabadi. Fracture mechanics analysis of anisotropic plates by the boundary element method. *Int. J. of Fracture*, 64:269–284, 1993.

P. Sollero and M. H. Aliabadi. Anisotropic analysis of composite laminates using the dual boundary element methods. *Composite Structures*, 31:229–234, 1995.

M. Suchar. On singular solutions in the theory of anisotropic plates. *Bulletin de l'Academie Polonaise des Sciences: Series Science Techniques*, 12:29–38, 1964.

S. Syngellakis and E. Elzein. Plate buckling loads by the boundary element method. *International Journal for Numerical Methods in Engineering*, 37:1763–1778, 1994.

W. S. Venturini. *A study of boundary element method and its application on engineering problems*. PhD thesis, University of São Paulo, São Carlos School of Engineering, 1988. In Portuguese.

J. Wang. The fundamental solutions of orthotropic shallow shells. *Acta Mechanica*, 94: 113–121, 1992.

J. Wang and K. Schweizerhof. The fundamental solution of moderately thick laminated anisotropic shallow shells. *Int. J. Engng. Sci.*, 33:995–1004, 1995.

J. Wang and K. Schweizerhof. Study on free vibration of moderately thick orthotropic laminated shallow shells by boundary-domain elements. *Applied Mathematical Modelling*, 20:579–584, 1996.

J. Wang and K. Schweizerhof. Free vibration of laminated anisotropic shallow shells including transverse shear deformation by the boundary-domain element method. *Computers and Structures*, 62:151–156, 1997.

P. H. Wen, M. H. Aliabadi, and A. Young. Application of dual reciprocity method to plates and shells. *Engn. Anal. with Boundary Elements*, 24:583–590, 2000.

B. C. Wu and N. J. Altiero. A new numerical method for the analysis of anisotropic thin plate bending problems. *Computer Meth. in Appl. Mechanics and Engineering*, 25: 343–353, 1981.

C. Zhang. Transient elastodynamic antiplane crack analysis of anisotropic solids. *Int. J. of Solids and Structures*, 37:6107–6130, 2000.

J. D. Zhang and S. N. Atluri. A boundary/interior element method for quasi-static and transient response analysis of shallow shells. *Computers and Structures*, 24:213–223, 1986.